UNIVERSITY OF KWAZULU-NATAL

NEW FAMILIES OF EXACT SOLUTIONS FOR COMPACT STARS

DIDIER KILEBA MATONDO

NEW FAMILIES OF EXACT SOLUTIONS FOR COMPACT STARS

DIDIER KILEBA MATONDO

This dissertation is submitted to the School of Mathematics, Statistics and Computer Science, College of Agriculture, Engineering and Science, University of KwaZulu-Natal, Durban, in fulfilment of the requirements for the degree of Doctor of Philosophy.

August 10, 2018

As the candidate's supervisors, we have approved this dissertation for submission.

Signed:	Prof S. D. Maharaj	August 10, 2018.
Signed:	Prof S. Ray	August 10, 2018.

Abstract

In this thesis we present new families of exact solutions to the Einstein and Einstein-Maxwell field equations which are relevant in the description of highly compact stellar objects. We first impose a linear equation of state to generate exact solutions in terms of elementary functions which contain earlier quark models, including those of Thirukkanesh and Maharaj (*Class. Quantum Grav.* **25**, 235001 (2008)) and Mafa Takisa and Maharaj (*Astrophys. Space Sci.* **354**, 463 (2013)). Secondly, we find exact solutions in terms of elementary functions, Bessel and modified Bessel functions through the Finch and Skea geometry which satisfy all criteria for physical acceptability. From these models we regain the uncharged model of Finch and Skea (*Class. Quantum Grav.* **6**, 467 (1989)) and the charged model of Hansraj and Maharaj (*Int. J. Mod. Phys. D* **15**, 1311 (2006)) as particular cases. Thirdly, we find new exact stellar models by imposing a symmetry condition on spacetime, namely a conformal Killing vector. We find solutions to the field equations with the help of the gravitational potentials related explicitly by the conformal vector established by Manjonjo *et al* (*Eur. Phys. J. Plus* **132**, 62 (2017)). For each approach, we select a particular model to study the physical features and then masses and radii with accurate ranges consistent with observed numerical values of compact objects such as SAX J1808.4-3658, LMC X-4, SMC X-1, EXO 1785, Cen X-3, 4U1820-30, PSR J1903+327, Vela X-1 and PSR J1614-2230 are generated. The physical features in all cases are studied comprehensively, and we show that our solutions are stable, well behaved and have realistic physical features.

Declaration I - Plagiarism

I, Didier Kileba Matondo, declare that

1. The research reported in this thesis, except where otherwise indicated, is my original research.

2. This thesis has not been submitted for any degree or examination at any other university.

3. This thesis does not contain other persons' data, pictures, graphs or other information, unless specifically acknowledged as being sourced from other persons.

4. This thesis does not contain other persons' writing, unless specifically acknowledged as being sourced from other researchers. Where other written sources have been quoted, then:

    a. Their words have been re-written but the general information attributed to them has been referenced.

    b. Where their exact words have been used, then their writing has been placed in italics and inside quotation marks and referenced.

5. This thesis does not contain text, graphics or tables copied and pasted from the Internet unless specifically acknowledged, and the source being detailed in the thesis and in the References sections.

Signed: Didier Kileba Matondo August 10, 2018

Declaration II - Publications

DETAILS OF CONTRIBUTION TO PUBLICATIONS that form part and/or include research presented in this thesis

- Publication 1

  D. Kileba Matondo and S.D. Maharaj, New charged anisotropic compact model, *Astrophys. Space Sci.* **361**, 221 (2016).

- Publication 2

  S.D. Maharaj, D. Kileba Matondo, P. Mafa Takisa, A family of Finch and Skea relativistic stars, *Int. J. Mod. Phys. D* **26**, 1750014 (2016).

- Publication 3

  D. Kileba Matondo, P. Mafa Takisa, S.D. Maharaj and S. Ray, Prediction of stellar masses with Finch and Skea geometry, *Astrophys. Space Sci.* **362**, 186 (2017).

- Publication 4

  D. Kileba Matondo, S.D. Maharaj and S. Ray, Relativistic stars with conformal symmetry, *Eur. Phys. J. C* **78**, 437 (2018).

- Publication 5

  D. Kileba Matondo, S.D. Maharaj and S. Ray, Charged isotropic model with conformal symmetry, *Astrophys. Space Sci.* submitted (2018).

Dedication

In memory of Kileba Mayemba André and Bakedinga Kela Agnes: my late parents, with love and eternal appreciation.

Acknowledgments

I wish to express my heartfelt gratitude to the following persons and organisations for their support in various ways to the completion of this thesis:

- My supervisor Professor Sunil D. Maharaj, for his support, guidance and encouragement which brought this work towards a completion. As my mentor, he has taught me more than I could ever give him credit for here. He has shown me, by his example, what a good scientist should be.
- My co-supervisor Professor S. Ray, for his wonderful collaboration, comments and suggestions during my postgraduate research.
- The National Research Foundation (NRF) and the University of KwaZulu-Natal for the financial support through the award of an NRF PhD scholarship.
- Members of staff in the School of Mathematics, Statistics and Computer Science, for the unconditional administrative assistance.
- All my friends in the School of Mathematics, Statistics and Computer Science through their personal and scholarly interactions, their suggestions at various points of my research. My special words of thanks should also go to Dr. Pedro Mafa, for always being so kind, helpful and motivating.
- My family for their love and encouragement. I am very indebted to my spouse Beatrice Umba and my sister Sylvie Kileba who supported me in every possible way to see the completion of this thesis.

Contents

List of Tables

List of Figures

Chapter 1

Introduction

At the beginning of the 20^{th} century, Einstein initiated the general theory of relativity as an extension of special relativity to describe gravity in a new approach. The essence of this new way is to show that the relative acceleration of particles is not viewed as a consequence of gravitational forces but emanates rather from the geometry of the spacetime in which the particles are moving. It was emphasized by Davies (1989) that general relativity involves the theoretical predictions which are consistent with observational results in astrophysics. The relationship between the spacetime geometry describing the motion of matter and the density of matter-energy is based on the Einstein and Einstein-Maxwell field equations. Exact solutions to the Einstein field equations made it possible to discover many properties of compact objects and their structures in relativistic astrophysics. Schwarzschild (1916a, 1916b) proposed the first solutions of Einstein field equations describing the exterior and interior gravitational field of the compact stellar models. In an extension, Reissner (1916) and Nördstrom (1918) found an exterior solution for a static spherically symmetric charged star, known as Reissner-Nördstrom exterior metric. The investigation of Kerr (1963) for an uncharged body in rotating motion, led to an exterior solution where mass and angular momentum effects have been taken in account. The Kerr-Newman exterior solution is the extension of the Kerr metric, also found by Newman

and Janis (1965), for a rotating stellar body in the presence of an electric field.

In the investigation of Delgaty and Lake (1998), several exact solutions to Einstein equations were subjected to tests based on the following criteria: non-singularity at the centre, regularity and monotonic decrease of the energy density and isotropic pressure inside the star, vanishing of the pressure at the surface and causality condition. An additional condition was imposed to the speed of sound to be monotonically decreasing. There are only few families of exact solutions that satisfy all physical criteria. The Finch and Skea (1989) solution has completely satisfied all the physical requirements set out. The exact solution generated by Finch and Skea (1989) for the interior of a 4−dimensional perfect fluid sphere is consistent for an exact relativistic model of a superdense star. The Finch and Skea model provides a simple ansatz which was used by many investigators. Hansraj and Maharaj (2006) have extended this model to incorporate the electric field in the field equations. Pandya *et al* (2015) found a new class of solutions where it is assumed that the interior of the static spherically symmetric spacetime is anisotropic. The complete generalisation of the model admitting anisotropy in the presence of charge was investigated by Maharaj *et al* (2016).

In the work of Delgaty and Lake (1998), the isotropy in the pressure is one of the elementary criteria for physical acceptability that a relatistic star has to satisfy. Substantial investigations have been devoted to understand the properties of stellar interior matter in order to produce realistic stellar models. The high energy density and strong gravitational potentials in the interior of compact stars seem to be at the root of a physical phenomenon generating the radial and tangential pressures. It was shown by a number of investigators that the critical mass, critical surface redshift and stability of highly compact bodies are substantialy affected by anisotropic matter. The work of Bowers and Liang (1974) created a new way in the question related to the possible role of anisotropic equations of state for relativistic stellar bodies by incorporing the factor of anisotropy in the equation of hydrostatic equilibrium. The presence of the nuclear interactions in stellar interior of the symmetric static rela-

tivistic configurations are anisotropic. Ruderman (1972) shows that this is possible when the energy density reaches high values. In the recent past a number of authors have investigated solutions to the Einstein field equations with anisotropic matter, in particular we have Bowers and Liang (1974), Dev and Gleiser (2002, 2003), Herrera *et al* (1979), Herrera and Santos (1995), Heintzmann and Hillebrandt (1975), Maharaj and Maartens (1989) and Mak and Harko (2002, 2003). The presence of the electromagnetic field also affects the physical features of a stellar model. Some recent studies involving a nonzero electric field are given by Bonnor (1965), Picanço and Malheiro (2007), Picanço *et al* (2004), Ray *et al* (2003), Hansraj and Maharaj (2006), Thirukkanesh and Maharaj (2008), Mafa Takisa and Maharaj (2013a, 2013b), Kileba Matondo and Maharaj (2013), Maurya and Gupta (2014) and Gupta *et al* (2011).

The understanding of the behaviour of compact bodies in relativistic astrophysics comes under exact solutions to the Einstein-Maxwell system of equations. These exact solutions result from some assumption on the spacetime and matter. The existence of a symmetry in the spacetime manifolds represents a good approach to finding a solution. An example of a symmetry is a conformal Killing vector. Conformal motions in static spherically symmetric spastimes have been a major work of Maartens *et al* (1995, 1996). The work of Tupper *et al* (2012) gives a complete classification of all spherically symmetric spacetimes in terms of conformal motions through decomposition into 2+2 reducible spacetimes. If a conformal Killing vector exists then some conditions are imposed on the gravitational potentials which gives an opportunity to solve the Einstein field equations. Herrera *et al* (1984) were the first to show that conformal symmetry presents a major interest in relativistic astrophysics to model dense stars.

In this thesis, we intend to find new classes of exact solutions to the Einstein and Einstein-Maxwell field equations which are physically reasonable in different approaches. We impose first a linear equation of state on the matter distribution. Secondly, from the Finch and Skea ansatz, a new family of exact solutions with

a barotropic equation of state can be generated. Thirdly, the explicit relationship between the gravitational potentials in the presence of conformal symmetry simplifies the Einstein field equations to be solved. In order to achieve this objective, this thesis is organised as follows:

- Chapter 1: Introduction.
- Chapter 2: In this chapter, we generate new exact solutions to the Einstein-Maxwell field equations which are relevant in the description of highly compact stellar objects. The relativistic star is charged and anisotropic with a quark equation of state. Exact solutions of the field equations are found in terms of elementary functions. Here, we regain earlier quark models with uncharged and charged matter distributions. A physical analysis shows that the matter distributions are well behaved and regular throughout the stellar structure. A range of stellar masses are generated for particular parameter values in the electric field. In particular the observed mass for a binary pulsar is regained.
- Chapter 3: Several new families of exact solution to the Einstein-Maxwell system of differential equations are generated for anisotropic charged matter. We consider the Finch and Skea spacetime geometry which satisfies all criteria for physical acceptability. The exact solutions is expressed in terms of elementary functions, Bessel functions and modified Bessel functions. When a parameter is restricted to be an integer then the special functions reduce to simple elementary functions. The uncharged model of Finch and Skea (1989) and the charged model of Hansraj and Maharaj (2006) are regained as special cases. The solutions obtained admit a barotropic equation of state. A graphical analysis indicates that the matter and electric quantities are well behaved.
- Chapter 4: In this chapter we use a particular solution of the generalised Finch and Skea model of Maharaj *et al* (2016) to study the mass and radius. We generate masses and radii for three cases: charged anisotropic, charged isotropic and uncharged isotropic distributions for observed compact objects. Physical

features of the model show the non-negligible influence of charge and anisotropy on the mass and radius within the stellar objects. The model parameters values are fixed based on physical requirements and stability conditions of compact stars. We show that the model is consistent with the observed masses of selected pulsars PSR J1614-2230, PSR J1903+0327, 4U 1820-30, Cen X-3, EXO 1785-248 and LMC X-4. The investigation reveals that the Finch and Skea geometry is physically relevant for the study of observed compact stars.

- Chapter 5: Here, we study exact models for anisotropic gravitating stars with conformal symmetry. The gravitational potentials are related explicitly by the conformal vector. We use this relationship between the metric potentials to generate new classes of exact solutions to the field equations. We identify a particular model to study the physical features and demonstrate that the model is well behaved. In particular the criteria for stability are satisfied. We regain masses, radii and surface redshifts for the compact objects PSR J1614-2230 and SAX J1808.4-3658.

- Chapter 6: We investigate the behaviour of a charged isotropic model with conformal symmetry. The relationship between the gravitational potentials arising from the conformal condition is used to generate a new class of exact solutions to the Einstein-Maxwell equations. A specific form of the electric field intensity and the metric potential is required to avoid a singularity at the centre. We can find simple elementary functions for the matter variables and the potentials with relativistic profiles. The causality conditions, stability conditions and energy conditions are satisfied. Masses, radii, cental densities and surface redshifts are generated, and the values are consistent with the compact stars 4U 1538-52 and PSR J1614-2230.

- Chapter 7: Conclusion.

Chapter 2

New charged anisotropic compact stars

2.1 Introduction

To obtain an understanding of the gravitational dynamics of a general relativistic star it is necessary to solve the Einstein-Maxwell equations. The matter distribution may be anisotropic in the presence of an electromagnetic field. On physical grounds we should include an equation of state relating the radial pressure to the energy density in a barotropic distribution. In this way we can model relativistic compact objects including dark energy stars, quark stars, gravastars, neutron stars and ultradense matter. For some recent models investigating the properties of charged anisotropic stars see the treatments of Feroze and Siddiqui (2014), Thirukkanesh and Ragel (2014), Maurya and Gupta (2014), Maurya *et al* (2015), Pandya *et al* (2015), Bhar *et al* (2015) and Murad (2016).

These exact solutions of the Einstein-Maxwell system are essential for describing astrophysical processes. Our study in this chapter is related to describing the stellar interior with a spherically symmetric anisotropic charged matter distribution. We impose a quark equation of state on the model. The physical features of quark

stars have been recently investigated by Malaver (2014), Mafa Takisa *et al* (2014b), Sunzu *et al* (2014) and Paul *et al* (2011). The investigations of Sharma *et al* (2001) show that the redshift, luminosity and maximum mass of a compact body are affected by the electric field and anisotropy. The works of Mak and Harko (2004), Komathiraj and Maharaj (2007a, 2007b) and Maharaj and Komathiraj (2007) show the significant role of the electromagnetic field in describing the gravitational behaviour of compact stars composed of quark matter. The role of anisotropy has been highlighted by Dev and Gleiser (2002, 2003). By making a specific choice of the electric field, Hansraj and Maharaj (2006) obtained solutions with isotropic pressures to the Einstein-Maxwell system. These solutions satisfy a barotropic equation of state and contain the Finch and Skea (1989) model. Charged anisotropic models with a linear equation of state were found by Thirukkanesh and Maharaj (2008). Mafa Takisa and Maharaj (2013a) utilised a linear equation of state to generate regular solutions of anisotropic spherically symmetric charged distributions which can be related to observed astronomical objects.

The main objective of this chapter is to generate a new class of exact solutions to the Einstein-Maxwell system of equations that is physically acceptable. We generalise the solution to the Einstein-Maxwell system, with no singularity in the charge distribution at the centre, obtained by Mafa Takisa and Maharaj (2013a) by generating a new class of exact solutions. The physical features such as the gravitational potentials, electric field intensity, charge distribution and matter distribution are well behaved. These new exact solutions describe a charged relativistic sphere with anisotropic pressures and a linear quark equation of state. In §2.2, we give the expression of the line element modelling the interior of relativistic star which allows us to rewrite the Einstein-Maxwell equations in terms of new variables. In §2.3, we present the basic assumptions for the physical models. We make a choice for one of the gravitational potentials and the electric field intensity which allow us to integrate the field equations. Three new classes of exact solutions to the Einstein-Maxwell field equations, in terms of elementary functions, are determined in §2.3.

The first class is unphysical and the other two classes satisfy the physical criteria. In §2.4, we demonstrate how our exact solutions regain the uncharged anisotropic solution found by Thirukkanesh and Maharaj (2008), and the charged anisotropic solution found by Mafa Takisa and Maharaj (2013a). In §2.5, we study the physical features of our models and present graphs for the energy density, radial pressure, electric field intensity, charge density and mass. The graphs indicate that the matter and electromagnetic quantities are well behaved. In §2.6, we generate stellar masses and show that our charged general relativistic solutions can be related to observed astronomical objects.

2.2 Field equations

The line element for static spherically symmetric spacetime, modelling the interior of the relativistic star, has the form

$$ds^2 = -e^{2\nu(r)}dt^2 + e^{2\lambda(r)}dr^2 + r^2(d\theta^2 + \sin^2\theta d\phi^2). \tag{2.1}$$

The functions $\lambda(r)$ and $\nu(r)$ correspond to the gravitational potentials. The energy momentum tensor $\mathbf{T}$ has the general form

$$T_{ab} = \text{diag}(-\rho - \frac{1}{2}E^2,\ p_r - \frac{1}{2}E^2,\ p_t + \frac{1}{2}E^2,\ p_t + \frac{1}{2}E^2), \tag{2.2}$$

where the quantities ρ, p_r, p_t and E are respectively, energy density, radial pressure, tangential pressure and electric field intensity. Then the Einstein-Maxwell system of equations can be written in the form

$$\frac{1}{r^2}\left[r(1-e^{-2\lambda})\right]' = \rho + \frac{1}{2}E^2, \tag{2.3a}$$

$$-\frac{1}{r^2}(1-e^{-2\lambda}) + \frac{2\nu'}{r}e^{-2\lambda} = p_r - \frac{1}{2}E^2, \tag{2.3b}$$

$$e^{-2\lambda}\left(\nu'' + \nu'^2 + \frac{\nu'}{r} - \nu'\lambda' - \frac{\lambda'}{r}\right) = p_t + \frac{1}{2}E^2, \tag{2.3c}$$

$$\frac{1}{r^2}e^{-\lambda}(r^2E)' = \sigma, \tag{2.3d}$$

in terms of coordinate r. An equivalent form of the Einstein-Maxwell field equations is obtained if we introduce the transformation

$$x = Cr^2, \quad Z(x) = e^{-2\lambda(r)}, \quad A^2y^2(x) = e^{2\nu(r)}, \tag{2.4}$$

where A and C are constants. This transformation was first used by Durgapal and Bannerji (1983). The line element (2.1) then has the form

$$ds^2 = -A^2y^2(x)dt^2 + \frac{1}{4Cx Z(x)}dx^2 + \frac{x}{C}\left(d\theta^2 + \sin^2\theta d\phi^2\right), \tag{2.5}$$

in terms of the variable x. The field equations (2.3) become

$$\frac{\rho}{C} = -2\dot{Z} + \frac{1-Z}{x} - \frac{E^2}{2C}, \tag{2.6a}$$

$$\frac{p_r}{C} = 4Z\frac{\dot{y}}{y} + \frac{Z-1}{x} + \frac{E^2}{2C}, \tag{2.6b}$$

$$\frac{p_t}{C} = 4xZ\frac{\ddot{y}}{y} + (4Z + 2x\dot{Z})\frac{\dot{y}}{y} + \dot{Z} - \frac{E^2}{2C}, \tag{2.6c}$$

$$\frac{\sigma^2}{C} = \frac{4Z}{x}(x\dot{E} + E)^2. \tag{2.6d}$$

The mass of a gravitating object, within the stellar radius, is important for comparison with observations. The mass contained within a radius x of the sphere is given by the expression

$$M(x) = \frac{1}{4C^{3/2}}\int_0^x \sqrt{\omega}\rho(\omega)\, d\omega. \tag{2.7}$$

This expression is sometimes called the mass function. For a physically realistic relativistic star, we expect that the matter distribution should obey a barotropic equation of state of the form $p_r = p_r(\rho)$. For a charged anisotropic matter distribution we consider the linear relationship

$$p_r = \alpha\rho - \beta, \tag{2.8}$$

where α and β are constants. The constant $\beta = \alpha\rho_s$ where ρ_s is the surface density of the star.

Then the Einstein-Maxwell equations governing the gravitational interactions of a charged anisotropic body, with a linear equation of state, can be written as

$$\frac{\rho}{C} = \frac{1-Z}{x} - 2\dot{Z} - \frac{E^2}{2C}, \tag{2.9a}$$

$$p_r = \alpha\rho - \beta, \tag{2.9b}$$

$$p_t = p_r + \Delta, \tag{2.9c}$$

$$\Delta = 4CxZ\frac{\ddot{y}}{y} + 2C\left(x\dot{Z} + \frac{4Z}{1+\alpha}\right)\frac{\dot{y}}{y} + \left(\frac{1+5\alpha}{1+\alpha}\right)C\dot{Z} - \frac{C(1-Z)}{x} + \frac{2\beta}{1+\alpha}, \tag{2.9d}$$

$$\frac{E^2}{2C} = \frac{1-Z}{x} - \left(\frac{1}{1+\alpha}\right)\left(2\alpha\dot{Z} + 4Z\frac{\dot{y}}{y} + \frac{\beta}{C}\right), \tag{2.9e}$$

$$\frac{\sigma^2}{C} = \frac{4Z}{x}(x\dot{E} + E)^2. \tag{2.9f}$$

The quantity $\Delta = p_t - p_r$ is defined as the measure of anisotropy and vanishes for isotropic pressures. The system of equations (2.9) is nonlinear consisting of six equations with eight independent variables y, Z, ρ, p_r, p_t, E, σ and Δ. We need to select two of the variables involved in the integration process to solve the system (2.9).

2.3 Physical models

To generate a new class of solutions to the Einstein-Maxwell system requires a choice for one of the gravitational potentials and the electric field intensity. In our approach we make the particular choice

$$Z = \frac{1 + (a-b)\,x}{1+ax}, \tag{2.10a}$$

$$\frac{E^2}{C} = \frac{la^3x^3 + sa^2x^2 + k(3+ax)}{(1+ax)^2}, \tag{2.10b}$$

where a, b, s, k, l are real constants. It is important to note that we keep the same form for the gravitational potential first used by Thirukkanesh and Maharaj (2008). The function Z is finite at the centre $x = 0$ and regular in the interior. The function for the electrical field E is a generalised form that contains previous studies as special cases. The function E is finite at the centre and well behaved in the stellar interior. When $l = s = 0$ we regain the models of Thirukkanesh and Maharaj (2008). If $l = 0$ then the exact models of Mafa Takisa and Maharaj (2013a) are obtained. For

particular choices of the parameters a and b we regain other earlier models: charged Hansraj and Maharaj (2006) stars ($a = b = 1$), charged Maharaj and Komathiraj (2007) stars ($a = 1$), uncharged Finch and Skea (1989) stars ($a = b = 1$), uncharged Durgapal and Bannerji (1983) neutron stars ($a = 1, b = 3/2$), and uncharged Tikekar (1990) superdense stars ($a = 7, b = 8$). The function E is finite at the centre and well behaved in the stellar interior.

From (2.10a), (2.10b) and (2.9e) we obtain the first order equation

$$\begin{aligned}\frac{\dot{y}}{y} &= \frac{4\alpha b-(1+\alpha)(la^3x^3+sa^2x^2+k(3+ax))}{8(1+ax)\left[1+(a-b)x\right]}\\ &\quad -\frac{\beta(1+ax)}{4C\left[1+(a-b)x\right]}+\frac{(1+\alpha)b}{4\left[1+(a-b)x\right]}.\end{aligned} \tag{2.11}$$

It is necessary to integrate (2.11) to complete the model of a charged gravitating sphere. It is convenient to categorise our solutions in terms of the constant b. We consider, in turn, the following three cases: $b = 0$, $b = a$, $b \neq a$.

2.3.1 The case $b = 0$

When $b = 0$, (2.11) assumes the simple form

$$\frac{\dot{y}}{y} = \frac{(1+\alpha)(la^3x^3+sa^2x^2+k(3+ax))}{-8\left(1+ax\right)^2}-\frac{\beta}{4C}. \tag{2.12}$$

This gives after integration the solution

$$y = D\left(1+ax\right)^{(-(3l+k-2s))(1+\alpha)/(8a)}\exp\left[F(x)\right], \tag{2.13}$$

where D is a constant of integration and

$$\begin{aligned}F(x) &= \frac{(1+\alpha)}{16(1+ax)}\left[4k-2asx(2+ax)+l(3+9ax+3a^2x^2-a^3x^3)\right]\\ &\quad -\frac{\beta x}{4C}.\end{aligned} \tag{2.14}$$

The energy density $\rho = -\frac{E^2}{2}$ generated by the potential y in (2.13) is negative and the model is unphysical.

2.3.2 The case $b = a$

When $b = a$, the differential equation (2.11) yields the form

$$\begin{aligned}\frac{\dot{y}}{y} &= \frac{4\alpha a-(1+\alpha)(la^3x^3+sa^2x^2+k(3+ax))}{8(1+ax)}\\ &\quad -\frac{\beta(1+ax)}{4C}+\frac{(1+\alpha)a}{4}.\end{aligned} \tag{2.15}$$

This equation has solution

$$y = D\,(1+ax)^{(4\alpha a-(s+2k)(1+\alpha)+l(1+\alpha))/(8a)}\exp\left[G(x)\right], \tag{2.16}$$

where D is a constant of integration and the function $G(x)$ is given by

$$\begin{aligned}G(x) &= -\frac{x^3}{16C}\left[2C(s-k)(1+\alpha)-a(C(sx-4)(1+\alpha)+2\beta x)-4\beta\right]\\ &\quad -\frac{l(1+\alpha)}{48ac}\left(11+6ax-3a^2x^2+2a^3x^3\right).\end{aligned} \tag{2.17}$$

Then the complete solution to the Einstein-Maxwell field equations (2.9) can be written as

$$e^{2\lambda} = 1+ax, \tag{2.18a}$$

$$e^{2\nu} = A^2D^2\,(1+ax)^{(4\alpha a-(s+2k)(1+\alpha)+l(1+\alpha))/(4a)}\exp\left[2G(x)\right], \tag{2.18b}$$

$$\frac{\rho}{C} = \frac{-la^3x^3-sa^2x^2+(2a-k)(3+ax)}{2(1+ax)^2}, \tag{2.18c}$$

$$p_r = \alpha\rho-\beta, \tag{2.18d}$$

$$p_t = p_r+\Delta, \tag{2.18e}$$

$$\begin{aligned}\Delta &= \frac{1}{16C(1+ax)^3}\left[C^2(k^2x(3+ax)^2(1+\alpha)^2+a^2x(a^4l^2x^6(1+\alpha)^2\right.\\ &\quad +2a^3lx^4(-2+sx)(1+\alpha)^2-4(-3+(8-9\alpha)\alpha+4sx(2+\alpha))\\ &\quad -4ax(2lx(5+3\alpha)-2(2+3\alpha(1+\alpha))+sx(6+\alpha(5+3\alpha)))\\ &\quad +a^2x^2((-2+sx)^2(1+\alpha)^2-4lx(8+\alpha(7+3\alpha))))\\ &\quad +2k(-24+ax(a^3lx^4(1+\alpha)^2+a^2x^2(-2+3lx+sx)(1+\alpha)^2\\ &\quad -2(12+\alpha(5+9\alpha))+ax(3sx(1+\alpha)^2-2(7+9\alpha+6\alpha^2)))))\\ &\quad \left.+4Cx(1+ax)^2(3k(1+\alpha)+a^3lx^3(1+\alpha)\right.\end{aligned}$$

$$+a^2x(-2+sx)(1+\alpha)+a(-4-6\alpha+kx(1+\alpha)))\beta$$
$$+4x(1+ax)^4\beta^2\big], \tag{2.18f}$$
$$\frac{E^2}{C} = \frac{la^3x^3+sa^2x^2+k(3+ax)}{(1+ax)^2}, \tag{2.18g}$$
$$\frac{\sigma^2}{C} = \frac{C\left[k(6+ax(3+ax))+a^2x^2(2s(2+ax)+alx(5+3ax))\right]^2}{x(k(3+ax)+a^2x^2(s+alx))(1+ax)^5}. \tag{2.18h}$$

The energy density ρ generated by the potential y in (2.16) is nonnegative. The solution (2.18) is an exact solution of the Einstein-Maxwell system when $a=b$.

We can compute the mass function explicitly from (2.7). In this case we can write the mass function in terms of x by

$$\begin{aligned} M(x) = \frac{1}{8C^{3/2}}\Bigg[&\frac{l\left(-6a^3x^3+14a^2x^2-70ax-105\right)x^{1/2}}{15a(1+ax)} \\ &-\frac{5(6a(k-2a)x)x^{1/2}}{15a(1+ax)}-\frac{s(-15-10ax+2a^2x^2)x^{1/2}}{15a(1+ax)} \\ &+\left(\frac{7l-5s}{a^{3/2}}\right)\arctan(\sqrt{ax})\Bigg]. \end{aligned} \tag{2.19}$$

We can regain the mass functions of Thirukkanesh and Maharaj (2008) ($l=s=0$) and Mafa Takisa and Maharaj (2013a) ($l=0$) from (2.20) as particular cases in the presence of charge. Note that their models necessarily contain an inverse tangent function. In our model when

$$l=\frac{5}{7}s, \tag{2.20}$$

the inverse tangent function is not present in the expression for $M(x)$.

2.3.3 The case $b \neq a$

The most interesting case is when $b \neq a$. When $b \neq a$, the solution of (2.11) can be written in the form

$$y = D(1+ax)^m\left[1+(a-b)x\right]^n\exp\left[F(x)\right], \tag{2.21}$$

where D is a constant of integration. The constants m, n and the function $F(x)$ are given by

$$n = \frac{1}{8Cb(a-b)^2}\left[a^2C((s+2K)(1+\alpha)-4b\alpha)\right.$$

$$
\begin{aligned}
&+abC(2b(1+5\alpha)-5k(1+\alpha))\\
&+b^2(3Ck(1+\alpha)-2bC(1+3x)+2\beta)\big]-\frac{a^3l(1+\alpha)}{8b},\\
m &= \frac{4b\alpha-(s+2k)(1+\alpha)+l(1+\alpha)}{8b},\\
F(x) &= -\frac{ax}{16C(a-b)^2}\left[(2C(1+\alpha)(s(a-b)+l(b-2a)))\right.\\
&\left.+(4(a-b)\beta+aCl(1+\alpha)(a-b)x)\right].
\end{aligned}
$$

Then we can write the exact solution for the system (2.9) as

$$e^{2\lambda} = \frac{1+ax}{1+(a-b)x}, \tag{2.22a}$$

$$
\begin{aligned}
e^{2\nu} &= A^2D^2[1+(a-b)x]^{2n}(1+ax)^{2m}\\
&\times\exp\left[-\frac{ax(2C(1+\alpha)(s(a-b)+l(b-2a)))}{8C(a-b)^2}\right.\\
&\left.-\frac{ax(4(a-b)\beta+aCl(1+\alpha)(a-b)x)}{8C(a-b)^2}\right],
\end{aligned}
\tag{2.22b}
$$

$$\frac{\rho}{C} = -\frac{(k-2b)(3+ax)+a^2x^2(s+alx)}{2(1+ax)^2}, \tag{2.22c}$$

$$p_r = \alpha\rho-\beta, \tag{2.22d}$$

$$p_t = p_r+\Delta, \tag{2.22e}$$

$$
\begin{aligned}
\Delta &= \frac{Ck}{8(1+ax)^3(1+(a-b)x)}\left[-24+x(a^4lx^4(1+\alpha)^2\right.\\
&-6b(2+\alpha)(-1+3\alpha)x+a^3x^3(4(-1+\alpha)+(3l+s)(1+\alpha)^2x)\\
&+a^2x^2(3sx(1+\alpha)^2+8(-2+3\alpha)-2bx(-1+\alpha(4+\alpha)))\\
&\left.+2ax(2(-9+5\alpha)+bx(1-3\alpha(7+2\alpha)))\right]\\
&+\frac{Cx}{16(1+ax)^3(1+(a-b)x)}\\
&\times\left[4b^2(3+ax(4+ax)+12\alpha+6\alpha ax(5+ax)+(3+ax)^2\alpha^2)\right.\\
&+a^4s^2x^4(1+\alpha)^2-8a^3lx^2(5+3\alpha)+a^4lx^3(a^2lx^3(1+\alpha)^2\\
&-32(2+\alpha)-8ax(3+\alpha))+2a^2sx(-8(2+\alpha)+ax(-8(3+\alpha)\\
&+ax(-8+alx^2(1+\alpha)^2)))-4ab(20\alpha+24\alpha ax)\\
&-4a^2bsx^2(-6+\alpha+3\alpha^2+ax(-1+\alpha)(3+\alpha))\\
&\left.-4a^3bx^2(4\alpha+lx(-8+\alpha(-1+3\alpha)+ax(-5+\alpha^2)))\right]\\
&+\frac{\beta x}{4(1+ax)(1+(a-b)x)}\left[(1+\alpha)(k(3+ax)+a^2x^2(s+alx))\right.
\end{aligned}
$$

$$-2b(2+3\alpha+ax(1+\alpha))] + \frac{x(1+ax)\beta^2}{C(1+(a-b)x)} + \frac{k^2x(3+ax)^2(1+\alpha)^2}{16(1+ax)^3(1+(a-b)x)}, \tag{2.22f}$$

$$\frac{E^2}{C} = \frac{la^3x^3+sa^2x^2+k(3+ax)}{(1+ax)^2}, \tag{2.22g}$$

$$\frac{\sigma^2}{C} = \frac{(1+(a-b)x)}{x(1+ax)^5(k(3+ax)+a^2x^2(s+alx))} \times \left[k(6+ax(3+ax))+a^2x^2(2s(2+ax)+alx(5+3ax))\right]^2. \tag{2.22h}$$

As for the case $a = b$, the energy density ρ generated from (2.21) is nonnegative. This exact solution of the Einstein-Maxwell equations is similar in structure to that when $a = b$ in §2.3.2. However note that (2.22) is a new exact solution written completely in terms of elementary functions.

For this solution the mass function is given by

$$M(x) = \frac{1}{8C^{3/2}}\left[\frac{l\left(-6a^3x^3+14a^2x^2-70ax-105\right)x^{1/2}}{15a(1+ax)} - \frac{5(6a(k-2b)x)x^{1/2}}{15a(1+ax)} - \frac{s(-15-10ax+2a^2x^2)x^{1/2}}{15a(1+ax)} + \left(\frac{7l-5s}{a^{3/2}}\right)\arctan(\sqrt{ax})\right]. \tag{2.23}$$

This expression contains previously studied mass functions in the presence of charge. As in the previous case note that when

$$l = \frac{5}{7}s, \tag{2.24}$$

the inverse tangent function is absent in the expression for $M(x)$.

2.4 Known solutions

When we set $s = l = 0$ in (2.10b), then the gravitational potentials become

$$e^{2\lambda} = \frac{1+ax}{1+(a-b)x}, \tag{2.25a}$$

$$e^{2\nu} = A^2D^2[1+(a-b)x]^{2n}(1+ax)^{2m}\exp\left[-\frac{\alpha\beta x}{2C(a-b)}\right], \tag{2.25b}$$

where the constants m and n are given by

$$\begin{aligned} m &= \frac{4\alpha b-2k(1+\alpha)}{8b}, \\ n &= \frac{1}{8bC(a-b)^2}\left[b^2\left(3kC(1+\alpha)-2bC(1+3\alpha)+2\beta\right)\right. \\ &\quad \left.-abC\left(5k(1+\alpha)-2b(1+5\alpha)\right)+a^2C\left(2k(1+\alpha)-4\alpha b\right)\right]. \end{aligned}$$

This case corresponds to a charged anisotropic sphere with a linear equation of state. This particular model was first found by Thirukkanesh and Maharaj (2008).

If we set $l=0$ in (2.10b) then the term la^3x^3 in the electric field is no longer present. The model's metric potentials then become

$$e^{2\lambda} = \frac{1+ax}{1+(a-b)x}, \tag{2.26a}$$

$$e^{2\nu} = A^2D^2[1+(a-b)x]^{2n}(1+ax)^{2m}\exp\left[-\frac{ax[Cs(1+\alpha)+2\beta]}{4C(a-b)}\right], \tag{2.26b}$$

where the constants m and n are equivalent to

$$\begin{aligned} m &= \frac{4\alpha b-(s+2k)(1+\alpha)}{8b}, \\ n &= \frac{1}{8bC(a-b)^2}\left[b^2\left(3kC(1+\alpha)-2bC(1+3\alpha)+2\beta\right)\right. \\ &\quad \left.-abC\left(5k(1+\alpha)-2b(1+5\alpha)\right)+a^2C\left((s+2k)(1+\alpha)-4\alpha b\right)\right]. \end{aligned}$$

This case describes a model of a charged anisotropic sphere with a barotropic linear equation of state. The charged solution (2.26) was first found by Mafa Takisa and Maharaj (2013a). Our new class of solutions is therefore a generalisation of previously known models. It arises because of the additional term with the constant l added in the electric field intensity.

2.5 Physical features

In this chapter, we have presented a new general model of a relativistic astrophysical star, and integrated a differential equation of first order from the Maxwell-Einstein system of field equations. We can show that this solution is physically reasonable.

We utilise the exact solution obtained in §2.3.3 when $a \neq b$ for a graphical analysis. The software package Mathematica (Wolfram 2010) was used to generate plots for the matter variables. We made the choices $a = 2$, $b = 2.5$, $\alpha = 0.33$, $\beta = 0.198$, $C = 1$, $l = 1.5$, $s = 2.5$, $k = 0$ for the various parameters. We have made choices of the parameters similar to that in the analysis of Mafa Takisa and Maharaj (2013a) so that we can be consistent with their analysis. We generated the following graphical plots: Fig. 2.1 shows that the energy density ρ is positive, finite and strictly decreasing; The radial pressure p_r in Fig. 2.2, expressed in terms of ρ in accordance with the equation of state follows a similar evolution as the density energy; In Fig. 2.3 we observe the electric field E initially decreases and then increases after reaching a minimum. The charge density σ is a regular and decreasing function in Fig. 2.4 and, in Fig. 2.5, the mass function M is continuous, finite and strictly increasing. In the graphs plotted the dashed line corresponds to the case $l = 0$, and the solid line corresponds to the case $l \neq 0$, $s \neq 0$. The overall profiles of the matter variables ρ, p_r, E, σ and M in our investigation are similar to those generated by Mafa Takisa and Maharaj (2013a) when $l = 0$. However in the presence of the additional term in the electric field, including the parameter $l \neq 0$, we observe that there is some change in the gradients of the respective profiles. The density ρ, radial pressure p_r and mass M, have lower values when $l \neq 0$. The electric field and charge density have higher values when $l \neq 0$. The effect of parameter l is consequently to enhance and strengthen the effect of the electromagnetic field in the relativistic star.

2.6 Stellar masses

In this section we generate stellar masses which are consistent with the results of Sharma and Maharaj (2007), Thirukkanesh and Maharaj (2008), and Mafa Takisa and Maharaj (2013a). Therefore the solutions found in this chapter may be applied to realistic stellar astronomical bodies. We use the transformation

$$\tilde{a} = aR^2, \quad \tilde{b} = bR^2, \quad \tilde{\beta} = \beta R^2,$$
$$\tilde{k} = kR^2, \quad \tilde{s} = sR^2, \quad \tilde{l} = lR^2. \tag{2.27}$$

This is the same transformation, intended to include the additional parameter l, that was defined by Mafa Takisa and Maharaj (2013a). When $l = 0$ in (2.27) we obtain previous results. With the transformation (2.27) and setting $C = 1$, we can write the energy density (2.22c) and the mass function (2.23) as

$$\rho = \frac{(2\tilde{b} - \tilde{k})(3 + \tilde{a}y) - \tilde{s}\tilde{a}^2y^2 - \tilde{l}\tilde{a}^3y^3}{2R^2(1 + \tilde{a}y)^2}, \tag{2.28a}$$

$$\begin{aligned} M &= \frac{\tilde{l}r(-6\tilde{a}^3y^3 + 14\tilde{a}^2y^2 - 70\tilde{a}y - 105)}{120\tilde{a}(1 + \tilde{a}y)} \\ &\quad + \frac{r^3(-3\tilde{k} + 6\tilde{b} + 5\tilde{s})}{12R^2(1 + \tilde{a}y)} + \frac{\tilde{s}r(15 - 2\tilde{a}^2y^2)}{24\tilde{a}(1 + \tilde{a}y)} \\ &\quad + \frac{R(7\tilde{l} - 5\tilde{s})}{8a^{3/2}} \arctan(\sqrt{\tilde{a}y}), \end{aligned} \tag{2.28b}$$

where $y = \frac{r^2}{R^2}$.

If we set $\tilde{l} = 0$, $\tilde{s} \neq 0$, $\tilde{k} \neq 0$, with $E \neq 0$, then (2.28) yields

$$\rho = \frac{(2\tilde{b} - \tilde{k})(3 + \tilde{a}y) - \tilde{s}\tilde{a}^2y^2}{2R^2(1 + \tilde{a}y)^2}, \tag{2.29a}$$

$$\begin{aligned} M &= \frac{r^3(-3\tilde{k} + 6\tilde{b} + 5\tilde{s})}{12R^2(1 + \tilde{a}y)} + \frac{\tilde{s}r(15 - 2\tilde{a}^2y^2)}{24\tilde{a}(1 + \tilde{a}y)} \\ &\quad - \frac{5\tilde{s}R}{8a^{3/2}} \arctan(\sqrt{\tilde{a}y}). \end{aligned} \tag{2.29b}$$

These expressions above are related to the solutions in §2.4 when $l = 0$, found by Mafa Takisa and Maharaj (2013a). If we set $\tilde{l} = 0$, $\tilde{s} = 0$, $\tilde{k} \neq 0$ with $E \neq 0$, we obtain

$$\rho = \frac{(2\tilde{b} - \tilde{k})(3 + \tilde{a}y)}{2R^2(1 + \tilde{a}y)^2}, \tag{2.30a}$$

$$M = \frac{r^3(2\tilde{b} - \tilde{k})}{4R^2(1 + \tilde{a}y)}, \tag{2.30b}$$

which is related to the solutions in §2.4 when $s = l = 0$ found by Thirukkanesh and Maharaj (2008). If we set $\tilde{l} = 0, \tilde{s} = 0, \tilde{k} = 0$ with $E = 0$, we obtain

$$\rho = \frac{\tilde{b}(3 + \tilde{a}y)}{R^2(1 + \tilde{a}y)^2}, \tag{2.31a}$$

$$M = \frac{\tilde{b}r^3}{2R^2(1 + \tilde{a}y)}, \tag{2.31b}$$

which are the solutions attributed to Sharma and Maharaj (2007).

We have produced a variety of stellar masses for particular choices of the parameters $\tilde{a}$ and $\tilde{b}$. These are presented in the following tables: Table 2.1 (Stellar masses with $l = 0, s = 0$), Table 2.2 (Stellar masses with $l = 0, s \neq 0$), Table 2.3 (Stellar masses with $l \neq 0, s \neq 0$) and Table 2.4 (Comparative masses). We have set $r = 7.07$ km and $R = 43.245$ km which are the values used by Dey*et al* (1998, 1999). For the electric field we have set $\tilde{k} = 37.403$, $\tilde{s} = 0.137$ and $\tilde{l} = 0.111$.

For $l = 0$, $s = 0$ and $k = 0$ our model reduces to an uncharged stellar body as that in Sharma and Maharaj (2007) in terms of the masses generated. When $l = 0$, $s = 0$ and $k \neq 0$, the masses obtained are similar to those found by Thirukkanesh and Maharaj (2008) for a charged relativistic star model. Note that for $l = 0$, $s \neq 0$ and $k \neq 0$ we find a charged relativistic stellar body and the stellar masses are consistent with the values generated by Mafa Takisa and Maharaj (2013a). To distinguish between the various cases in the presence of the electrical field we let $k \neq 0$, $l = 0$, $s = 0$ in Table 2.1, $k \neq 0$, $l = 0$, $s \neq 0$ in Table 2.2 and $k \neq 0$, $l \neq 0$, $s \neq 0$ in Table 2.3. We have also included the case for $k = 0$, in all tables, so that we can compare with uncharged masses. In Table 2.4 we gather all results and provide a comparative table. It is interesting to observe the effect of the electric field on the masses generated. The introduction of the new parameter l does not appear to appreciably change the mass for the parameter values chosen; a different set of parameters can produce a different profile for the mass. In particular observe that the parameter values $\tilde{b} = 54.34$ and $\tilde{a} = 53.340$ correspond to the analysis of Dey *et al.* (1998, 1999) for an equation of state with strange matter. The values obtained are consistent with results of observed masses for the X-ray binary pulsar

SAX J1808.4-3658. Consequently our new charged general relativistic solutions of the Einstein-Maxwell system are of astrophysical importance.

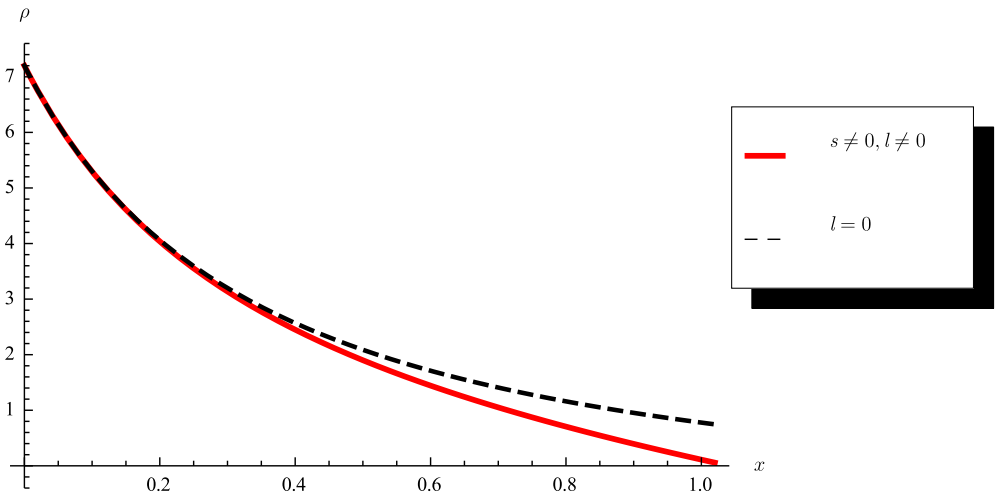

Figure 2.1 – Energy density.

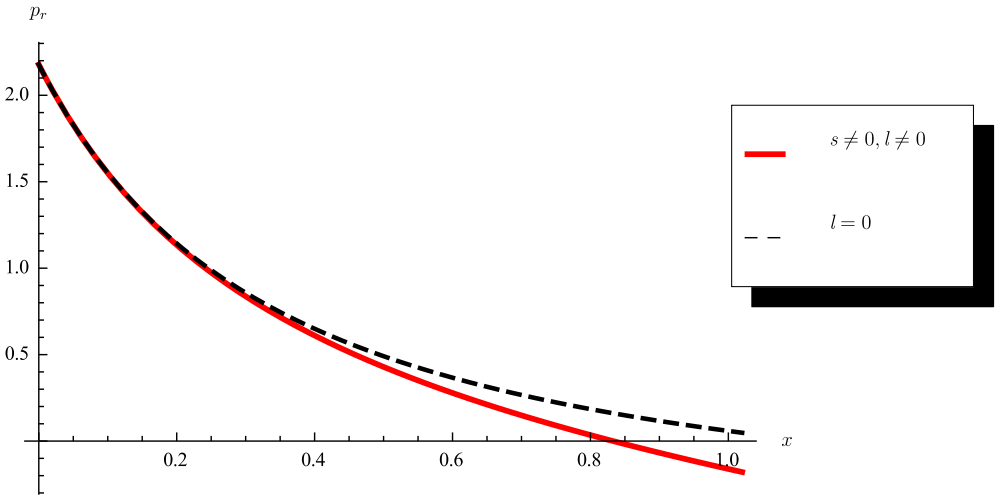

Figure 2.2 – Radial pressure.

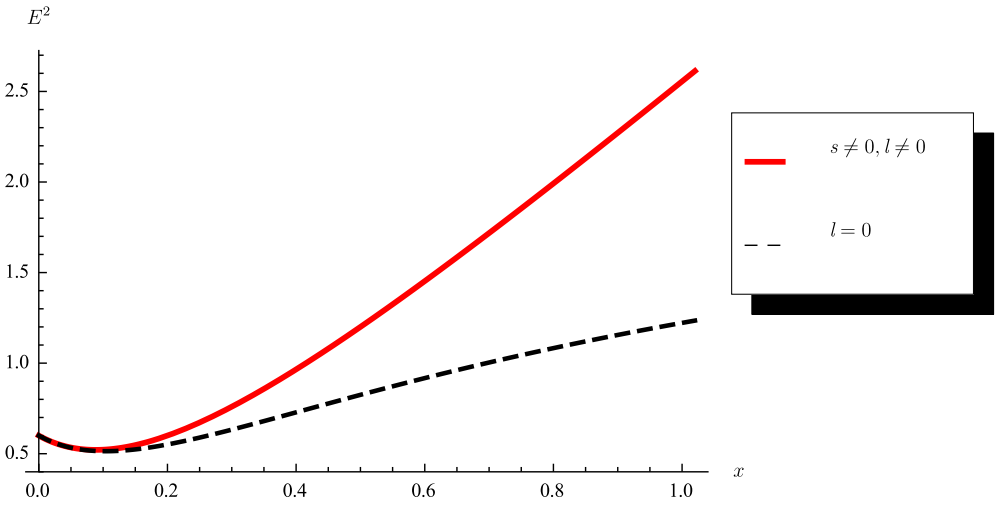

Figure 2.3 – Electric field intensity.

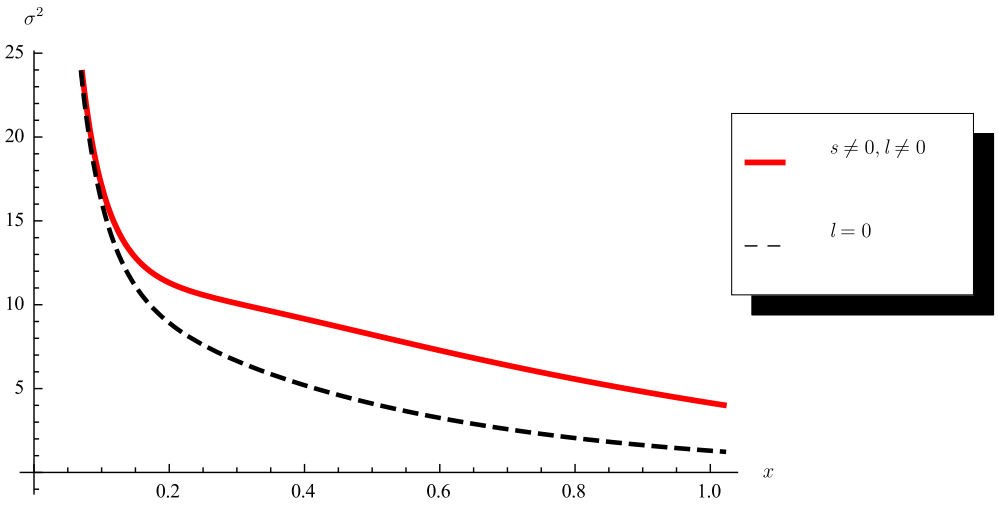

Figure 2.4 – Charge density.

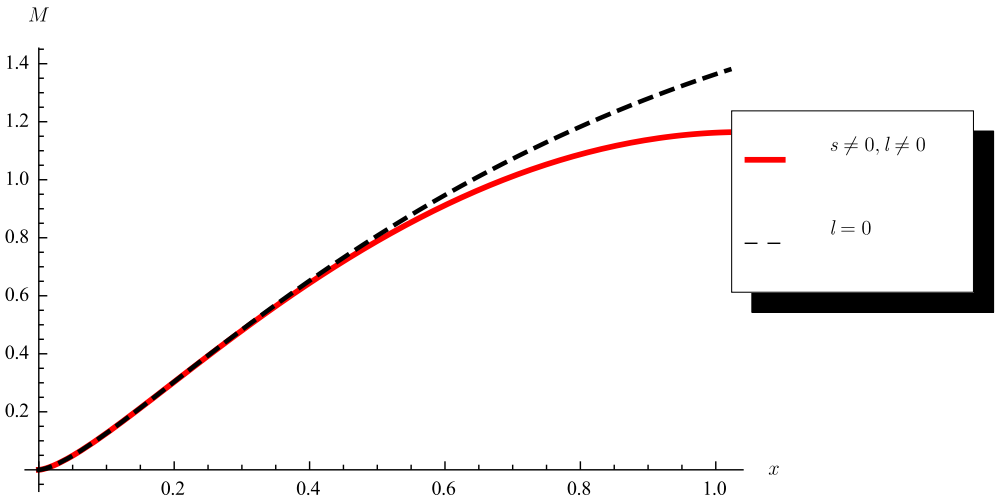

Figure 2.5 – Mass function.

Table 2.1 – Stellar masses with $l = 0, s = 0$

$\tilde{b}$	$\tilde{a}$	$M(M_{\odot})$ $k = s = l = 0$ $E = 0$	$M(M_{\odot})$ $l = 0, s = 0$ $E \neq 0$
30	23.681	1.175	0.4426
40	36.346	1.298	0.6911
50	48.307	1.396	0.8738
54.34	53.340	1.434	0.9399
60	59.788	1.478	1.0169
70	70.920	1.547	1.1333
80	81.786	1.607	1.2308
90	92.442	1.659	1.3141
100	102.929	1.706	1.3864

Table 2.2 – Stellar masses with $l = 0, s \neq 0$

$\tilde{b}$	$\tilde{a}$	$M(M_{\odot})$ $k = s = l = 0$ $E = 0$	$M(M_{\odot})$ $l = 0, s \neq 0$ $E \neq 0$
30	23.681	1.175	0.4425
40	36.346	1.298	0.6909
50	48.307	1.396	0.8736
54.34	53.340	1.434	0.9396
60	59.788	1.478	1.0165
70	70.920	1.547	1.1329
80	81.786	1.607	1.2303
90	92.442	1.659	1.3136
100	102.929	1.706	1.3860

Table 2.3 – Stellar masses with $l \neq 0, s \neq 0$

$\tilde{b}$	$\tilde{a}$	$M(M_{\odot})$ $k = s = l = 0$ $E = 0$	$M(M_{\odot})$ $l \neq 0, s \neq 0$ $E \neq 0$
30	23.681	1.176	0.4424
40	36.346	1.298	0.6907
50	48.307	1.396	0.8733
54.34	53.340	1.434	0.9393
60	59.788	1.478	1.0162
70	70.920	1.547	1.1324
80	81.786	1.607	1.2297
90	92.442	1.659	1.3129
100	102.929	1.706	1.3850

Table 2.4 – Comparative masses

$\tilde{b}$	$\tilde{a}$	$M(M_\odot)$ $k=s=l=0$ $E=0$	$M(M_\odot)$ $l=0, s=0$ $E\neq 0$	$M(M_\odot)$ $l=0, s\neq 0$ $E\neq 0$	$M(M_\odot)$ $(l\neq 0, s\neq 0)$ $E\neq 0$
30	23.681	1.175	0.4426	0.4425	0.4424
40	36.346	1.298	0.6911	0.6909	0.6907
50	48.307	1.396	0.8738	0.8736	0.8733
54.34	53.340	1.434	0.9399	0.9396	0.9393
60	59.788	1.478	1.0169	1.0165	1.0162
70	70.920	1.547	1.1333	1.1329	1.1324
80	81.786	1.607	1.2308	1.2303	1.2297
90	92.442	1.659	1.3141	1.3136	1.3129
100	102.929	1.706	1.3864	1.3860	1.3850

Chapter 3

Family of Finch and Skea relativistic stars

3.1 Introduction

The Einstein-Maxwell system of equations has generated much interest recently. Exact solutions may be used to describe the dynamics of charged anisotropic matter in a relativistic stellar setting. The modelling of highly compact objects such as dark energy stars, gravastars, ultradense stars and neutron stars then becomes possible in general relativity. Stars with anisotropic pressures and an electric field have been studied by Maurya and Gupta (2014), Maurya *et al* (2015), Pandya *et al* (2015), Bhar *et al* (2015) , Fatema and Murad (2013), Murad and Fatema (2013) and Murad (2016). Solutions with an equation of state may be related to observed astronomical objects as shown by Maharaj and Mafa Takisa (2012), Mafa Takisa *et al* (2014a, 2014b) and Sunzu *et al* (2014a, 2014b).

In spite of numerous exact solutions that have been found with a static spherically symmetric field only a few families of models are known which satisfy all the criteria for a physically acceptable relativistic star. An ansatz that does lead to a physically valid model is that of Finch and Skea (1989) with uncharged matter. Charged

Finch-Skea stars were found by Hansraj and Maharaj (2006); these models are given in terms of Bessel functions and obey a barotropic equation of state. Tikekar and Jotania (2007) found a two parameter family of solutions describing strange stars and other compact distributions of matter in equilibrium. Stars with a quadratic equation of state with the Finch-Skea geometry were analysed by Sharma and Ratanpal (2013). This category of stars was extended by Pandya *et al* (2015) for a generalized form of the gravitational potential. Kalam *et al* (2014) proposed quintessence stars with both dark energy and anisotropic pressures. Strange stars admitting a Chaplygin equation of state were investigated by Bhar (2015). The Finch and Skea (1989) geometry has been studied in matter distributions with lower and higher dimensions. Banerjee *et al* (2013) produced a class of interior solutions, corresponding to the BTZ exterior spacetime (Banados *et al* 1992), in $2+1$ dimensions. Bhar *et al* (2015) also produced anisotropic stars in $2+1$ dimensions and a quark equation of state. In higher dimensions the Finch-Skea metrics, and generalisations, also arise as shown by Patel *et al* (1997) and Chilambwe and Hansraj (2015). It is interesting to observe that the Finch-Skea spacetimes also arise in the 5-dimensional Einstein-Gauss-Bonnet modified theory of gravity in Hansraj *et al* (2015). This suggests that the Finch-Skea geometry may play an important role in more general Lovelock polynomials with a Lagrangian containing higher order terms.

The above references highlight the importance of the Finch and Skea (1989) potentials in many different physical applications. We therefore perform a systematic study of the Einstein-Maxwell equations with the Finch-Skea geometry in the presence of anisotropy and charge as it satisfies all physical requirements for a general relativistic stellar configuration and is widely used in the modelling process. Hansraj and Maharaj (2006) found the charged analogue of the Finch-Skea star. In this chapter we extend the Hansraj and Maharaj approach by adding anisotropy to the field equations. We generate the master gravitational equation in §3.2 which is obtained with the help of the Einstein-Maxwell system. We make a particular choice for one of the gravitational potentials, the electric field intensity and the anisotropic

term. Three classes of solution are possible depending on the quantity $a^2-\alpha$. In §3.3 we treat the case where $a^2-\alpha=0$. In §3.4 we consider the case $a^2-\alpha>0$ and we set $a=-1,1,3$. For these values of a we find new classes of exact solution to the Einstein-Maxwell system in terms of elementary functions. In §3.5 our study concerns the case $a^2-\alpha<0$. As in the previous section we make the choices $a=-1,1,3$ and new classes of exact solutions to the Einstein-Maxwell system are obtained in terms of elementary functions. The equation of state is established in §3.6 for a particular model. The other classes of models also admit an equation of state. The physical analysis of the charged anisotropic model is presented in §3.7 with graphs generated for particular parameter values for the electric field.

3.2 The model

The line element has the form

$$ds^2=-e^{2\nu(r)}dt^2+e^{2\lambda(r)}dr^2+r^2(d\theta^2+\sin^2\theta d\phi^2), \tag{3.1}$$

where $\nu(r)$ and $\lambda(r)$ are the potentials for a static spherical field. We now introduce the transformation

$$x=Cr^2,\quad Z(x)=e^{-2\lambda(r)},\quad A^2y^2(x)=e^{2\nu(r)}, \tag{3.2}$$

where A and C are constants. This transformation was first used by Durgapal and Bannerji (1983). The line element (3.1) then has the form

$$ds^2 = -A^2y^2(x)dt^2+\frac{1}{4Cx Z(x)}dx^2+\frac{x}{C}\left(d\theta^2+\sin^2\theta d\phi^2\right), \tag{3.3}$$

in terms of the variable x. The Einstein-Maxwell field equations become

$$\frac{\rho}{C} = -2\dot{Z}+\frac{1-Z}{x}-\frac{E^2}{2C}, \tag{3.4a}$$

$$\frac{p_r}{C} = 4Z\frac{\dot{y}}{y}+\frac{Z-1}{x}+\frac{E^2}{2C}, \tag{3.4b}$$

$$\frac{p_t}{C} = 4xZ\frac{\ddot{y}}{y}+(4Z+2x\dot{Z})\frac{\dot{y}}{y}+\dot{Z}-\frac{E^2}{2C}, \tag{3.4c}$$

$$\frac{\sigma^2}{C} = \frac{4Z}{x}(x\dot{E}+E)^2, \tag{3.4d}$$

in terms of the new variables. In the above ρ is the energy density, p_r is the radial pressure, p_t is the tangential pressure, E is the electric field and σ is the charge density. The conservation equation is

$$\frac{dp_r}{dx} = -\frac{1}{x}\left[p_r - p_t + x(\rho+p_r)\frac{d\nu}{dx}\right] + \frac{E}{x}\frac{d}{dx}(xE). \tag{3.5}$$

The mass of the graviting object contained within a radius x of the sphere is

$$M(x) = \frac{1}{4C^{3/2}}\int_0^x \sqrt{\omega}\rho(\omega)\ d\omega. \tag{3.6}$$

This quantity is sometimes called the mass function and is important for comparison with observations.

For a physically realistic relativistic star, we expect that the matter distribution should obey a barotropic equation of state. For a charged anisotropic matter distribution we consider the relationship

$$p_r = p_r(\rho), \tag{3.7}$$

where α and β are constants. From (3.4*b*) and (3.4*c*) we can write

$$4xZ\frac{\ddot{y}}{y} + 2x\dot{Z}\frac{\dot{y}}{y} + \dot{Z} - \frac{Z-1}{x} - \frac{E^2}{C} = \frac{\Delta}{C}, \tag{3.8}$$

where $\Delta = p_t - p_r$ is the measure of anisotropy. We can solve the Einstein-Maxwell field equations by choosing specific forms for the gravitational potential Z, the electric field intensity E and anisotropy Δ which are physically reasonable. Therefore we make the choices

$$Z = \frac{1}{1+ax}, \tag{3.9a}$$

$$\frac{E^2}{C} = \frac{(\alpha-\beta)x}{(1+ax)^2}, \tag{3.9b}$$

$$\frac{\Delta}{C} = \frac{\beta x}{(1+ax)^2}, \tag{3.9c}$$

where a, α, β are real constants. The electric field E depends on the real parameters α and β. The form (3.9*b*) is physically reasonable since E^2 remains regular and

positive throughout the sphere if $\alpha > \beta$. In addition the field intensity E becomes zero at the stellar centre and attains a maximum value of $E = \sqrt{(\alpha - \beta)C}/(4a)$ when $r = 1/\sqrt{aC}$. The anisotropy Δ is a decreasing function after reaching a maximum and will have small values close to the stellar boundary. Substitution of (3.9) into (3.8) gives

$$4(1 + ax)\ddot{y} - 2a\dot{y} + (a^2 - \alpha)y = 0, \tag{3.10}$$

which is the master equation.

There are three categories of solutions in terms of different values of the parameter α. The three cases correspond to

$$a^2 - \alpha = 0, \quad a^2 - \alpha > 0, \quad a^2 - \alpha < 0, \tag{3.11}$$

which generates new models.

3.3 The case $a^2 - \alpha = 0$

With $a^2 - \alpha = 0$, equation (3.10) becomes

$$4(1 + ax)\ddot{y} - 2a\dot{y} = 0. \tag{3.12}$$

Equation (3.12) is integrated to give

$$y(x) = \frac{(2 + 2ax)^{3/2}}{3a}c_1 + c_2, \tag{3.13}$$

where c_1 and c_2 are constants.

The complete solution of the Einstein-Maxwell system is then given by

$$e^{2\lambda} = 1 + ax, \tag{3.14a}$$

$$e^{2\nu} = A^2\left[\frac{(2 + 2ax)^{3/2}}{3a}c_1 + c_2\right]^2, \tag{3.14b}$$

$$\frac{\rho}{C} = \frac{6a + 2a^2x + (-\alpha + \beta)x}{2(1 + ax)^2}, \tag{3.14c}$$

$$\frac{p_r}{C} = \frac{a}{1 + ax} + \frac{(\alpha - \beta)x}{2(1 + ax)^2}$$

$$+\frac{24ac_1}{4c_1(1+ax)^2+3ac_2\sqrt{2(1+ax)}}, \tag{3.14d}$$

$$\frac{p_t}{C} = \frac{-2a+(-\alpha+\beta)x}{2(1+ax)^2} + \frac{12\sqrt{2}ac_1}{3ac_2\sqrt{1+ax}+2\sqrt{2}c_1(1+ax)^2}, \tag{3.14e}$$

$$\frac{E^2}{C} = \frac{(\alpha-\beta)x}{(1+ax)^2}, \tag{3.14f}$$

$$\frac{\sigma^2}{C} = \frac{C(\alpha-\beta)(3+ax)^2}{(1+ax)^5}. \tag{3.14g}$$

The line element for this solution (3.14) is given by

$$ds^2 = -A^2\left[\frac{(2+2ax)^{3/2}}{3a}c_1+c_2\right]^2 dt^2 + \frac{1+ax}{4Cx}dx^2+\frac{x}{C}(d\theta^2+\sin\theta^2 d\phi^2). \tag{3.15}$$

It is interesting to note that when $\alpha=\beta$ then the electric field vanishes and we obtain an uncharged anisotropic model.

3.4 The case $a^2-\alpha>0$

When $a^2-\alpha>0$ then (3.10) has a more complicated form. However we can transform it to a standard Bessel equation. We can simplify (3.10) with the transformation

$$V = (1+ax)^{\frac{1}{2}}, \tag{3.16a}$$

$$y = Y(1+ax)^{\frac{2+a}{4}}. \tag{3.16b}$$

Then (3.10) becomes

$$V^2\frac{d^2Y}{dV^2}+V\frac{dY}{dV}+\left((a^2-\alpha)V^2-\left(\frac{2+a}{2}\right)^2\right)Y = 0, \tag{3.17}$$

where $V=y^{2/(2+a)}Y^{-2/(2+a)}$. Now we use the transformation

$$w=(a^2-\alpha)^{1/2}V, \tag{3.18}$$

to obtain

$$w^2\frac{d^2Y}{dw^2}+w\frac{dY}{dw}+\left(w^2-\left(\frac{a+2}{2}\right)^2\right)Y \;=\; 0, \tag{3.19}$$

which is a Bessel equation of order $\frac{a+2}{2}$. In general the solution of (3.19) is a series. The general solution is a sum of linearly independent Bessel functions $J_{\frac{a+2}{2}}(w)$, of the first kind, and $\mathcal{Y}_{-\frac{a+2}{2}}(w)$, of the second kind, so that

$$Y(w)=b_1J_{\frac{a+2}{2}}(w)+b_2\mathcal{Y}_{-\frac{a+2}{2}}(w), \tag{3.20}$$

and b_1, b_2 are arbitrary constants.

The form of the solution in (3.20) is difficult to use in the modelling process. For specific values of a, when $\frac{a}{2}+1$ is a half-integer, it is possible to write the general solution of (3.20) as a sum of products of Legendre polynomials and trigonometric functions so that elementary functions arise. The solution has a simpler representation when a is an integer. If $a=-1,1,3,...$ then the solution (3.20) can be written as Bessel functions of half-integer order $J_{\frac{1}{2}}$, $J_{-\frac{1}{2}}$, $J_{\frac{3}{2}}$, $J_{-\frac{3}{2}}$, $J_{\frac{5}{2}}$, $J_{-\frac{5}{2}}$,... (see Watson (1996)). We show that this is possible for the cases $a=-1$, $a=1$, $a=3$.

3.4.1 Model I: $a=-1$

For $a=-1$, the solution (3.20) can be written as

$$Y(w)=b_1J_{\frac{1}{2}}(w)+b_2J_{-\frac{1}{2}}(w), \tag{3.21}$$

where

$$J_{\frac{1}{2}}(w) \;=\; \sqrt{\frac{2}{\pi w}}\sin(w), \tag{3.22a}$$

$$J_{-\frac{1}{2}}(w) \;=\; -\sqrt{\frac{2}{\pi w}}\cos(w). \tag{3.22b}$$

Then the general solution of (3.10) is given by

$$y(x) \;=\; (1-\alpha)^{-1/4}$$

$$\times \left[c_1 \sin\left(\sqrt{(1-\alpha)(1-x)}\right) + c_2 \cos\left(\sqrt{(1-\alpha)(1-x)}\right)\right], \quad (3.23)$$

where $c_1 = \sqrt{\frac{2}{\pi}} b_1$ and $c_2 = -\sqrt{\frac{2}{\pi}} b_2$ are new constants. The complete exact solution of the Einstein-Maxwell system has the form

$$\begin{aligned}
e^{2\lambda} &= 1-x, && (3.24a)\\
e^{2\nu} &= (1-\alpha)^{-1/2} A^2 \\
&\quad \times \left[c_1 \sin\left(\sqrt{(1-\alpha)(1-x)}\right) + c_2 \cos\left(\sqrt{(1-\alpha)(1-x)}\right)\right]^2, && (3.24b)\\
\frac{\rho}{C} &= \frac{-6 + x(2+\beta-\alpha)}{2(1-x)^2}, && (3.24c)\\
\frac{p_r}{C} &= -\left[2(1-\alpha)\left(c_1 - c_2 \tan\left(\sqrt{(1-\alpha)(1-x)}\right)\right)\right] \\
&\quad \times \left[c_2(1-x) + c_1(1-x)\tan\left(\sqrt{(1-\alpha)(1-x)}\right)\right]^{-1} \\
&\quad \times \left[\sqrt{(1-\alpha)(1-x)}\right]^{-1} + \frac{1}{1-x} + \frac{(\alpha-\beta)x}{2(1-x)^2}, && (3.24d)\\
\frac{p_t}{C} &= \left[4c_1(-1+\alpha) + c_2\sqrt{(1-\alpha)(1-x)}\,(2 + x(-2+\alpha+\beta))\right. \\
&\quad + \left(c_1\sqrt{(1-\alpha)(1-x)}(2 + x(-2+\alpha+\beta)) + 4c_2(1-\alpha)\right) \\
&\quad \times \tan\left(\sqrt{(1-\alpha)(1-x)}\right)\Big] \left[2\sqrt{(1-\alpha)(1-x)}\right. \\
&\quad \left. \times \left(c_2(1-x)^2 + c_1(1-x)^2 \tan\left(\sqrt{(1-\alpha)(1-x)}\right)\right)\right]^{-1}, && (3.24e)\\
\frac{E^2}{C} &= \frac{(\alpha-\beta)x}{(1-x)^2}, && (3.24f)\\
\frac{\sigma^2}{C} &= \frac{C(\alpha-\beta)(-3+x)^2}{(1-x)^5}. && (3.24g)
\end{aligned}$$

This is a new solution to the Einstein-Maxwell system. The line element for this case is

$$\begin{aligned}
ds^2 &= -(\alpha-1)^{-1/2} A^2 \\
&\quad \times \left[c_1 \sin\left(\sqrt{(1-\alpha)(1-x)}\right) + c_2 \cos\left(\sqrt{(1-\alpha)(1-x)}\right)\right]^2 dt^2 \\
&\quad + \frac{1-x}{4Cx} dx^2 + \frac{x}{C}\left(d\theta^2 + \sin^2\theta d\phi^2\right). && (3.25)
\end{aligned}$$

3.4.2 Model II: $a = 1$

When $a = 1$, (3.20) is of the form

$$Y(w) = b_1 J_{\frac{3}{2}}(w) + b_2 J_{-\frac{3}{2}}(w), \tag{3.26}$$

where

$$J_{\frac{3}{2}}(w) = \sqrt{\frac{2}{\pi w}}\left[\frac{\sin(w)}{w} - \cos(w)\right], \tag{3.27a}$$

$$J_{-\frac{3}{2}}(w) = -\sqrt{\frac{2}{\pi w}}\left[\frac{\cos(w)}{w} + \sin(w)\right]. \tag{3.27b}$$

Then the general solution to (3.10) is

$$\begin{aligned} y(x) &= (1-\alpha)^{-3/4} \\ &\times \left[c_2 \cos\left(\sqrt{(1-\alpha)(1+x)}\right) + c_1 \sin\left(\sqrt{(1-\alpha)(1+x)}\right)\right. \\ &-c_1\sqrt{(1-\alpha)(1+x)}\cos\left(\sqrt{(1-\alpha)(1+x)}\right) \\ &\left.+c_2\sqrt{(1-\alpha)(1+x)}\sin\left(\sqrt{(1-\alpha)(1+x)}\right)\right], \end{aligned} \tag{3.28}$$

where we introduced the constants $c_1 = \sqrt{\frac{2}{\pi}}b_1$ and $c_2 = -\sqrt{\frac{2}{\pi}}b_2$. This form of solution is similar to previous studies. With the help of the general solution (3.28), we can write the complete exact charged anisotropic solution of the Einstein-Maxwell system as

$$e^{2\lambda} = 1 + x, \tag{3.29a}$$

$$\begin{aligned} e^{2\nu} &= (1-\alpha)^{-3/2}A^2\left[c_2\sqrt{(1-\alpha)(1+x)}\sin\left(\sqrt{(1-\alpha)(1+x)}\right)\right. \\ &-c_1\sqrt{(1-\alpha)(1+x)}\cos\left(\sqrt{(1-\alpha)(1+x)}\right) \\ &\left.+c_2\cos\left(\sqrt{(1-\alpha)(1+x)}\right) + c_1\sin\left(\sqrt{(1-\alpha)(1+x)}\right)\right]^2, \end{aligned} \tag{3.29b}$$

$$\frac{\rho}{C} = \frac{6 + x(2+\beta-\alpha)}{2(1+x)^2}, \tag{3.29c}$$

$$\begin{aligned} \frac{p_r}{C} &= \frac{1}{2(1+x)^2}\left[\left(\frac{c_1}{\tan(\sqrt{(1-\alpha)(1+x)})} - c_2\right)\right. \\ &\left.\times(2 + (2-\alpha+\beta)x)\sqrt{(1-\alpha)(1+x)}\right. \end{aligned}$$

$$+(2-4\alpha+(2-3\alpha-\beta)x)\left(c_1+\frac{c_2}{\tan(\sqrt{(1-\alpha)(1+x)})}\right)\Bigg]$$
$$\times\left[\frac{c_2-c_1(\sqrt{(1-\alpha)(1+x)})}{\tan(\sqrt{(1-\alpha)(1+x)})}+c_1+c_2\sqrt{(1-\alpha)(1+x)}\right]^{-1}, \quad (3.29d)$$

$$\frac{p_t}{C} = \frac{1}{2(1+x)^2}\left[\frac{c_1(2+(2+\alpha-\beta)x)\sqrt{(1-\alpha)(1+x)}}{\tan(\sqrt{(1-\alpha)(1+x)})}\right.$$
$$+c_2(-2+(-2-\alpha+\beta)x)\sqrt{(1-\alpha)(1+x)}$$
$$\left.+(2-4\alpha+(2-3\alpha+\beta)x)\left(c_1+\frac{c_2}{\tan(\sqrt{(1-\alpha)(1+x)})}\right)\right]$$
$$\times\left[\frac{c_2-c_1(\sqrt{(1-\alpha)(1+x)})}{\tan(\sqrt{(1-\alpha)(1+x)})}+c_1+c_2\sqrt{(1-\alpha)(1+x)}\right]^{-1}, \quad (3.29e)$$

$$\frac{E^2}{C} = \frac{(\alpha-\beta)x}{(1+x)^2}, \quad (3.29f)$$

$$\frac{\sigma^2}{C} = \frac{C(3+x)^2(\alpha-\beta)}{(1+x)^5}. \quad (3.29g)$$

The system (3.29) gives the exact solution of the Einstein-Maxwell system expressed in terms of elementary functions. This is a new solution. We can consider the result (3.29) as a generalisation of the Hansraj and Maharaj (2006) model; when $\beta = 0$ the pressures are isotropic and we regain their model. When $\alpha = 0$ and $\beta = 0$ then we have an uncharged isotropic star which was the model first found by Finch and Skea (1989). We can write the line element in terms of the coordinate x as

$$ds^2 = -(1-\alpha)^{-3/2}A^2\left[c_2\sqrt{(1-\alpha)(1+x)}\sin\left(\sqrt{(1-\alpha)(1+x)}\right)\right.$$
$$-c_1\sqrt{(1-\alpha)(1+x)}\cos\left(\sqrt{(1-\alpha)(1+x)}\right)$$
$$\left.+c_2\cos\left(\sqrt{(1-\alpha)(1+x)}\right)+c_1\sin\left(\sqrt{(1-\alpha)(1+x)}\right)\right]^2dt^2$$
$$+\frac{1+x}{4Cx}dx^2+\frac{x}{C}(d\theta^2+\sin^2\theta d\phi^2). \quad (3.30)$$

The metric (3.30) may be interpreted as the anisotropic, charged generalisation of the Finch and Skea (1989) solution.

3.4.3 Model III: $a = 3$

When $a = 3$, (3.20) is of the form

$$Y(w) = b_1 J_{\frac{5}{2}}(w) + b_2 J_{-\frac{5}{2}}(w), \tag{3.31}$$

where

$$J_{\frac{5}{2}}(w) = \sqrt{\frac{2}{\pi w}}\left(\frac{3\sin w}{w^2} - \frac{3\cos w}{w} - \sin w\right), \tag{3.32a}$$

$$J_{-\frac{5}{2}}(w) = \sqrt{\frac{2}{\pi w}}\left(-\frac{3\cos w}{w^2} - \frac{3\sin w}{w} + \cos w\right). \tag{3.32b}$$

Then the general solution to (3.10) is

$$\begin{aligned} y(x) &= (9-\alpha)^{-5/4}\left[-3c_1\sqrt{(9-\alpha)(1+3x)}\cos\sqrt{(9-\alpha)(1+3x)}\right. \\ &\quad + (c_2(9-\alpha)(1+3x) - 3c_2)\cos\sqrt{(9-\alpha)(1+3x)} \\ &\quad -3c_2\sqrt{(9-\alpha)(1+3x)}\sin\sqrt{(9-\alpha)(1+3x)} \\ &\quad \left. + (3c_1 - c_1(9-\alpha)(1+3x))\sin\sqrt{(9-\alpha)(1+3x)}\right], \end{aligned} \tag{3.33}$$

where we have defined $c_1 = a\sqrt{\frac{2}{\pi}}$ and $c_2 = b\sqrt{\frac{2}{\pi}}$ as new constants. The complete exact solution to the Einstein-Maxwell system for this case is thus given by

$$e^{2\lambda} = 1 + 3x, \tag{3.34a}$$

$$\begin{aligned} e^{2\nu} &= A^2(9-\alpha)^{-5/2}\left[-3c_1\sqrt{(9-\alpha)(1+3x)}\cos\sqrt{(9-\alpha)(1+3x)}\right. \\ &\quad + (c_2(9-\alpha)(1+3x) - 3c_2)\cos\sqrt{(9-\alpha)(1+3x)} \\ &\quad -3c_2\sqrt{(9-\alpha)(1+3x)}\sin\sqrt{(9-\alpha)(1+3x)} \\ &\quad \left. + (3c_1 - c_1(9-\alpha)(1+3x))\sin\sqrt{(9-\alpha)(1+3x)}\right]^2, \end{aligned} \tag{3.34b}$$

$$\frac{\rho}{C} = \frac{18 + (18 - \alpha + \beta)\,x}{2(1+3x)^2}, \tag{3.34c}$$

$$\begin{aligned} \frac{p_r}{C} &= 6\,(9-\alpha)\,(1+3x)^{-1}\left[-c_2 - c_1\sqrt{(9-\alpha)(1+3x)}\right. \\ &\quad \left. +(c_1 - c_2\sqrt{(9-\alpha)(1+3x)})\tan(\sqrt{(9-\alpha)(1+3x)})\right] \\ &\quad \times\left[-3c_1\sqrt{(9-\alpha)(1+3x)} + c_2((9-\alpha)(1+3x) - 3)\right. \\ &\quad \left. -3c_2\sqrt{(9-\alpha)(1+3x)}\tan(\sqrt{(9-\alpha)(1+3x)})\right. \end{aligned}$$

$$+(3c_1-c_1(9-\alpha)(1+3x))\tan(\sqrt{(9-\alpha)(1+3x)})\Big]^{-1}$$
$$-\frac{6+(18-\alpha+\beta)x}{12(9-\alpha)(1+3x)}, \tag{3.34d}$$

$$\frac{p_t}{C} = 6\,(9-\alpha)\,(1+3x)^{-1}\Big[-c_2-c_1\sqrt{(9-\alpha)(1+3x)}$$
$$+(c_1-c_2\sqrt{(9-\alpha)(1+3x)})\tan(\sqrt{(9-\alpha)(1+3x)})\Big]$$
$$\times\Big[-3c_1\sqrt{(9-\alpha)(1+3x)}+c_2((9-\alpha)(1+3x)-3)$$
$$-3c_2\sqrt{(9-\alpha)(1+3x)}\tan(\sqrt{(9-\alpha)(1+3x)})$$
$$+(3c_1-c_1(9-\alpha)(1+3x))\tan(\sqrt{(9-\alpha)(1+3x)})\Big]^{-1}$$
$$-\frac{6+(18-\alpha-\beta)x}{12(9-\alpha)(1+3x)}, \tag{3.34e}$$

$$\frac{E^2}{C} = \frac{(\alpha-\beta)x}{(1+3x)^2}, \tag{3.34f}$$

$$\frac{\sigma^2}{C} = \frac{9C(\alpha-\beta)(1+x)^2}{(1+3x)^5}. \tag{3.34g}$$

This is a new category of exact models for a charged, anisotropic matter distribution. The line element is given by

$$ds^2 = -A^2(9-\alpha)^{-5/2}\Big[-3c_1\sqrt{(9-\alpha)(1+3x)}\cos\sqrt{(9-\alpha)(1+3x)}$$
$$+(c_2(9-\alpha)(1+3x)-3c_2)\cos\sqrt{(9-\alpha)(1+3x)}$$
$$-3c_2\sqrt{(9-\alpha)(1+3x)}\sin\sqrt{(9-\alpha)(1+3x)}$$
$$+(3c_1-c_1(9-\alpha)(1+3x))\sin\sqrt{(9-\alpha)(1+3x)}\Big]^2dt^2$$
$$+\frac{1+3x}{4Cx}dx^2+\frac{x}{C}(d\theta^2+\sin^2\theta d\phi^2). \tag{3.35}$$

3.5 The case $a^2-\alpha<0$

We now consider the case $a^2-\alpha<0$ and write the differential equation (3.10) as

$$4(1+ax)\ddot{y}-2a\dot{y}-(\alpha-a^2)y=0. \tag{3.36}$$

Keeping the same transformation (3.16) of §3.4, the equation (3.36) takes the form

$$V^2\frac{d^2Y}{dV^2}+V\frac{dY}{dV}-\left((\alpha-a^2)V^2+\left(\frac{2+a}{2}\right)^2\right)Y=0, \tag{3.37}$$

where $V = y^{2/(2+a)}Y^{-2/(2+a)}$. We cannot use the variable w of §3.4 as $a^2 - \alpha < 0$. It is important to use a new variable $\tilde{w}$. By taking

$$\tilde{w} = (\alpha - a^2)^{\frac{1}{2}}V, \tag{3.38}$$

equation (3.36) becomes

$$\tilde{w}^2\frac{d^2Y}{d\tilde{w}^2} + \tilde{w}\frac{dY}{d\tilde{w}} - \left(\tilde{w}^2 + \left(\frac{2+a}{2}\right)^2\right)Y = 0. \tag{3.39}$$

Equation (3.39) is the modified Bessel differential equation of order $\frac{2+a}{2}$. The general solution of (3.39) is a sum of linearly independent modified Bessel functions given by

$$Y(\tilde{w}) = b_1 I_{\frac{a+2}{2}}(\tilde{w}) + b_2 K_{-\frac{a+2}{2}}(\tilde{w}), \tag{3.40}$$

where b_1, b_2 are arbitrary constants. The quantities $I_{\frac{a+2}{2}}(\tilde{w})$, $K_{-\frac{a+2}{2}}(\tilde{w})$ are called modified Bessel functions of the first and second kind respectively. The form of the solution of (3.40) is complicated but can be written in terms of elementary functions when $\frac{a}{2}+1$ is a half-integer. For these parameter values the solution is usually written in terms of hyperbolic functions. For $a = -1, 1, 3, ...$ the solution of (3.39) can be written with the help of modified Bessel functions of half-integer order $I_{\frac{1}{2}}$, $I_{-\frac{1}{2}}$, $I_{\frac{3}{2}}$, $I_{-\frac{3}{2}}$, $I_{\frac{5}{2}}$, $I_{-\frac{5}{2}}$,... We now consider the cases where $a = -1$, $a = 1$ and $a = 3$.

3.5.1 Model I: $a = -1$

When $a = -1$ the solution (3.40) takes the form

$$Y(\tilde{w}) = b_1 I_{\frac{1}{2}}(\tilde{w}) + b_2 I_{-\frac{1}{2}}(\tilde{w}), \tag{3.41}$$

where

$$I_{\frac{1}{2}}(\tilde{w}) = \sqrt{\frac{2}{\pi\tilde{w}}}\sinh(\tilde{w}), \tag{3.42a}$$

$$I_{-\frac{1}{2}}(\tilde{w}) = \sqrt{\frac{2}{\pi\tilde{w}}}\cosh(\tilde{w}). \tag{3.42b}$$

Then the general solution of (3.36) is given by

$$y(x) = (\alpha - 1)^{-\frac{1}{4}}$$

$$\times \left[c_1 \sinh(\sqrt{(\alpha-1)(1-x)}) + c_2 \cosh(\sqrt{(\alpha-1)(1-x)})\right], \quad (3.43)$$

where $c_1 = \sqrt{\frac{2}{\pi}} b_1$ and $c_2 = \sqrt{\frac{2}{\pi}} b_2$ are new constants. Then the complete exact solution of the Einstein-Maxwell system is

$$\begin{aligned}
e^{2\lambda} &= 1-x, && (3.44a)\\
e^{2\nu} &= (\alpha-1)^{-\frac{1}{2}} A^2 \\
&\quad \times \left[c_1 \sinh(\sqrt{(\alpha-1)(1-x)}) + c_2 \cosh(\sqrt{(\alpha-1)(1-x)})\right]^2, && (3.44b)\\
\frac{\rho}{C} &= \frac{-6+x(2+\beta-\alpha)}{2(1-x)^2}, && (3.44c)\\
\frac{p_r}{C} &= \frac{1}{1-x} + \frac{(\alpha-\beta)x}{2(1-x)^2} \\
&\quad +(1-x)^{-1}\left[2(1-\alpha)(c_1 + c_2 \tanh(\sqrt{(\alpha-1)(1-x)}))\right] \\
&\quad \times \left[\sqrt{(\alpha-1)(1-x)}(c_2 + c_1 \tanh(\sqrt{(\alpha-1)(1-x)}))\right]^{-1}, && (3.44d)\\
\frac{p_t}{C} &= \Big[+c_2\sqrt{(\alpha-1)(1-x)}(2+x(-2+\alpha+\beta)) - 4c_1(-1+\alpha) \\
&\quad +(c_1\sqrt{(\alpha-1)(1-x)}(2+x(-2+\alpha+\beta)) \\
&\quad -4c_2(-1+\alpha))\tanh(\sqrt{(\alpha-1)(1-x)})\Big](1-x)^{-2} \\
&\quad \times \left[2\sqrt{(\alpha-1)(1-x)}(c_2 + c_1 \tanh(\sqrt{(\alpha-1)(1-x)}))\right]^{-1}, && (3.44e)\\
\frac{E^2}{C} &= \frac{(\alpha-\beta)x}{(1-x)^2}, && (3.44f)\\
\frac{\sigma^2}{C} &= \frac{C(\alpha-\beta)(-3+x)^2}{(1-x)^5}. && (3.44g)
\end{aligned}$$

This is a new solution to the Einstein-Maxwell system in terms of hyperbolic functions. The line element for this case is

$$\begin{aligned}
ds^2 &= -(\alpha-1)^{-\frac{1}{2}} A^2 \\
&\quad \times \left[c_1 \sinh(\sqrt{(\alpha-1)(1-x)}) + c_2 \cosh(\sqrt{(\alpha-1)(1-x)})\right]^2 dt^2 \\
&\quad + \frac{1-x}{4Cx} dx^2 + \frac{x}{C}(d\theta^2 + \sin^2\theta d\phi^2). && (3.45)
\end{aligned}$$

3.5.2 Model II: $a = 1$

For $a = 1$ the solution (3.40) becomes

$$Y(\tilde{w}) = b_1 I_{\frac{3}{2}}(\tilde{w}) + b_2 I_{-\frac{3}{2}}(\tilde{w}), \tag{3.46}$$

where the modified Bessel functions are given by

$$I_{\frac{3}{2}}(\tilde{w}) = \sqrt{\frac{2}{\pi\tilde{w}}}\left[-\frac{\sinh(\tilde{w})}{\tilde{w}} + \cosh(\tilde{w})\right], \tag{3.47a}$$

$$I_{-\frac{3}{2}}(\tilde{w}) = \sqrt{\frac{2}{\pi\tilde{w}}}\left[-\frac{\cosh(\tilde{w})}{\tilde{w}} + \sinh(\tilde{w})\right], \tag{3.47b}$$

Then the general solution of the equation (3.36) takes the form

$$\begin{aligned} y(x) &= (\alpha-1)^{-\frac{3}{4}}\left[c_1\sqrt{(\alpha-1)(1+x)}\sinh\left(\sqrt{(\alpha-1)(1+x)}\right)\right. \\ &\quad -c_2\sinh\left(\sqrt{(\alpha-1)(1+x)}\right) - c_1\cosh\left(\sqrt{(\alpha-1)(1+x)}\right) \\ &\quad \left.+c_2\sqrt{(\alpha-1)(1+x)}\cosh\left(\sqrt{(\alpha-1)(1+x)}\right)\right], \end{aligned} \tag{3.48}$$

where $c_1 = b_2\sqrt{\frac{2}{\pi}}$ and $c_2 = b_1\sqrt{\frac{2}{\pi}}$ are new constants. The complete exact solution to the Einstein-Maxwell system for this case can be written as

$$e^{2\lambda} = 1 + x, \tag{3.49a}$$

$$\begin{aligned} e^{2\nu} &= (\alpha-1)^{-\frac{3}{2}}\left[c_1\sqrt{(\alpha-1)(1+x)}\sinh\left(\sqrt{(\alpha-1)(1+x)}\right)\right. \\ &\quad -c_2\sinh\left(\sqrt{(\alpha-1)(1+x)}\right) - c_1\cosh\left(\sqrt{(\alpha-1)(1+x)}\right) \\ &\quad \left.+c_2\sqrt{(\alpha-1)(1+x)}\cosh\left(\sqrt{(\alpha-1)(1+x)}\right)\right]^2, \end{aligned} \tag{3.49b}$$

$$\frac{\rho}{C} = \frac{6-(\alpha-1)x+(1+\beta)x}{2(1+x)^2}, \tag{3.49c}$$

$$\begin{aligned} \frac{p_r}{C} &= \frac{1}{2(1+x)^2}\left[c_2\sqrt{(\alpha-1)(1+x)}(2+x(2-\alpha+\beta))\right. \\ &\quad -c_1(-2+4\alpha+x(-2+3\alpha+\beta)) \\ &\quad +\left(c_1\sqrt{(\alpha-1)(1+x)}(2+x(2-\alpha+\beta))\right. \\ &\quad \left.\left.-c_2(-2+4\alpha+x(-2+3\alpha+\beta))\right)\tanh\left(\sqrt{(\alpha-1)(1+x)}\right)\right] \\ &\quad \times\left[c_1 - c_2\sqrt{(\alpha-1)(1+x)}\right. \\ &\quad \left.+\left(c_2 - c_1\sqrt{(\alpha-1)(1+x)}\right)\tanh\left(\sqrt{(\alpha-1)(1+x)}\right)\right]^{-1}, \end{aligned} \tag{3.49d}$$

$$
\begin{aligned}
\frac{p_t}{C} &= \frac{1}{2(1+x)^2}\left[-c_2\sqrt{(\alpha-1)(1+x)}\,(-2+x(-2+\alpha+\beta))\right.\\
&\quad +c_1\,(2-4\alpha+x(2-3\alpha+\beta))\\
&\quad +c_1\left(\frac{c_2}{c_1}(2-4\alpha+x(2-3\alpha+\beta))\right.\\
&\quad \left.+\sqrt{(\alpha-1)(1+x)}(x(2-\alpha-\beta)+2)\right)\\
&\quad \left.\times\tanh\left(\sqrt{(\alpha-1)(1+x)}\right)\right]\\
&\quad \times\left[c_1-c_2\sqrt{(\alpha-1)(1+x)}+c_2\tanh\left(\sqrt{(\alpha-1)(1+x)}\right)\right.\\
&\quad \left.-c_1\sqrt{(\alpha-1)(1+x)}\tanh\left(\sqrt{(\alpha-1)(1+x)}\right)\right]^{-1}, \qquad (3.49e)\\
\frac{E^2}{C} &= \frac{(\alpha-1)x+(1-\beta)x}{(1+ax)^2}, \qquad (3.49f)\\
\frac{\sigma^2}{C} &= \frac{C((1-\beta)+(\alpha-1))(3+ax)^2}{(1+ax)^5}. \qquad (3.49g)
\end{aligned}
$$

Equations (3.49) represent a new solution in terms of hyperbolic functions. This result is a generalisation of the corresponding metric of Hansraj and Maharaj (2006); when $\beta = 0$ the anisotropy vanishes and we regain their model. The line element takes the form

$$
\begin{aligned}
ds^2 &= -(\alpha-1)^{-\frac{3}{2}}\left[c_1\sqrt{(\alpha-1)(1+x)}\sinh\left(\sqrt{(\alpha-1)(1+x)}\right)\right.\\
&\quad -c_2\sinh\left(\sqrt{(\alpha-1)(1+x)}\right)-c_1\cosh\left(\sqrt{(\alpha-1)(1+x)}\right)\\
&\quad \left.+c_2\sqrt{(\alpha-1)(1+x)}\cosh\left(\sqrt{(\alpha-1)(1+x)}\right)\right]^2dt^2\\
&\quad +\frac{1+x}{4Cx}dx^2+\frac{x}{C}(d\theta^2+\sin^2\theta d\phi^2). \qquad (3.50)
\end{aligned}
$$

3.5.3 Model III: $a = 3$

When $a = 3$ we can write the solution (3.40) as

$$
Y(\tilde{w}) = b_1 I_{\frac{5}{2}}(\tilde{w}) + b_2 I_{-\frac{5}{2}}(\tilde{w}), \qquad (3.51)
$$

where b_1 , b_2 are constants and $I_{\frac{5}{2}}$, $I_{-\frac{5}{2}}$ are modified Bessel functions which may be expressed in terms of hyperbolic functions as

$$
I_{\frac{5}{2}}(\tilde{w}) = \sqrt{\frac{2}{\pi\tilde{w}}}\left(\frac{3\sinh(\tilde{w})}{\tilde{w}^2}-\frac{3\cosh(\tilde{w})}{\tilde{w}}+\sinh(\tilde{w})\right), \qquad (3.52a)
$$

$$I_{-\frac{5}{2}}(\tilde{w}) = \sqrt{\frac{2}{\pi\tilde{w}}}\left(\frac{3\cosh(\tilde{w})}{\tilde{w}^2} - \frac{3\sinh(\tilde{w})}{w} + \cosh(\tilde{w})\right). \tag{3.52b}$$

Then the general solution to the differential equation in this case may be written as

$$\begin{aligned} y(x) &= (\alpha-9)^{-5/4} \\ &\quad \times[((3+(\alpha-9)(1+3x))c_1 - 3c_2T(x))\sinh(T(x)) \\ &\quad +((3+(\alpha-9)(1+3x))c_2 - 3c_1T(x))\cosh(T(x))], \end{aligned} \tag{3.53}$$

where $c_1 = b_1\sqrt{\frac{2}{\pi}}$ and $c_2 = b_2\sqrt{\frac{2}{\pi}}$ are new constants. The complete solution to the Einstein-Maxwell equations is given by

$$e^{2\lambda} = 1+3x, \tag{3.54a}$$

$$\begin{aligned} e^{2\nu} &= A^2(\alpha-9)^{-5/2} \\ &\quad \times[((3+(\alpha-9)(1+3x))c_1 - 3c_2T(x))\sinh(T(x)) \\ &\quad +((3+(\alpha-9)(1+3x))c_2 - 3c_1T(x))\cosh(T(x))]^2, \end{aligned} \tag{3.54b}$$

$$\frac{\rho}{C} = \frac{18+(18-\alpha+\beta)\,x}{2(1+3x)^2}, \tag{3.54c}$$

$$\begin{aligned} \frac{p_r}{C} &= \frac{-6+(-18+\alpha-\beta)x}{2(1+3x)^2}\,[12(1+3x)(\alpha-9)(-c_2+c_1T(x) \\ &\quad +(-c_1+c_1T(x))\tanh(T(x)))] \\ &\quad \times\big[2(1+3x)^2(-3c_1T(x)+c_2(3+(\alpha-9)(1+3x)) \\ &\quad +(-3c_2T(x)+c_1(3+(\alpha-9)(1+3x)))\tanh(T(x)))\big]^{-1}, \end{aligned} \tag{3.54d}$$

$$\begin{aligned} \frac{p_t}{C} &= \big[-(3c_1\,(T(x))^2\,(-30+4\alpha+x(-54+7\alpha-\beta)) \\ &\quad +c_2T(x)(-18(-8+\alpha)+x(-6(-297+\beta) \\ &\quad +\alpha(-354+17\alpha+\beta)+3x(\alpha-9)(-162+17\alpha+\beta)))) \\ &\quad -(3c_2(\alpha-9)(1+3x)(-30+4\alpha+x(-54+7\alpha-\beta)) \\ &\quad +c_1T(x)(-18(-8+\alpha)+x(-6(-297+\beta) \\ &\quad +\alpha(-354+17\alpha+\beta)+3x(\alpha-9)(-162+17\alpha+\beta)))) \\ &\quad \times\tanh(T(x))] \\ &\quad \times\big[2(1+3x)^2T(x)\,(3c_1T(x)-c_2(-6+3x(\alpha-9)+\alpha) \\ &\quad +(3c_2T(x)-c_1(-6+3x(\alpha-9)+\alpha))\tanh(T(x)))\big]^{-1}, \end{aligned} \tag{3.54e}$$

$$\frac{E^2}{C} = \frac{(9-(9-\alpha)-\beta)\,x}{(1+3x)^2}, \tag{3.54f}$$

$$\frac{\sigma^2}{C} = \frac{9C\,(9-(9-\alpha)-\beta)\,(1+x)^2}{(1+3x)^5}, \tag{3.54g}$$

where we have set $T(x) \equiv \sqrt{(\alpha-9)(1+3x)}$.

We have found another class of new solutions which allows for more complex behaviour in the potentials than the earlier cases. For our new solution to the Einstein-Maxwell system given by equations (3.54), the line element has the form

$$\begin{aligned} ds^2 = & -A^2(\alpha-9)^{-5/2} \\ & \times[((3+(\alpha-9)(1+3x))c_1 - 3c_2T(x))\sinh(T(x)) \\ & +((3+(\alpha-9)(1+3x))c_2 - 3c_1T(x))\cosh(T(x))]^2\,dt^2 \\ & +\frac{1+3x}{4Cx}dx^2 + \frac{x}{C}(d\theta^2+\sin^2\theta d\phi^2). \end{aligned} \tag{3.55}$$

3.6 Equation of state

An equation of state relating the radial pressure p_r to the energy density ρ is a desirable physical feature in a relativistic stellar model. The expressions for the radial pressure p_r are complicated but all the models found in this chapter admit an equation of state. We illustrate this for the model found in §3.4.2. From equation (3.29c) in §3.4.2 we can establish the expression

$$x^2 + \frac{4\rho - C(2+\beta-\alpha)}{2\rho}x + \frac{\rho-3C}{\rho} = 0. \tag{3.56}$$

To solve this equation, with distinct real roots, we impose the following condition, where the discriminant of the quadratic equation (3.56) is positive. We have that

$$\left(\frac{C}{2\rho}(2+\beta-\alpha)\right)^2 + \frac{2C}{\rho}(4-\beta+\alpha) > 0. \tag{3.57}$$

Hence the variable x is written in terms of ρ as

$$x = \frac{1}{2}\sqrt{\left(\frac{C}{2\rho}(2+\beta-\alpha)\right)^2 + \frac{2C}{\rho}(4-\beta+\alpha)}$$

$$-\left[1-\frac{C}{4\rho}(2+\beta-\alpha)\right]. \tag{3.58}$$

Then from (3.29d) we can write p_r as a function of ρ. Therefore, we have an equation of state of the form

$$\begin{aligned}\frac{p_r}{C} &= [-c_2\,(-2+4\alpha+(-2+3\alpha+\beta)(-1+F(\rho)))\\ &\quad +c_1(2+(2-\alpha+\beta)(-1+F(\rho)))\sqrt{(1-\alpha)F(\rho)}\\ &\quad -(c_1(-2+4\alpha+(-2+3\alpha+\beta)(-1+F(\rho)))\\ &\quad +c_2(2+(2-\alpha+\beta)(-1\\ &\quad +F(\rho)))\sqrt{(1-\alpha)F(\rho)})\tan(\sqrt{(1-\alpha)F(\rho)})\Big]\\ &\quad \times\Big[2(F(\rho))^2(c_2-c_1\sqrt{(1-\alpha)F(\rho)}+(c_1\\ &\quad +c_2\sqrt{(1-\alpha)F(\rho)})\tan(\sqrt{(1-\alpha)F(\rho)}))\Big]^{-1}, \end{aligned}\tag{3.59}$$

where we have set

$$F(\rho) = \frac{1}{2}\sqrt{\left(\frac{C}{2\rho}(2-\alpha+\beta)\right)^2+\frac{2C}{\rho}(4+\alpha-\beta)}+\frac{C}{4\rho}(2-\alpha+\beta).$$

Consequently the model in §3.4.2 has an equation of state of the general form

$$p_r = p_r(\rho), \tag{3.60}$$

which is barotropic.

Another quantity of physical interest is the speed of sound $\frac{dp_r}{d\rho}$. With the help of (3.59) and (3.29), the expression for the speed of sound in terms of the radial coordinate r becomes

$$\begin{aligned}\frac{dp_r}{d\rho} &= \frac{2+\alpha-\beta+(2-\alpha+\beta)cr^2}{-10-\alpha+\beta+cr^2(-2-\alpha+\beta)}\\ &\quad -\left[\frac{1}{-10-\alpha+\beta+cr^2(-2-\alpha+\beta)}\right]\\ &\quad \times\big[(-1+\alpha)(1+cr^2)(2(-2+cr^2(-1+\alpha)+\alpha)(1+\gamma^2)\\ &\quad +2(-1+\gamma^2)\cos(2\Omega(r))+6\gamma\Omega(r)\cos(2\Omega(r))\\ &\quad +(-3\Omega(r)\sin(2\Omega(r))+\gamma(-4+3\gamma\Omega(r)))\sin(2\Omega(r)))]\end{aligned}$$

$$\times \left[(-1+\gamma\Omega(r))\cos(\Omega(r)) - (\Omega(r)+\gamma)\sin(\Omega(r))\right]^{-2}, \tag{3.61}$$

where $\gamma = \frac{c_1}{c_2}$ is a constant and $\Omega(r) = \sqrt{(1-\alpha)(1+cr^2)}$. This expression is complicated but it is interesting to note that it is possible to find an analytic expression for the speed of sound. Graphical plots can be generated for $\frac{dp_r}{d\rho}$ as we show in the next section.

3.7 Physical models

Some brief comments about the physical features of the new solutions to the Einstein-Maxwell system are made in this section. In this chapter, we have presented several new models for a relativistic astrophysical star. The underlying equation was the Bessel differential equation which governs the solution of the Maxwell-Einstein system of field equations. The solutions found have matter variables which are regular and well behaved in the interior of the star. As an example we showed in this section that the exact solutions found in §3.4.2 are physically reasonable. The matter variables are plotted graphically. The software package Mathematica (Wolfram 2010) was used for the plots with the choice of parameters $a = 1$, $c_1 = 6.685$, $\alpha = 0.59$, $\gamma = -89.87631$, $C = 1$, $\beta = 0.175$, $c_2 = -0.07438$.

For a physically realistic relativistic star the equation of state is complex and depends on parameters such as the temperature, the number fraction of a specific particle interior species and strong entropy gradients. As a simplifying assumption for a charged anisotropic matter distribution we assume the barotropic relationship. The expressions for the matter and geometrical variables are in terms of Bessel functions which makes it difficult to study the behaviour of the physical features. We can obtain simpler forms for these quantities by expanding them in terms of Taylor series up to order r^2. This makes it possible to investigate the physical behaviour for small values of r. We obtain the quantities:

$$e^{2\lambda} = 1 + r^2, \tag{3.62a}$$

$$e^{2\nu} = 1 + 2.90788r^2, \tag{3.62b}$$
$$\frac{\rho}{C} = 3 - 5.2075r^2, \tag{3.62c}$$
$$\frac{p_r}{C} = 5.81673 - 14.2278r^2, \tag{3.62d}$$
$$\frac{p_t}{C} = 5.81673 - 14.0528r^2, \tag{3.62e}$$
$$\frac{E^2}{C} = 0.415r^2, \tag{3.62f}$$
$$\frac{\sigma^2}{C} = 3.735 - 16.185r^2. \tag{3.62g}$$

It is clear from the above that the gravitational potentials and matter variables are finite and regular at the centre and in the spacetime region close to the centre. Note that our models in general are not asymptotically flat in the finite interior of the star; however the interior does match to the asymptotically flat vacuum exterior. To take into account the physical units and dimensional homogeneity in plotted matter variables, we make the following scaling: $x = r^2$, $r^2 = \tilde{r}^2/R^2$, $\rho = \tilde{\rho}R^2$, $p_r = \tilde{p_r}R^2$, $p_t = \tilde{p_t}R^2$, $E = \tilde{E}R^2$, $\sigma = \tilde{\sigma}R^2$, where R has the dimension of length. The numerical value $R = 3.75$ km has been chosen so that all the matter variables are well behaved. The quantities $\tilde{\rho}$, $\tilde{p_r}$, $\tilde{p_t}$, $\tilde{E}$ and $\tilde{\sigma}$ are the physically relevant quantities. For example the star density is of order 3.0×10^{15} gcm^{-3}. This is greater than the nuclear saturation density but it is in the range of quark stars with a linear equation of state (see for example Mafa Takisa *et al* (2014b)). The physical star radius is $\tilde{r}$ which is approximately 8.43 km. Note that different choices of the parameter values may produce other physical profiles.

The following plots were generated:

- Figure 3.1: Energy density.
- Figure 3.2: Radial and Tangential pressure.
- Figure 3.3: Electric field.
- Figure 3.4: Charge density.
- Figure 3.5: Mass function.

- Figure 3.6: Equations of state.
- Figure 3.7: Speed of sound.

Figure 3.1 shows that the energy density ρ is positive, finite and strictly decreasing. In Figure 3.2 we see that both the tangential and radial pressures are positive and monotonically decreasing functions. In Figure 3.3 the electric field is positive and monotonically increasing and attains a maximum value when $\tilde{r} = R$. The evolution of the charge density in Figure 3.4 is a decreasing function which is continuous. The mass function is an increasing function with increasing radius in Figure 3.5. We observe that the anisotropy does not affect appreciably the behaviour of the mass and for these three cases. We plotted the equation of state for different parameter values in Figure 3.6. We find that the anisotropy parameter β influences the evolution of the equation of state. In Figure 3.7 the speed of sound satisfies the causality principle $0 \leq \frac{dp_r}{d\rho} \leq 1$ and the speed of sound is less than the speed of light. The plots generated indicate that models found in this chapter are physically reasonable. A detailed study of the physical features such as the luminosity and the relationship to observed astronomical objects will be carried out in future work.

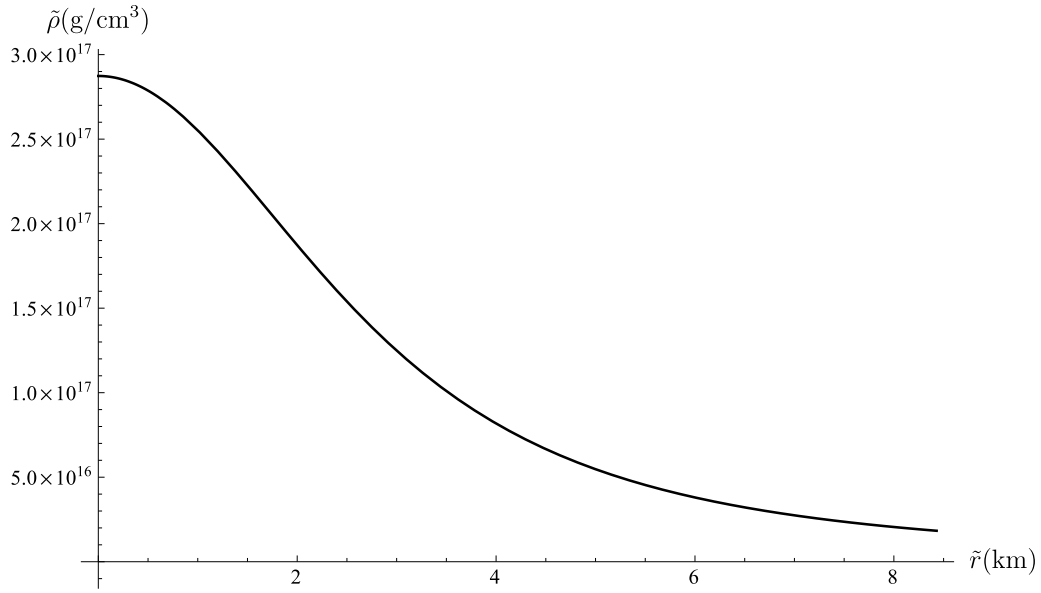

Figure 3.1 – Energy density

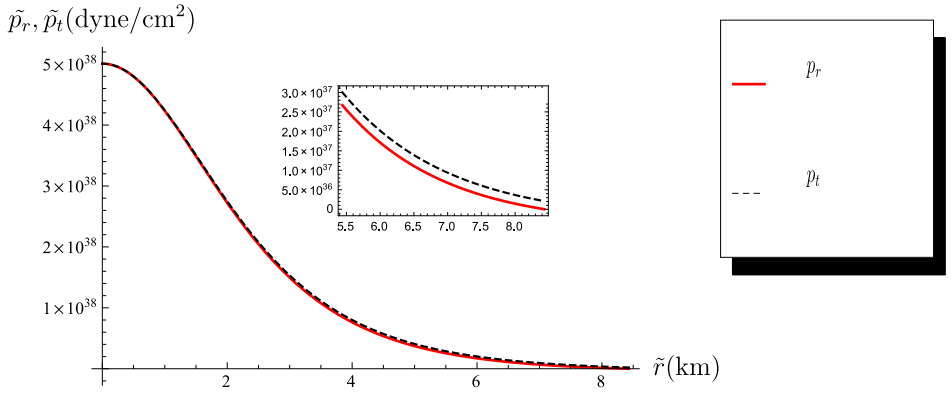

Figure 3.2 – Radial and tangential pressures

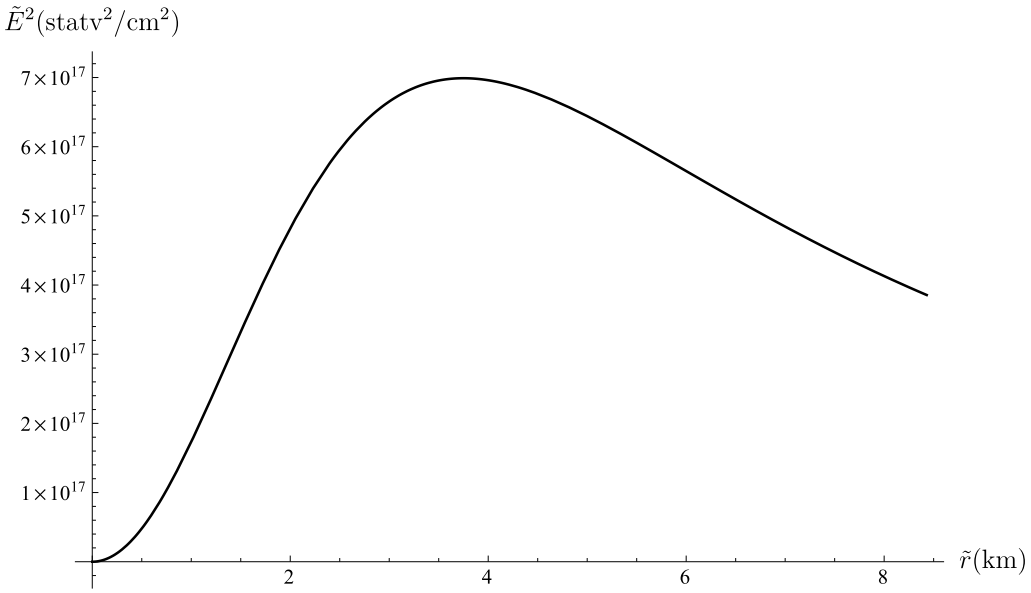

Figure 3.3 – Electric field intensity

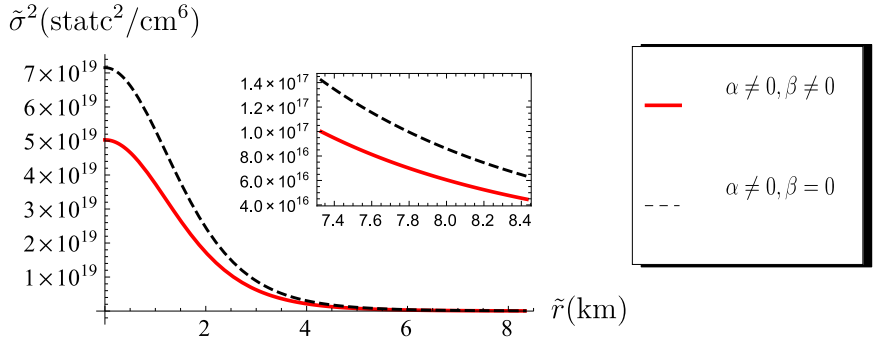

Figure 3.4 – Charge density

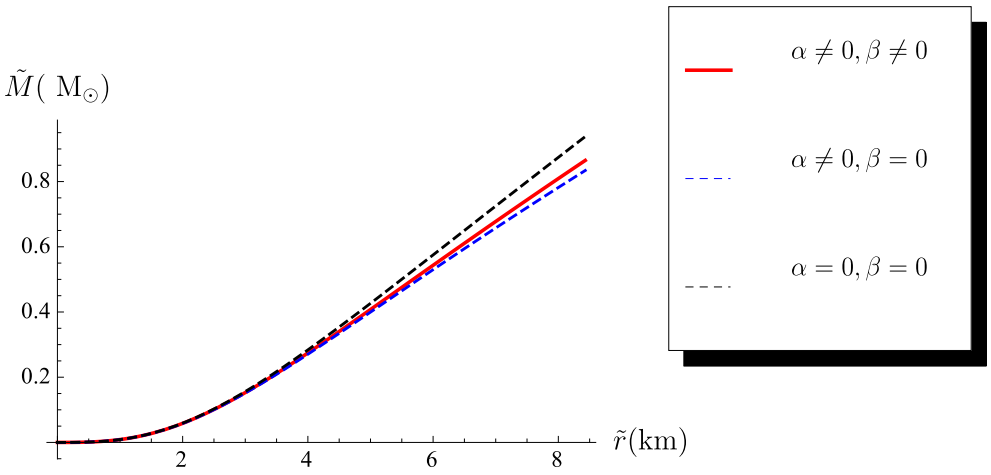

Figure 3.5 – Mass function

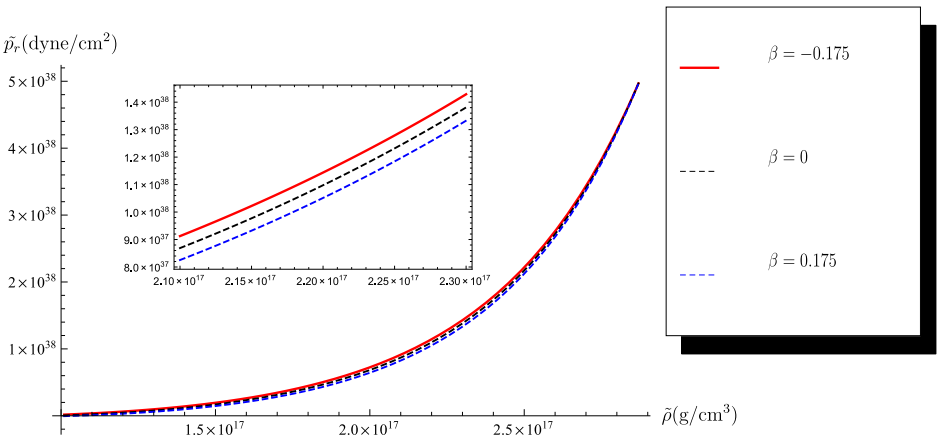

Figure 3.6 – Equations of state.

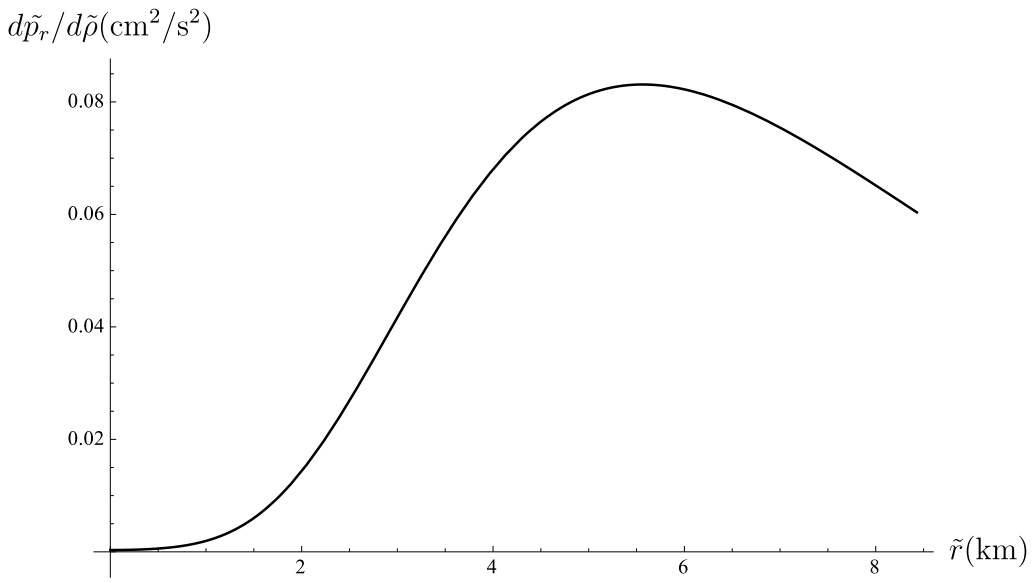

Figure 3.7 – Speed of sound.

Chapter 4

Prediction of stellar masses with Finch and Skea geometry

4.1 Introduction

The Einstein-Maxwell system of equations plays an important role in several applications in relativistic astrophysics. All astrophysical isolated systems (like the case of normal as well as compact stars) are generally considered to be charge neutral. However, global charge neutrality for extended systems is not easily attainable, and a sun-like star can hold up to 200 Coulomb of charge (Glendenning 2000). For the case of a highly dense compact star, the situation is much more complicated, and it has been shown in several models in the literature, that a highly dense compact star in general relativity can hold a large amount of charge. Now, an electric field, if present in the system, plays a crucial role in describing the equilibrium of the compact star, and this charge may even halt gravitational collapse as first shown by Bonnor (1965). The relevant requirement in relativistic astrophysics is to build stable equilibrium solutions of the Einstein-Maxwell system of equations, and to produce models of different stellar objects with strong gravitational fields by choosing relevant matter distributions. Models constructed in this way might be useful in

studying the physical characteristics of compact stellar bodies such as gravastars, neutron stars, quark stars, etc.

The studies of Ruderman (1972) and Canuto (1974), amongst others, have demonstrated that anisotropy may develop inside highly dense compact stellar objects. The conditions under which anisotropy might occur throughout the star, including the presence of the electromagnetic field or type 3A superfluid, have been investigated by Bowers and Liang (1917). Several anisotropic models have been investigated by Maurya and Gupta (2014), Maurya *et al* (2015), Pandya *et al* (2015), Bhar *et al* (2014), Murad (2013), Maharaj and Mafa Takisa (2012), Mafa Takisa *et al* (2014a, 2014b), Sunzu *et al* (2014a, 2014b) and Kileba Matondo and Maharaj (2016). Finch and Skea (1989) found a compact stellar model which was later shown to obey all the physical requirements for a realistic star as given by Delgaty and Lake (1998). Hence, many investigators have studied the Finch and Skea (1989) ansatz in different astrophysical contexts including Hansraj and Maharaj (2006), Tikekar and Jotania (2007) and Banerjee *et al* (2013). Recently the generalised Finch and Skea model with both anisotropy and the electric field was found by Maharaj *et al* (2016). This generalised model is regular and matter variables are well behaved with a barotropic equation of state. Therefore this model might be relevant in the description of the interior of a static charged anisotropic star.

In the recent past, there has been substantial improvement in observations of compact stars. The main challenge that remains is to determine with sufficient accuracy, the radius of these compact stars, primarily because their position is so far away. These recent probes with improved measurement techniques (e.g., the Shapiro delay method, to name one) and observational precisions reveal accurate measurement of the mass of some compact stars. Simultaneously, many theoretical teams have also tried to establish the accurate estimation of the radii of these new found masses for those stars. The combined effect of improved observational information of the mass and the theoretically predicted radius about such compact stellar objects have generated much interest about the internal matter content and accordingly the

spacetime geometry. Our treatment in this chapter shows that the Finch and Skea geometry produces masses and radii consistent with observations.

The investigation of Maharaj *et al* (2016) shows that the Finch and Skea geometry may be generalised to include charge and anisotropy. In this chapter we use a particular solution in the charged anisotropic model in Maharaj *et al* (2016) to investigate the physical features and show that this model is consistent with observed compact stars. We aim to find the maximum masses and the radii of the selected pulsars PSR J1416-2230, PSR J1903+0327, 4U 1820-30, Cen X-3, EXO 1785-248 and LMC X-4. In §4.2, the Einstein-Maxwell field equations and the Maharaj *et al* (2016) solution are presented. Physical requirements for acceptability for a stellar model in general relativity is presented in §4.3. We generate in §4.4, masses and radii, for particular parameter values, for charged anisotropic, charged isotropic and uncharged isotropic cases. These results are presented in Table 4.1, Table 4.2 and Table 4.3. Graphical plots of the physical quantities for two pulsars PSR J1614-2230 and LMC X-4 are displayed in §4.4. A detailed discussion of the masses and radii and their relationship to observed objects is given.

4.2 The model

In this section we choose a static gravitational field described by the following line element

$$ds^2 = -e^{2\nu(r)}dt^2 + e^{2\lambda(r)}dr^2 + r^2(d\theta^2 + \sin^2\theta d\phi^2), \tag{4.1}$$

where $\nu(r)$ and $\lambda(r)$ are the potentials for the static spherical field. The energy momentum tensor therefore has the general form

$$T_{ab} = \text{diag}\left(-\rho - \frac{1}{2}E^2, p_r - \frac{1}{2}E^2, p_t + \frac{1}{2}E^2, p_t + \frac{1}{2}E^2\right), \tag{4.2}$$

with the quantities ρ, p_r, p_t and E being respectively, the energy density, the radial pressure, the tangential pressure and the electric field intensity. Taking $\frac{8\pi G}{C^4} = 1$, the

Einstein-Maxwell field equations for charged anisotropic matter are given by

$$\frac{1}{r^2}\left[r(1-e^{-2\lambda})\right]' = \rho + \frac{1}{2}E^2, \tag{4.3}$$

$$-\frac{1}{r^2}(1-e^{-2\lambda}) + \frac{2\nu'}{r}e^{-2\lambda} = p_r - \frac{1}{2}E^2, \tag{4.4}$$

$$e^{-2\lambda}\left(\nu'' + \nu'^2 + \frac{\nu'}{r} - \nu'\lambda' - \frac{\lambda'}{r}\right) = p_t + \frac{1}{2}E^2, \tag{4.5}$$

$$\sigma = \frac{1}{r^2}e^{-\lambda}(r^2E)', \tag{4.6}$$

where primes represent differentiation with respect to r and σ the proper charge density. The mass of a charged stellar object contained within a radius r of the relativistic sphere is

$$M(r) = \frac{1}{2}\int_0^r (\rho_{unch}(\omega) + E^2)\omega^2 d\omega, \tag{4.7}$$

where $\rho_{unch}(\omega)$ is the energy density for uncharged case. An equivalent form of (4.3)-(4.6) can be obtain by using Durgapal and Bannerji (1983) transformation

$$x = Cr^2, \quad Z = e^{-2\lambda(r)}, \quad A^2y^2(x) = e^{2\nu(r)}, \tag{4.8}$$

with A and C are constants. The Einstein-Maxwell field equations then become

$$\frac{\rho}{C} = -2\dot{Z} + \frac{1-Z}{x} - \frac{E^2}{2C}, \tag{4.9}$$

$$\frac{p_r}{C} = 4Z\frac{\dot{y}}{y} + \frac{Z-1}{x} + \frac{E^2}{2C}, \tag{4.10}$$

$$\frac{p_t}{C} = 4xZ\frac{\ddot{y}}{y} + (4Z + 2x\dot{Z})\frac{\dot{y}}{y} + \dot{Z} - \frac{E^2}{2C}, \tag{4.11}$$

$$\frac{\sigma^2}{C} = \frac{4Z}{x}(x\dot{E} + E)^2, \tag{4.12}$$

It is necessary to select an exact solution of (4.3)-(4.6) to perform a physical analysis. Here we use a particular solution that arises in the models found by Maharaj *et al* (2016). The reason for this choice is that the gravitational potentials are regular in the interior, the matter variables have realistic profiles and a barotropic equation of state exists. In addition, this class of models contains the Finch and Skea

(1989) spacetime which has been shown to be consistent in the description of current observed astronomical bodies in several treatments. The relevant exact Einstein-Maxwell solution is given by

$$
\begin{aligned}
e^{2\lambda} &= 1+Cr^2, && (4.13a)\\
e^{2\nu} &= (1-\alpha)^{-3/2}A^2\left[c_2\cos\left(F(r)\right)-c_1F(r)\cos\left(F(r)\right)\right.\\
&\quad \left.+c_2F(r)\sin\left(F(r)\right)+c_1\sin\left(F(r)\right)\right]^2, && (4.13b)\\
\frac{\rho}{C} &= \frac{6+Cr^2(2+\beta-\alpha)}{2(1+Cr^2)^2}, && (4.13c)\\
\frac{p_r}{C} &= \left[\frac{2(1+Cr^2)^2\left(c_2-c_1(F(r))\right)}{\tan(F(r))}+2(1+Cr^2)^2\left(c_1+c_2F(r)\right)\right]^{-1}\\
&\quad \times\left[\frac{c_1\left(2+(2-\alpha+\beta)Cr^2\right)F(r)}{\tan(F(r))}\right.\\
&\quad -c_2\left(2+(2-\alpha+\beta)Cr^2\right)F(r)\\
&\quad -c_1\left(-2+4\alpha+(-2+3\alpha+\beta)r^2\right)\\
&\quad \left.-\frac{c_2\left(-2+4\alpha+(-2+3\alpha+\beta)Cr^2\right)}{\tan(F(r))}\right], && (4.13d)\\
\frac{p_t}{C} &= \frac{1}{2}\left[\frac{c_1(2+(2+\alpha-\beta)Cr^2)F(r)}{\tan(F(r))}\right.\\
&\quad +c_1\left(2-4\alpha+(2-3\alpha+\beta)Cr^2\right)\\
&\quad +c_2(-2+(-2-\alpha+\beta)Cr^2)F(r)\\
&\quad \left.+\frac{c_2\left(2-4\alpha+(2-3\alpha+\beta)Cr^2\right)}{\tan(F(r))}\right]\\
&\quad \times\left[\frac{(1+r^2)^2(c_2-c_1(F(r)))}{\tan(F(r))}+(1+Cr^2)^2\left(c_1+c_2F(r)\right)\right]^{-1}, && (4.13e)\\
\frac{E^2}{C} &= \frac{(\alpha-\beta)Cr^2}{(1+Cr^2)^2}, && (4.13f)\\
\frac{\sigma^2}{C} &= \frac{C(3+Cr^2)^2(\alpha-\beta)}{(1+Cr^2)^5}. && (4.13g)
\end{aligned}
$$

In addition, we have $F(r)=\sqrt{(1-\alpha)(1+Cr^2)}$ and, α and β are constants related to the electric field and anisotropy. We note that this exact model is given in terms of simple elementary functions which facilitates the physical analysis.

4.3 Physical requirements

For physical acceptability the model should comply with the following requirements throughout the star:

(i) The gravitational potentials and the matter variables should be well defined at the centre and regular throughout the star,

(ii) The energy density ρ at the centre of the star should be finite and decreasing in the interior $\left(\frac{d\rho}{dr} \leq 0\right)$,

(iii) The radial pressure p_r and the tangential pressure p_t must be positive, the speed of sound must be smaller than the speed of light $\left(\frac{dp_r}{d\rho} \leq 1\right)$ and the gradient of the pressure must be negative, $\left(\frac{dp_r}{dr} \leq 0\right)$ inside the stellar body,

(iv) At the stellar surface the radial pressure should vanish,

(v) The energy conditions: $\rho + p_r \geq 0$, $\rho + p_t \geq 0$ and $\rho - p_r - 2p_t \geq 0$ within the star,

(vi) For stability the adiabatic index $\Gamma = \dfrac{\rho + p_r}{p_r}\dfrac{dp_r}{d\rho} > \dfrac{4}{3}$, and

(vii) The metric functions $e^{2\lambda}$ and $e^{2\nu}$ should match smoothly to the Reissner-Nordström exterior metric

$$e^{2\nu(R)} = 1 - \frac{2M}{R} + \frac{Q^2}{R^2}, \tag{4.14}$$

$$e^{2\lambda(R)} = \left(1 - \frac{2M}{R} + \frac{Q^2}{R^2}\right)^{-1}, \tag{4.15}$$

at the surface of the sphere.

4.4 Physical analysis

To take into account the physical units and dimensional homogeneity in the matter variables, and also to compare with the results of previous investigations, we make

the following transformations:

$$\tilde{r} = r\mathcal{L}^2, \quad \rho = \tilde{\rho}\mathcal{L}^2, \quad p_r = \tilde{p_r}\mathcal{L}^2, \quad p_t = \tilde{p_t}\mathcal{L}^2,$$

where $\mathcal{L}$ is a parameter with dimension of *length*.

We analysed the behaviour of the model by taking the central density in the range of 1.5731×10^{14} gcm$^{-3} \leq \tilde{\rho}_c \leq 1.7825 \times 10^{15}$ gcm^{-3}, which corresponds to the range of parameters $0.11870 \leq C \leq 1.39500$. Starting from the lower bound density $\tilde{\rho}_c = 1.5731 \times 10^{14}$ gcm^{-3} and $C = 0.11870$, we obtain the fixed value of the parameter $\mathcal{L} = 2.674$ km, and the mass M of PSR 1614-2230 and radius R is generated. The parameter value $\mathcal{L} = 2.674$ km is fixed but the parameter C and the central density $\tilde{\rho}_c$ allowed to vary to generate specific stellar masses M and radii R for the rest of the pulsars, PSR J1614-2230, PSR J1903+0327, 4U 1820-30, Cen X-3, EXO 1785-248 and LMC X-4. We are concerned here with the uncharged isotropic case. The parameters used in the uncharged isotropic case have generated results which are consistent with the observational data. Consequently, we use these values to study charged isotropic and charged anisotropic bodies. We consider the electric charge E to be of the order of $E = 4.91959 \times 10^{20}$ V m^{-1} used in the work of Mafa Takisa *et al* (2014b), which corresponds to the values of $\alpha = 0.59$ and $\beta = 0.175$, so that we can generate specific numerical stellar masses M and radii R for the objects PSR J1614-2230, PSR J1903+0327, 4U 1820-30, Cen X-3, EXO 1785-248 and LMC X-4 for charged isotropic and charged anisotropic bodies. We also calculate the surface redshift Z_s. We find the values for the stellar radius R to be in the range 5.33-13.83 km, and the mass is in the range 1.04-1.97 $M_\odot$. The values of masses, radii, central densities and surface redshifts are given in Table 4.1 which corresponds to the charged anisotropic case. For the charged isotropic case the values are listed in Table 4.2. Finally in Table 4.3 the corresponding values for the isotropic case are provided. We note that similar values for the mass were obtained by Gangopadhyay *et al* (2013), and some other values were presented in the investigations Mafa Takisa *et al* (2014b), with a linear equation of state, and Mafa Takisa *et al* (2014a), with a quadratic equation of state. An interested reader, keen to

acquire a detailed knowledge of the observations of the above compact stellar objects, is referred to Gangopadhyay *et al* (2013) and the references therein. Our analysis here is more general as the equation of state is a general barotropic relationship. We have also provided the mass-radius $\frac{M}{R}$ (compactification factor) relationship for the six stellar pulsars in all tables. We note that the compactification factor is in the range of $\frac{M}{R} \sim \frac{1}{10}$ to $\frac{1}{4}$ which corresponds to neutron stars and ultra-compact stars as pointed out by Mafa Takisa and Maharaj (2013a). The Buchdahl (1959) requirement of $\frac{M}{R} < \frac{4}{9}$ for the all three cases is satisfied. The Andréasson (2009) requirement for charged cases $\sqrt{M} \leq \frac{\sqrt{R}}{3} + \sqrt{\frac{R}{9} + \frac{E^2R^3}{3}}$ in Table 4.2 and 4.3 are satisfied. Also the Buchdahl (1959) requirement of $\frac{M}{R} < \frac{4}{9}$ for uncharged case is satisfied too. The surface redshift Z_s can be measured from the X-ray spectrum which gives the compactness of the star. We observe that the surface redshift decreases with increase of radius for all six pulsars. The surface redshift Z_s is in the interval 0.4-0.5, and this range is approximately close to the values 0.36-0.49, found by Rahaman *et al* (2015); note also that these redshift values are in good agreement with the studies of Böhmer and Harko (2007) and Rahaman *et al* (2012). Also, we can highlight the condition of the upper bound (Buchdahl 1959), equivalent to $Z_s \leq 2$ for a realistic compact object has been met, and therefore our model is physically acceptable. Our redshift range values are also consistent with strange stellar objects which have a compactification factor higher than neutron stars with the upper bound $Z_s \leq 0.9$ as pointed out by Lindblom (1984).

By keeping the value of the mass constant and comparing the charged isotropic case to the uncharged isotropic case, the radius decreases relative to the uncharged isotropic case; this effect is expected since the new field is repulsive aiding the pressure to sustain the star against gravitational collapse. Also we notice that the charged anisotropic case has a bigger radius compared to the charged isotropic case. This feature likely arises as the effect of the anisotropy squeezes the sphere tangentially, which leads to increase of the radius of the star.

In order to compare the nature of the matter variables throughout the distri-

bution, we choose two particular stars: PSR J1614-2230 ($M = 1.97\ M_{\odot}$) bounds our upper limit and LMC X-4 ($M = 1.04\ M_{\odot}$) bounds our lower limit. Keeping all parameters unchanged and allowing the constants C, α and β to vary, we have shown the variations of density, pressures, anisotropy, mass, energy conditions, and speed of sound of both pulsars for the threes cases: charged anisotropic, charged isotropic and uncharged isotropic cases in Fig. 4.1, Fig. 4.2, and Fig. 4.3. The various physical variables throughout the compact stellar bodies are regular and well behaved. The energy density for the uncharged isotropic case is always greater than the energy density in charged anisotropic and the charged isotropic cases. Comparing between Fig. 4.1a and Fig. 4.2a we observe that the central energy density of LMC X-4 ($M = 1.04\ M_{\odot}$) has a value greater than the energy density of PSR J1614-2230 ($M = 1.97\ M_{\odot}$). Similar behaviour have been reported in the investigations of Singh *et al* (2016) and Sharma and Ratanpal (2013). We notice that the tangential and radial pressures in Figs. 4.1c, 4.1d, 4.2c, and 4.2d are radially decreasing outwards. In Figs 4.1e and 4.2e, the gradient of radial pressure is plotted. The gradient of radial pressure is decreasing, reaches a minimum and then increases towards the boundary as required. The behaviour of the anisotropy for both pulsars is displayed in Figs. 4.1f and 4.2f; it initially increases, reaches a maximum and then decreases. The anisotropy has lesser values for the PSR J1614-2230 when compared with the object MLC X-4. The speed of sound, as shown in Fig. 4.3a, is less than the speed of light, thus satisfying the condition of causality. The terms denoting the energy conditions, i.e., $\tilde{\rho} + \tilde{p_r}$, $\tilde{\rho} + \tilde{p_t}$ and $\tilde{r} - \tilde{p_r} - 2\tilde{p_t}$ versus radius for both pulsars are plotted in Figs. 4.1h and 4.2h. It can be observed that these quantities remain positive throughout the compact sphere and the energy conditions are satisfied. The profile of the adiabatic index Γ within the stellar matter is shown in Fig. 4.3c. It clearly shows that the variation of Γ throughout the star remains greater that $\frac{4}{3}$, which complies with the condition for stability of a relativistic stellar model.

It is interesting to note from our plots, that the presence of charge has apparently decreased the size of the star (comparing the Figs. 4.1g and 4.2g). However, natural

perception indicates that the presence of similar charges inside a compact stellar system will generate a repulsive force, thus bloating the size of the star. A careful observation of our results reveals that for a given constant central density (which defines the ultimate morphology of the star) the size of the star has actually increased due to the presence of charge. However our solutions allow for the presence of lower values of the central density for the uncharged case, thus making the size of the star large for the uncharged star, than the charged case. This essentially means that the presence of charge has allowed for a steeper equation of state of matter inside the star. This can be seen in the Figs. 4.1a and 4.2a for the density, and correspondingly in the Figs. 4.1g and 4.2g for the mass.

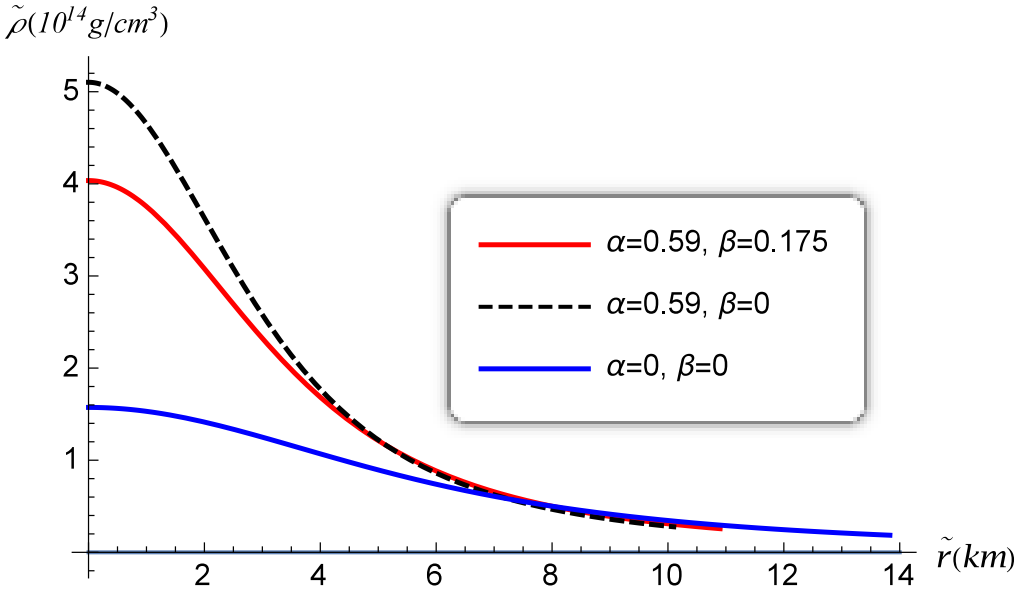

(a) Energy density

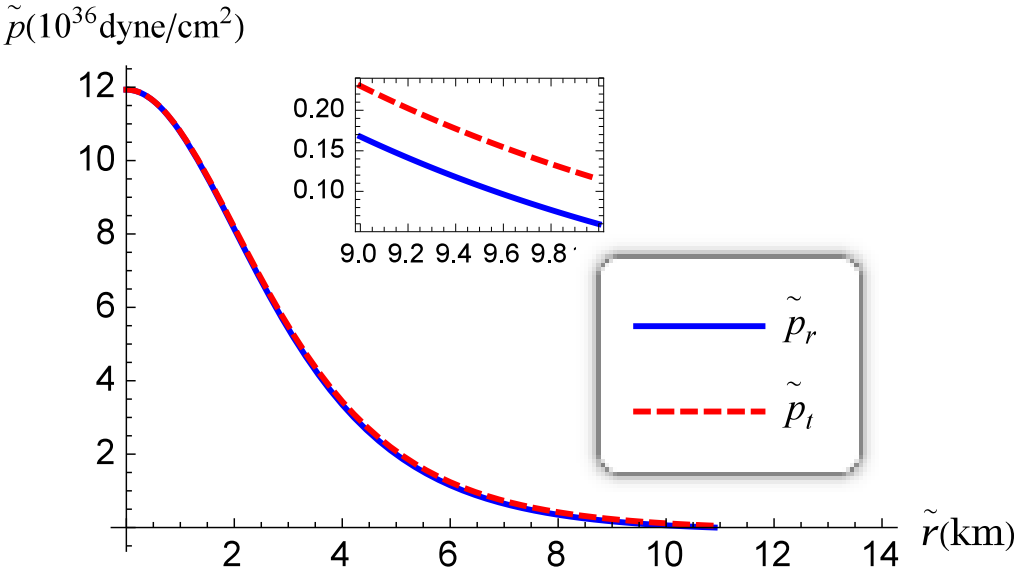

(b) Tangential and radial pressure

Figure 4.1 – Figures for PSR J1614 - 2230

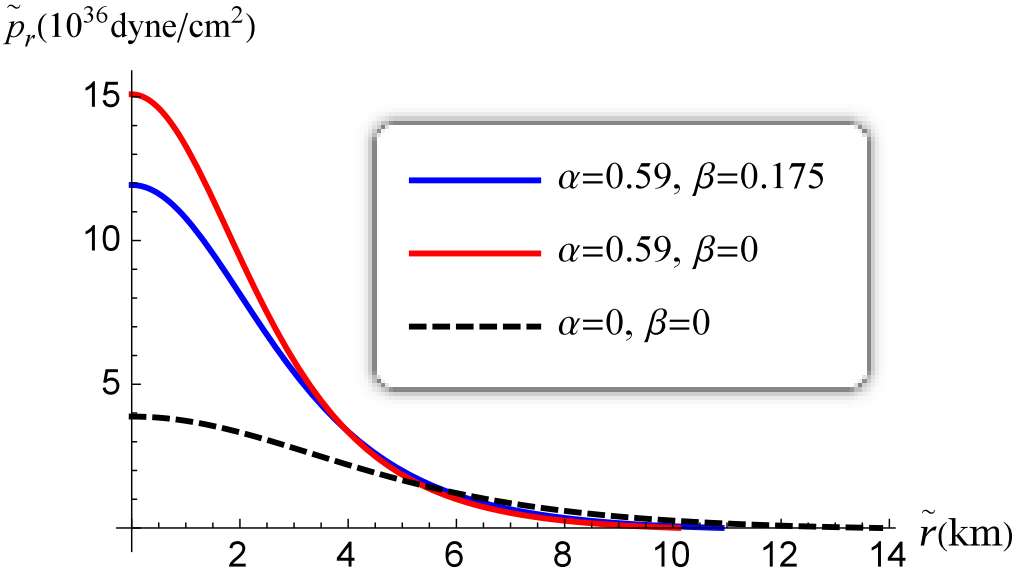

(c) Radial pressure

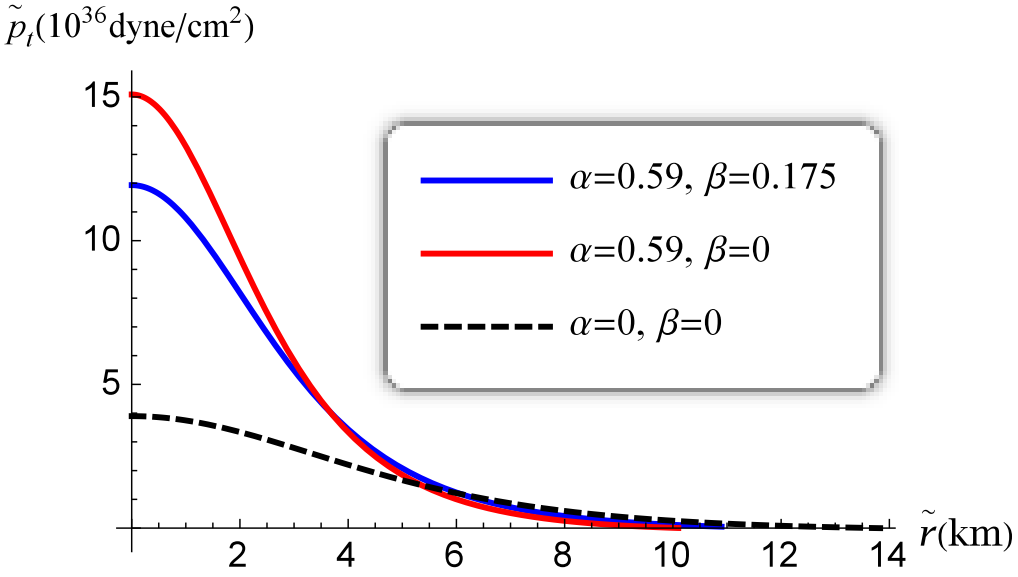

(d) Tangential pressure

Figure 4.1 – Figures for PSR J1614 - 2230

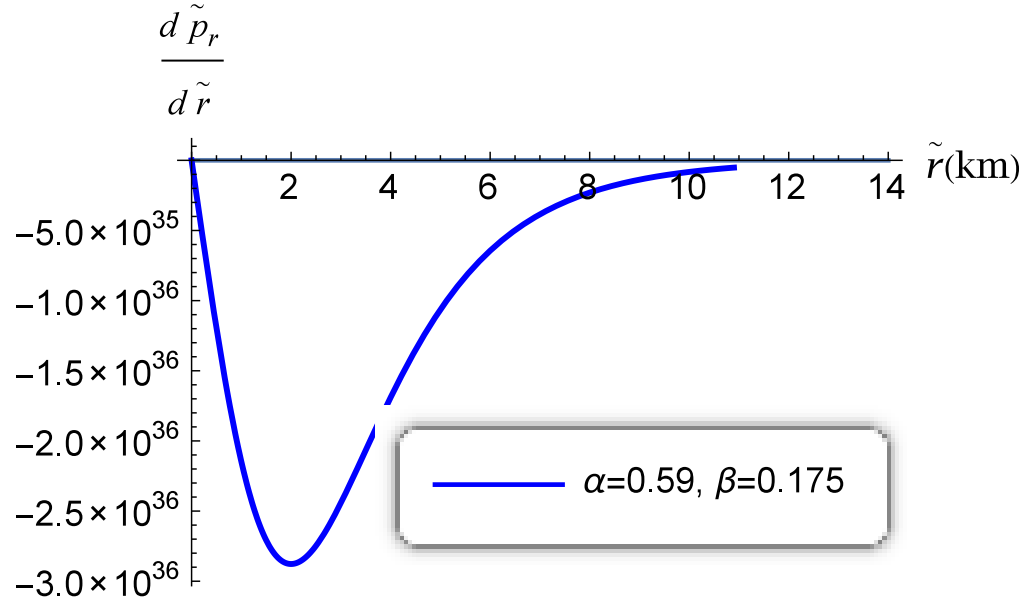

(e) Gradient of radial pressure

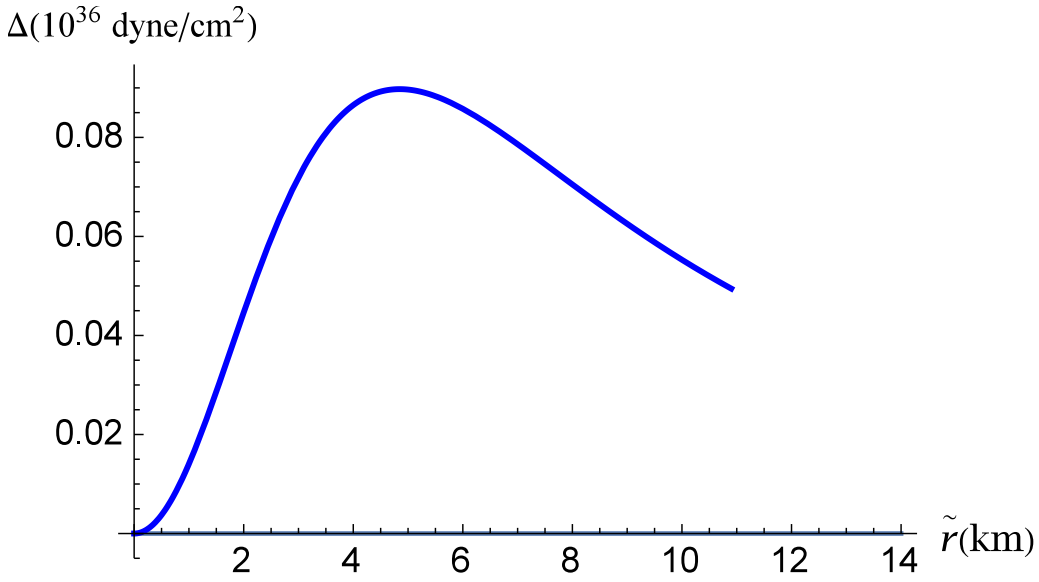

(f) Anisotropy

Figure 4.1 – Figures for PSR J1614 - 2230

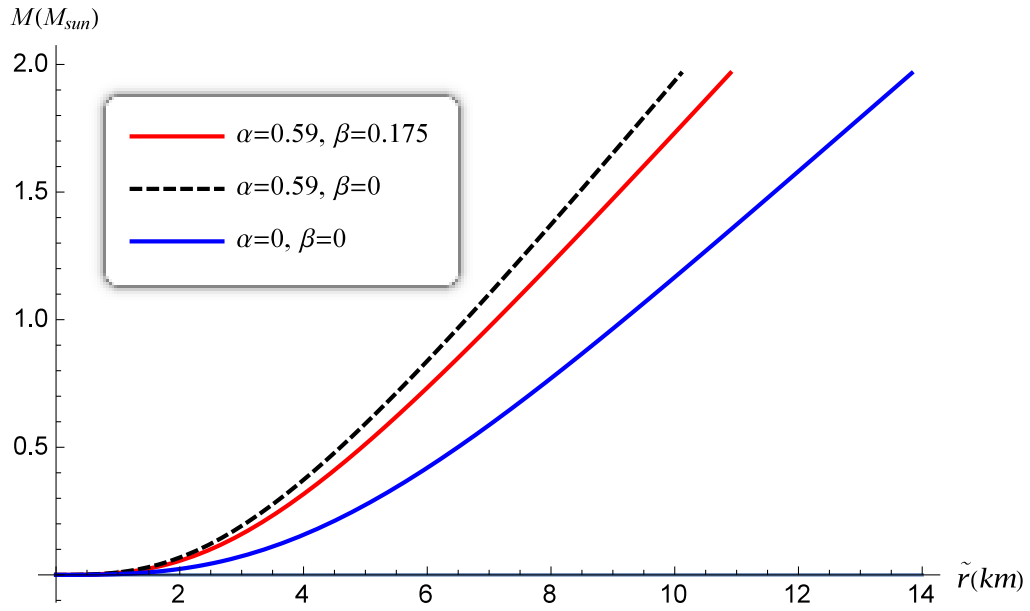

(g) Mass

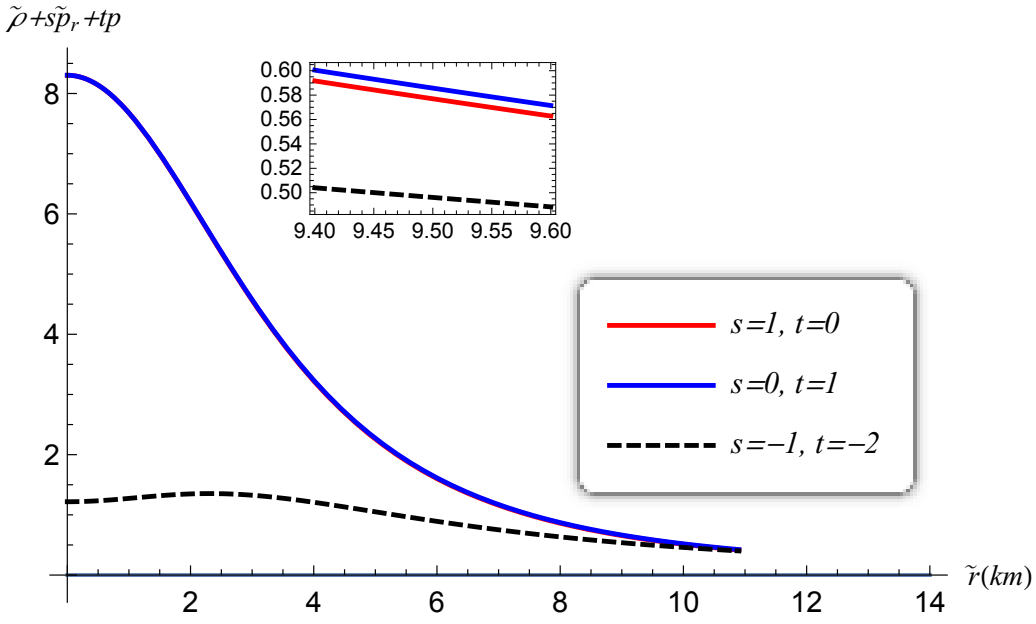

(h) Energy conditions

Figure 4.1 – Figures for PSR J1614 - 2230

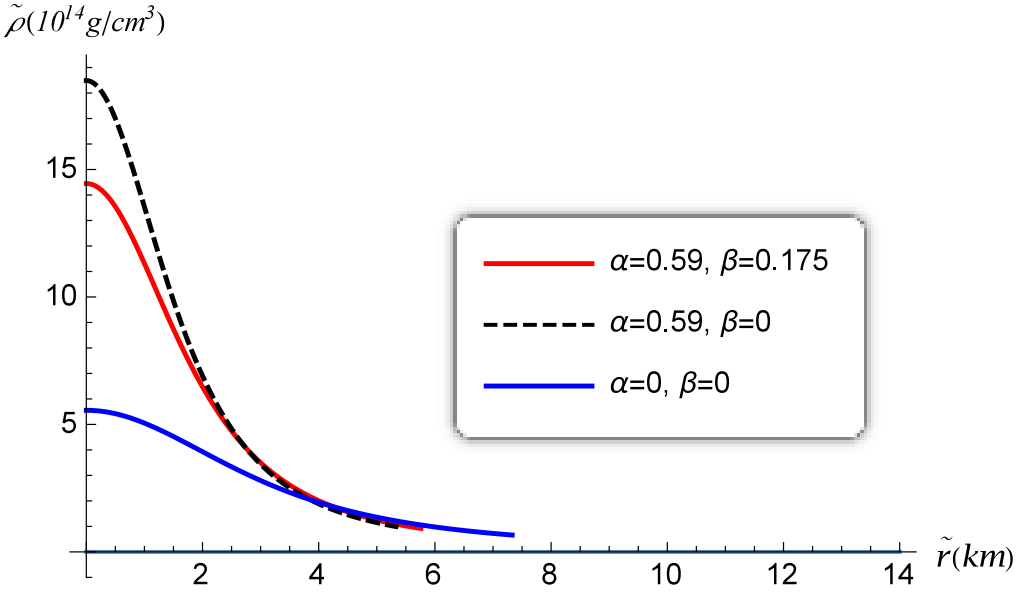

(a) Energy density

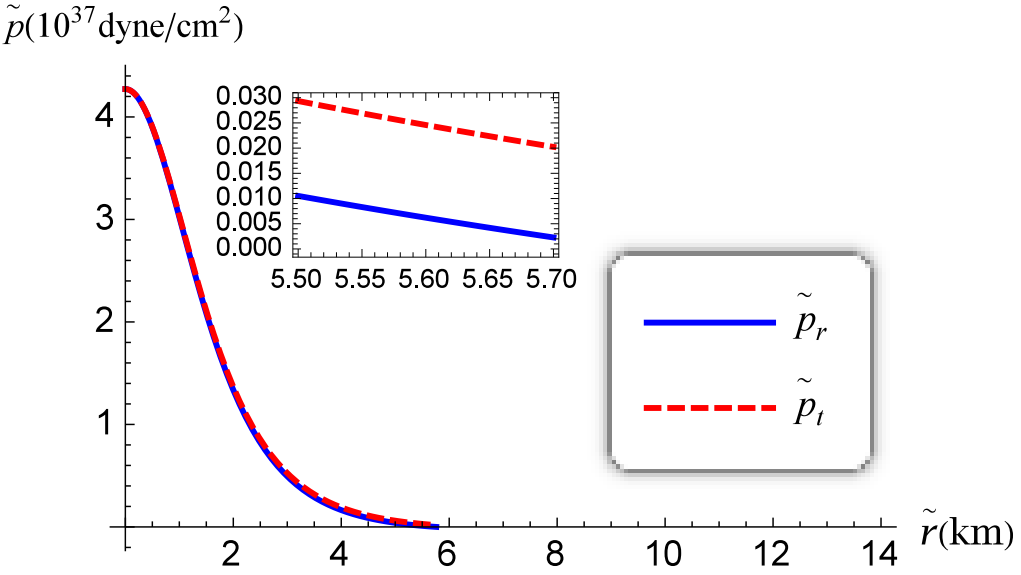

(b) Tangential and radial pressure

Figure 4.2 – Figures for LMC X-4.

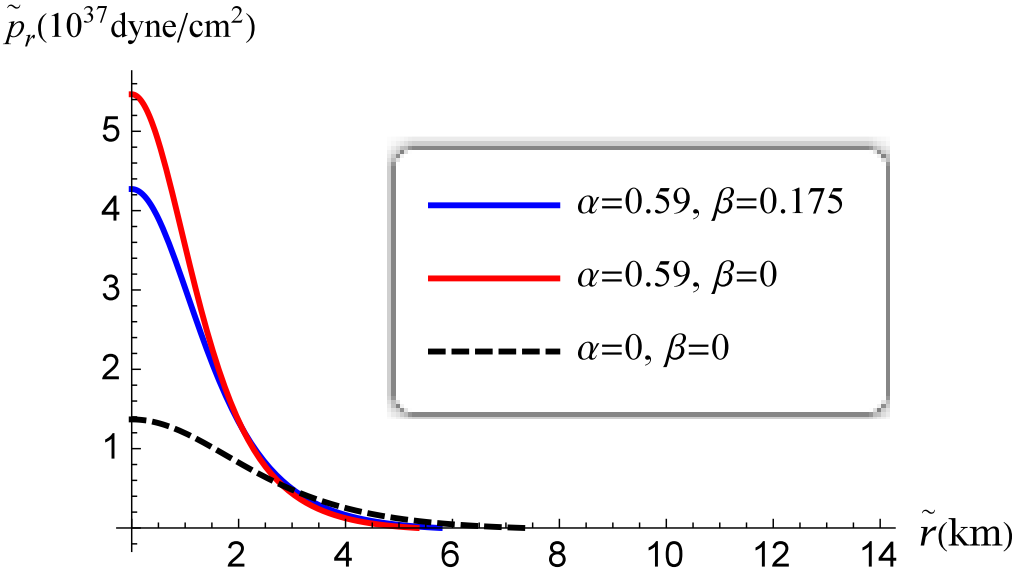

(c) Radial pressure

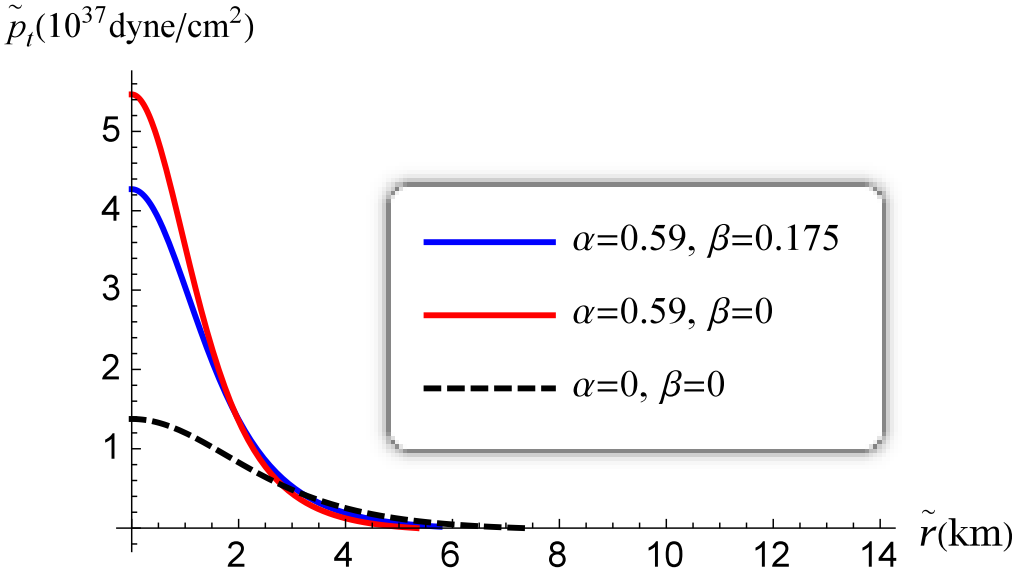

(d) Tangential pressure

Figure 4.2 – Figures for LMC X-4.

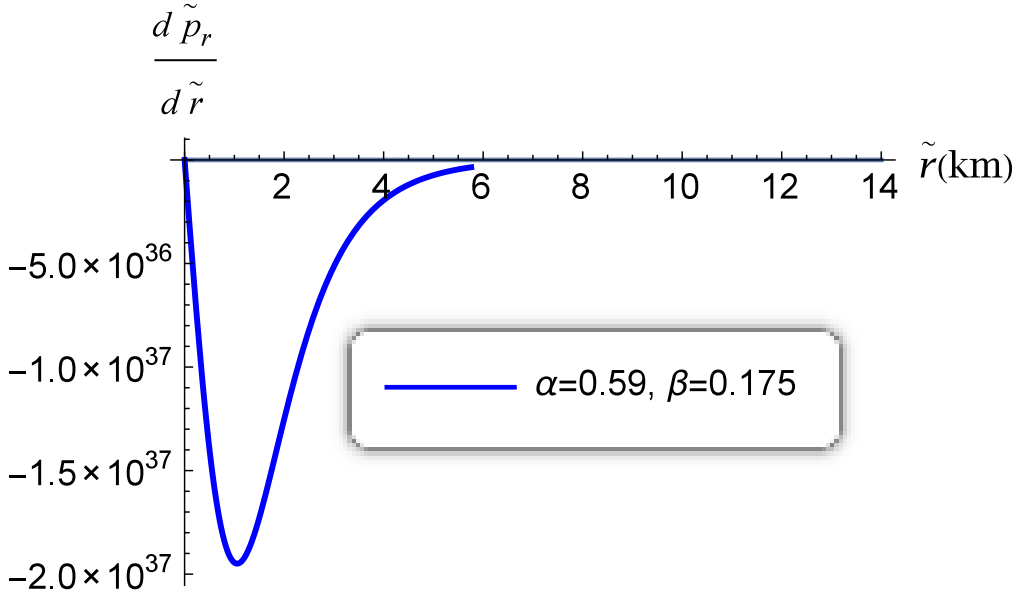

(e) Gradient of radial pressure

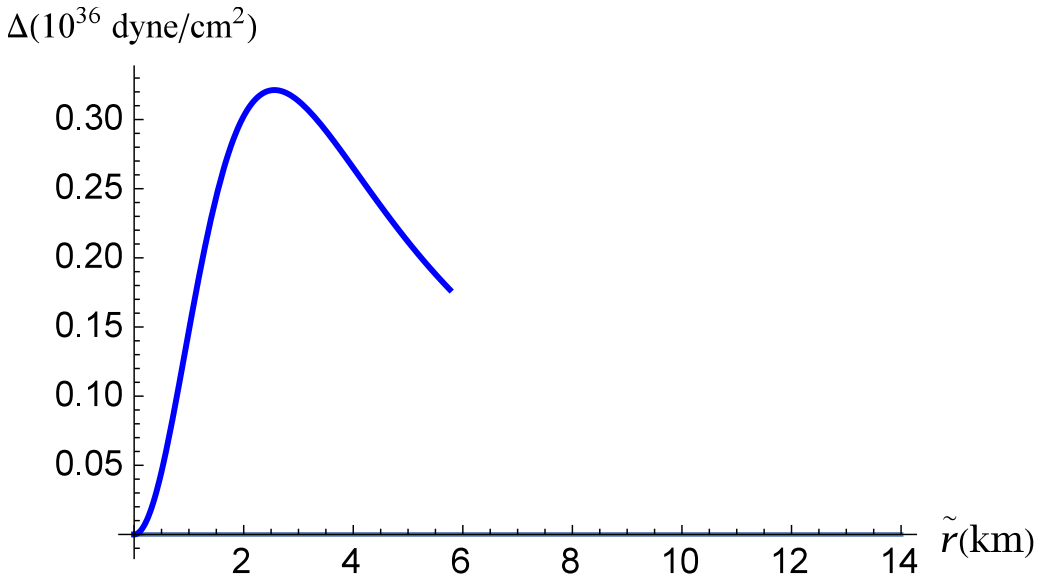

(f) Anisotropy

Figure 4.2 – Figures for LMC X-4.

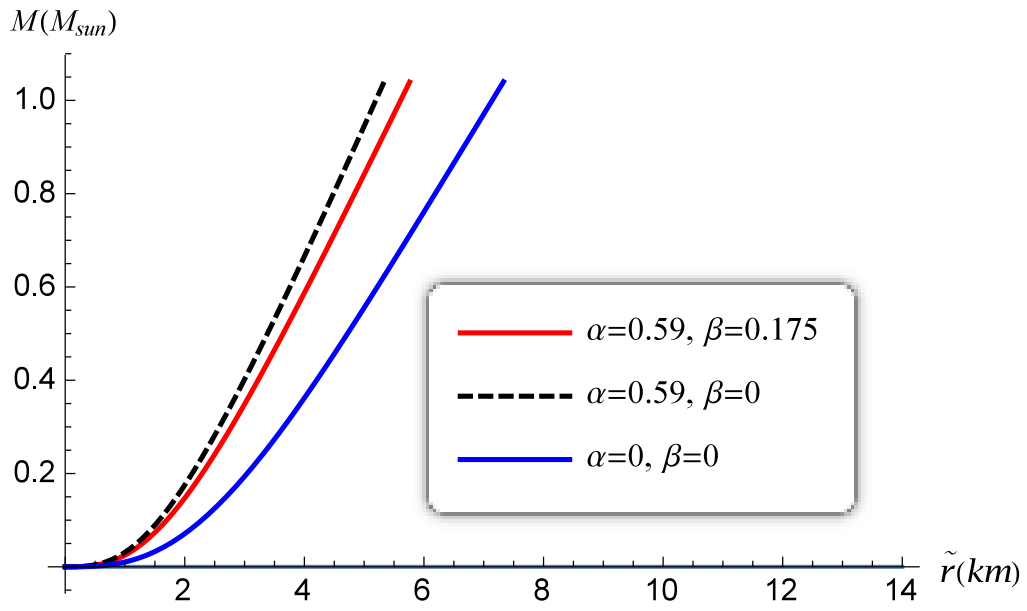

(g) Mass

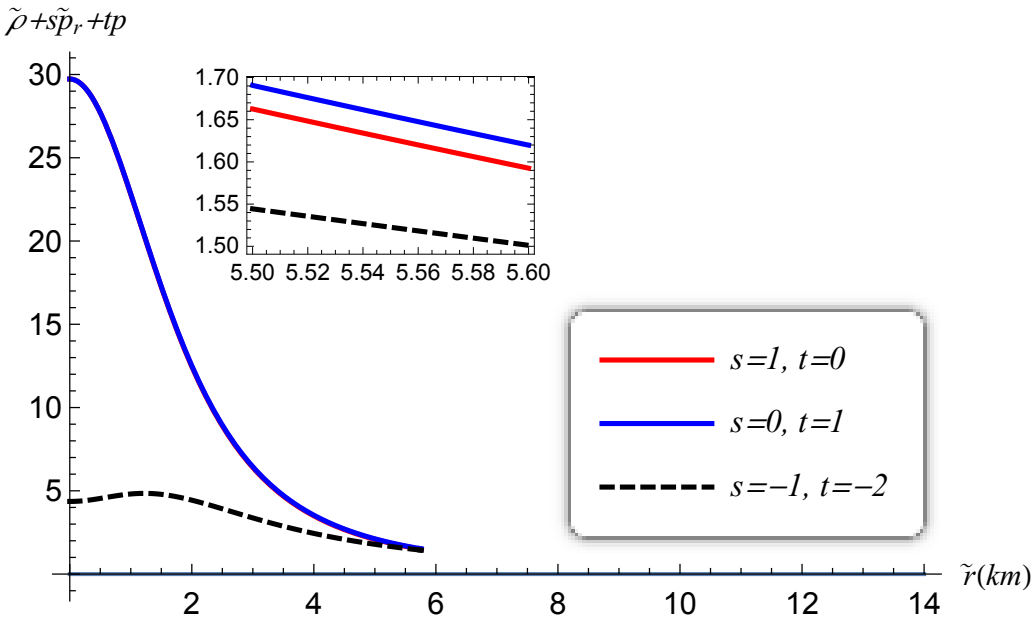

(h) Energy conditions

Figure 4.2 – Figures for LMC X-4.

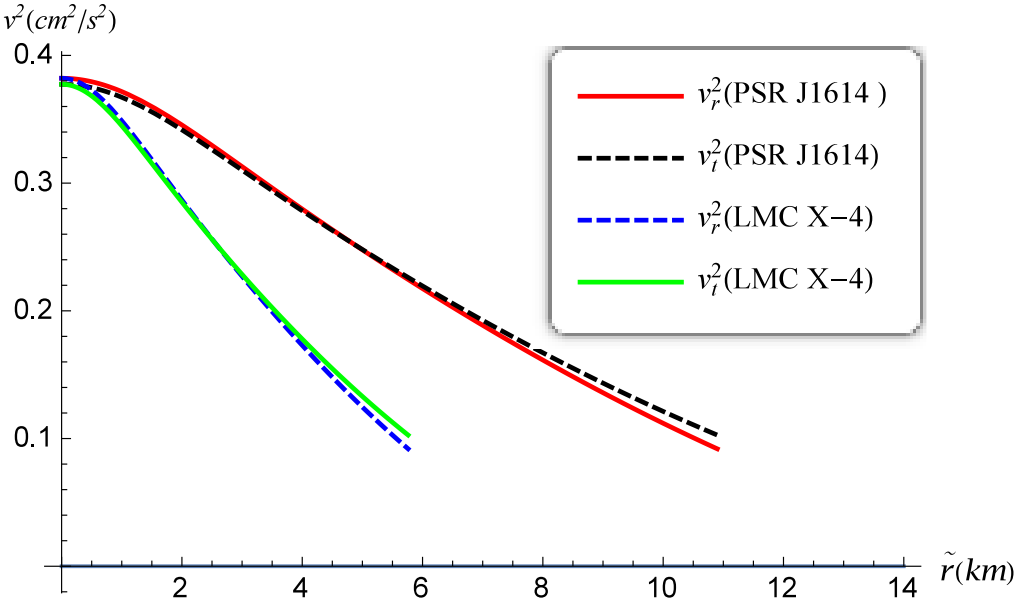

(a) Square of speeds of sound

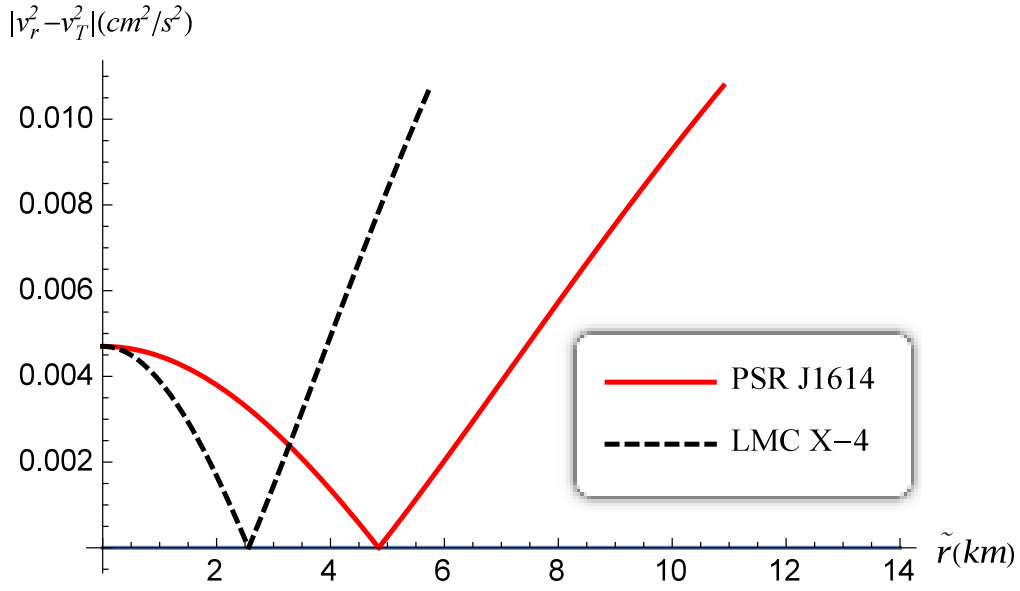

(b) The quantity $|v_t^2 - v_r^2|$

Figure 4.3 – Figures for PSRJ1614-2230 and LMC X-4.

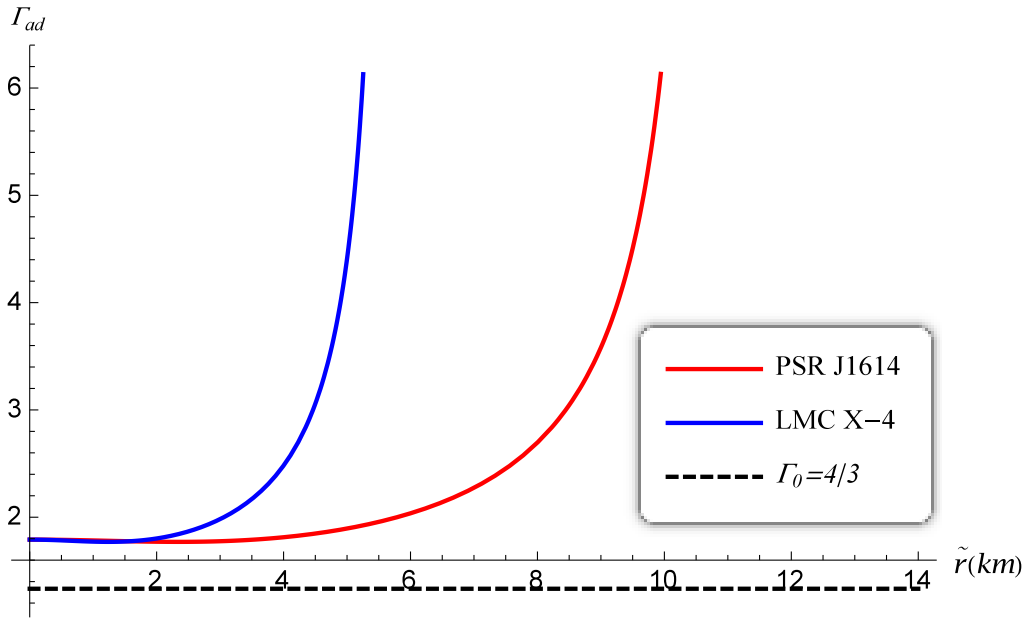

(c) Adiabatic index

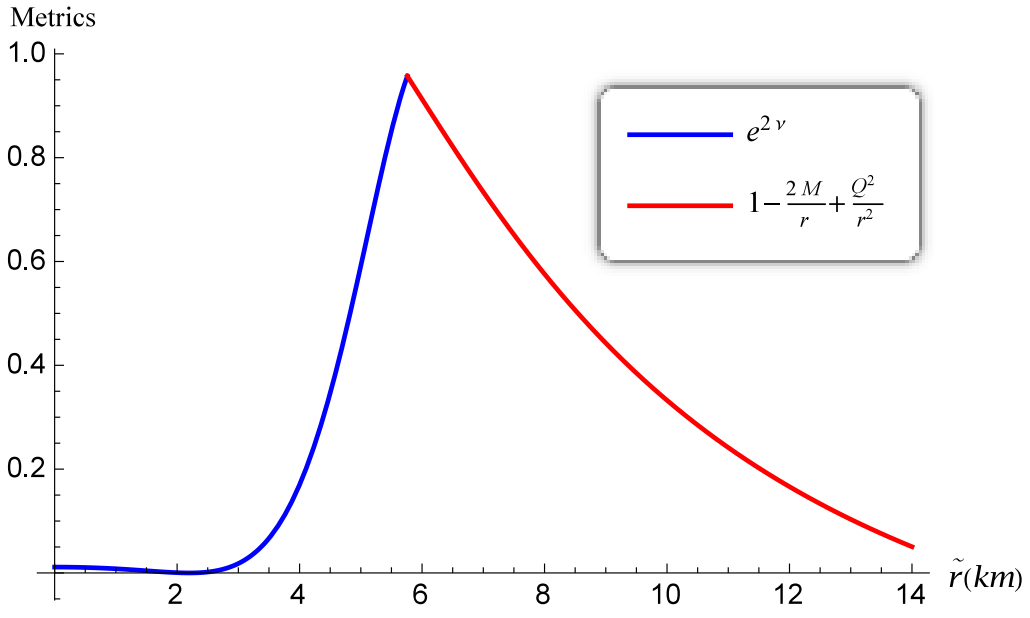

(d) Matching at the boundary for LMC X-4 for charged anisotropic case

Figure 4.3 – Figures for PSRJ1614-2230 and LMC X-4.

Table 4.1 – Charged anisotropic stars

Stars	C	$M(M_{\odot})$	R(km)	$\frac{M}{R}$	$\tilde{\rho}_c$(x10^{14}gcm^{-3})	Z_s
PSR J1614-2230	0.304500	1.97	10.90	0.18070	4.03545	0.56895
PSR J1903+0327	0.424300	1.667	9.237	0.18047	5.62312	0.56868
4U 1820-30	0.472320	1.58	8.55	0.18479	6.25951	0.55380
Cen X-3	0.531100	1.49	8.2568	0.18045	7.03851	0.56922
EXO 1785-248	0.697690	1.3	7.2039	0.18045	9.24627	0.56914
LMC X-4	1.090200	1.04	5.76	0.18055	14.4481	0.56889

Table 4.2 – Charged isotropic stars

Stars	C	$M(M_{\odot})$	R(km)	$\frac{M}{R}$	$\tilde{\rho}_c$(x10^{14}gcm^{-3})	Z_s
PSR J1614-2230	0.38500	1.97	10.10	0.19504	5.10229	0.59626
PSR J1903+0327	0.54286	1.667	8.55	0.19497	7.19436	0.59978
4U 1820-30	0.60429	1.58	8.1039	0.19496	8.00847	0.59979
Cen X-3	0.67949	1.49	7.6423	0.19496	9.00508	0.59979
EXO 1785-248	0.89262	1.3	6.6678	0.19496	11.8296	0.59971
LMC X-4	1.39500	1.04	5.33	0.19512	17.8249	0.59932

Table 4.3 – uncharged isotropic stars

Stars	C	$M(M_{\odot})$	R(km)	$\frac{M}{R}$	$\tilde{\rho}_c$(x10^{14}gcm^{-3})	Z_s
PSR J1614-2230	0.11870	1.97	13.83	0.14244	1.5731	0.42945
PSR J1903+0327	0.16342	1.667	11.746	0.14192	2.16576	0.42729
4U 1820-30	0.18192	1.58	11.1335	0.14191	2.41093	0.42760
Cen X-3	0.20456	1.49	10.449	0.14259	2.71097	0.42759
EXO 1785-248	0.268727	1.30	9.1604	0.14191	3.56136	0.42758
LMC X-4	0.41910	1.04	7.33	0.14188	5.55421	0.42722

Chapter 5

Relativistic stars with conformal symmetry

5.1 Introduction

A conformal symmetry in spacetime places restrictions on the gravitational potentials. This happens because in the presence of a conformal Killing vector, null geodesics are mapped to null geodesics; the change in the metric is proportional to the metric as it is Lie dragged along a congruence of curves. A conformal symmetry generates conserved quantities for photons. Several researchers have studied the Einstein equations for neutral matter and the Einstein-Maxwell equations for charged matter with a conformal symmetry. Exact solutions generated in this way are useful in relativistic astrophysics and may be used to model dense stars. Most studies in conformal motions have been completed in spherically symmetric spacetimes because of potential applications in cosmology and astrophysics.

Conformal motions in static spherically symmetric spacetimes have been extensively studied by Maartens *et al* (1995, 1996) and Tupper *et al* (2012). It has been pointed out that static spherical geometries do admit conformal symmetries which are nonstatic. A recent comprehensive treatment of conformal symmetries

in astrophysics, utilizing the Weyl tensor for conformally flat and non-conformally flat metrics, was completed by Manjonjo *et al* (2017). Several authors have used conformal symmetries to model compact objects in a general relativistic setting. Herrera *et al* (1984) and Herrera and Ponce (1985a, 1985b, 1985c), Maartens and Maharaj (1990) and Mak and Harko (2004) have modelled charged imperfect fluids in the presence of a conformal symmetry. New classes of compact stars with conformal symmetry and a linear equation of state were found by Esculpi and Aloma (2010). Rahaman *et al* (2017) and Shee *et al* (2016) studied anisotropic stars with a non-static conformal vector and a specific spacetime geometry. Clearly the assumption of a conformal symmetry has been useful in generating realistic astrophysical models.

In generating a stellar model, an equation of state should be imposed on the star based on physical considerations. However in our approach we have specified one of the gravitational potentials to yield an exact solution to the Einstein field equations with anisotropic matter distributions. This is an alternative approach using the gravitational metric rather than the equation of state arising from the microphysics. Our approach leads to an exact model with reasonable physical features. The presence of anisotropic pressure affects the values of the stellar mass, luminosity and other physical quantities. The investigations of Herrera and Santos (1997) indicate that local anisotropic pressure provides stability to the stellar sphere. It was showed by Dev and Gleiser (2002) that the structure and physical properties of stellar bodies are affected in the presence of anisotropy. The mass and surface redshift may vary depending on the nature of the anisotropic pressure. Gleiser and Dev (2004) demonstrated for smaller adiabatic indices associated with anisotropy that the stellar sphere becomes more stable when compared with isotropic pressure. Ruderman (1972) showed that in the high density range of order 10^{15}gcm^{-3}, where the nuclear interactions are relativistic, the distribution of matter is likely to be anisotropic. The presence of anisotropy has an important effect on the physical properties, stability and configuration of stellar matter distributions. It is interesting to observe that an equation of state may arise in particular models, involving the

radial pressure, by assuming special forms of the metrics in the spacetime geometry. Mafa Takisa and Maharaj (2013b) showed that solutions are possible with a quadratic equation of state relating the radial pressure to the energy density. Varela *et al* (2010) established a general approach indicating the role played by an equation of state in the process of dealing with anisotropic matter. Linear relationships involving radial pressure and the energy density exist in anisotropic stellar models of Mafa Takisa *et al* (2014a), Sunzu *et al* (2014a, 2014b) and Kileba Matondo and Maharaj (2016). Recently, a new approach with anisotropic pressure has been investigated with the Finch and Skea geometry by Maharaj *et al* (2016) and Kileba Matondo *et al* (2017).

Anisotropic pressure plays a prominent role in many processes in relativistic astrophysics. Weber (1999) has showed that the variation of the magnetic field intensity during the post main sequence of development of neutron stars, enables the matter distribution to produce pressure anisotropy. Several phenomena have been presented previously to describe the existence of anisotropic pressure inside the star. Kippenhahn and Weigert (1990) argue that the presence of anisotropic pressure within a stellar object is likely due to the presence of a solid core or the stellar fluid is a type-3A superfluid. Within the stellar object, pressure anisotropy could have arisen from several phase transitions and pion condensation as showed by Sokolov (1980) and Sawyer (1972). Sawyer and Scalapino (1973) have shown that when elementary particles such as pions condense, the anisotropic pressure has to be taken into account to describe a pion condensed phase configuration from the geometry of the π^{-1} modes. Bowers and Liang (1974) have studied the role played by the presence of anisotropy to describe stellar objects in relativistic astrophysics, and the effects arising on the physical quantities such as the compactness factor, redshift, mass and radius. Ivanov (2002) pointed out the link between the anisotropy and the redshift, and obtained higher surface redshifts when the strong energy condition and the dominant energy condition are satisfied. For stellar objects with high densities greater than nuclear matter density, it is required that the Tolman-Oppenheimer-Volkov

equation describing the equilibrium condition for charged fluid elements subject to gravitational, electric and hydrostatic forces, to be modified because of another interaction force due to the pressure anisotropy within the star. It was suggested by Usov (2004) that the existence of strong electric field could be generated by the presence of anisotropy. Sharma and Maharaj (2007) shown that in the presence of pressure anisotropy, compact stellar objects can be generated with a linear equation of state which can be applied to strange stars with quark matter. Recently, a class of static spherically symmetric objects with high anisotropic pressure in Tolman VII spacetime has been investigated by Bhar *et al* (2015). A model for compact star with large pressure anisotropy which satifies all physical requirements and causality conditions has been produced by Thirukkanesh and Ragel (2014).

The usual approach in the modelling process is to restrict the conformal symmetry or assume a functional form for the metric functions. This approach is ad hoc. Manjonjo *et al* (2017) have shown that the existence of a conformal Killing vector implies a relationship relating the gravitational potentials. This provides a systematic method of generating solutions of the Einstein and Einstein-Maxwell systems of field equations. We use the relationship of Manjonjo *et al* (2017) to find new classes of exact solutions with an anisotropic matter distribution in terms of simple elementary functions and study their physical features. We show that the exact solutions obtained are physically reasonable and may be related to observed astrophysical objects.

Solutions of dense relativistic stars found with conformal symmetry often have a singularity at the stellar centre. We seek exact solutions of the Einstein field equations which are regular at the centre. We select forms of the metric functions that enable the conformal relation of Manjonjo *et al* (2017) to be integrated. This helps to eliminate the singularity at the centre. In §5.2 the Einstein field equations are given. In §5.3 we give the conformal relationship between the potentials derived in Manjonjo *et al* (2017). Polynomial forms for one of the potentials enable the conformal relation to be integrated. Three classes of metrics which are regular at

the centre are found in §5.4, §5.5 and §5.6. In §5.7, we use the metric potentials, obtained in §5.4, to generate an exact solution to Einstein field equations. In §5.8, we study the physical features of the model. The matter variables and other physical quantities are also plotted for a particular choice of parameter values.

5.2 Field equations

The gravitational field in spherically symmetric spacetimes, modelling the interior of a static relativistic star, is given by

$$ds^2 = -e^{2\nu(r)}dt^2 + e^{2\lambda(r)}dr^2 + r^2(d\theta^2 + \sin^2\theta d\phi^2). \tag{5.1}$$

The expressions $\lambda(r)$ and $\nu(r)$ are arbitrary functions and represent gravity. The tensor $\mathbf{T}$ corresponds to energy momentum and has the general form

$$T_{ab} = \mathrm{diag}\left(-\rho,\ p_r,\ p_t,\ p_t\right), \tag{5.2}$$

where the quantities ρ, p_r, p_t and E are the energy density, radial pressure and tangential pressure respectively. Then the Einstein system of equations can be written in the form

$$\frac{1}{r^2}\left[r(1-e^{-2\lambda})\right]' = 8\pi\rho, \tag{5.3a}$$

$$-\frac{1}{r^2}(1-e^{-2\lambda}) + \frac{2\nu'}{r}e^{-2\lambda} = 8\pi p_r, \tag{5.3b}$$

$$e^{-2\lambda}\left(\nu'' + \nu'^2 + \frac{\nu'}{r} - \nu'\lambda' - \frac{\lambda'}{r}\right) = 8\pi p_t, \tag{5.3c}$$

in terms of the coordinate r. Primes denote differentiation with respect to r. We are using units in which $G = c = 1$.

The Durgapal and Bannerji (1983) form of the Einstein field equations is obtained if we introduce the transformation

$$x = Cr^2, \quad Z(x) = e^{-2\lambda(r)}, \quad A^2y^2(x) = e^{2\nu(r)}, \tag{5.4}$$

where A and C are constants. In terms of the new variables the line element (5.1) has the form

$$ds^2 = -A^2y^2(x)dt^2 + \frac{1}{4CxZ(x)}dx^2 + \frac{x}{C}\left(d\theta^2 + \sin^2\theta d\phi^2\right). \tag{5.5}$$

The field equations (5.3) become

$$\frac{8\pi\rho}{C} = -2\dot{Z} + \frac{1-Z}{x}, \tag{5.6a}$$

$$\frac{8\pi p_r}{C} = 4Z\frac{\dot{y}}{y} + \frac{Z-1}{x}, \tag{5.6b}$$

$$\frac{8\pi p_t}{C} = 4xZ\frac{\ddot{y}}{y} + (4Z + 2x\dot{Z})\frac{\dot{y}}{y} + \dot{Z}, \tag{5.6c}$$

which is an equivalent form. The mass contained within a radius x of the spherical star is given by the expression

$$M(x) = \frac{2\pi}{C^{3/2}}\int_0^x \sqrt{\omega}\rho(\omega)\, d\omega, \tag{5.7}$$

which is sometimes called the mass function.

5.3 Physical models

The field equations are highly nonlinear. If the spacetime manifold admits a symmetry then this often leads to simplification and an exact solution. For a conformal Killing vector to exist we have the requirement

$$\mathscr{L}_{\mathbf{X}}g_{ab} = 2\psi g_{ab}, \tag{5.8}$$

on the metric tensor field g_{ab}. Here $\mathscr{L}_{\mathbf{X}}$ is the Lie derivative along the integral curves of the vector field $\mathbf{X}$ and $\psi(x^a)$ is the conformal factor. The condition (5.8) places restrictions on the quantities associated with the spacetime curvature. In particular for the Ricci tensor R_{ab} and the Ricci scalar R we obtain respectively

$$\mathscr{L}_{\mathbf{X}}R_{ab} = 2\psi_{;ab} - g_{ab}\Box\psi, \tag{5.9a}$$

$$\mathscr{L}_{\mathbf{X}}R = -2\psi R - 6\Box\psi, \tag{5.9b}$$

where $\Box\psi = g^{ab}\psi_{;ab}$. Then the Einstein field equations $R_{ab} - \frac{1}{2}Rg_{ab} = 8\pi T_{ab}$ place restrictions on the matter variables in the presence of the conformal symmetry. The explicit conditions on the matter variables are given by Maartens *et al* (1986) and Coley and Tupper (1990).

It is required to make a choice for the gravitational potentials to generate a new class of solution to the Einstein system of equations. A variety of choices can be made that lead to physical models. Here we use the fact that the line element (5.1) admits conformal symmetries. If a conformal symmetry exists then the potentials ν and λ are related by

$$e^{\nu} = \tilde{a}r\cosh\left(b\int\frac{e^{\lambda}}{r}dr + c\right), \tag{5.10}$$

where $\tilde{a}$, b, c are constants. The result (5.10) was established by Manjonjo *et al* (2017). Combining (5.10) and the transformations (5.4), the relationship between y and Z can be written as

$$y = a\sqrt{x}\cosh\left(\frac{b}{2}\int\frac{dx}{x\sqrt{Z}} + c\right), \tag{5.11}$$

where $a = \tilde{a}/A\sqrt{C}$ is a real constant. Particular choices of the gravitational potential Z allow us to integrate (5.11) and find exact solutions to the Einstein system of equations.

There have been several exact solutions with anisotropy and conformal symmetry that have been found including the recent works of Shee *et al* (2016) and Rahaman *et al* (2017). Here we show that other classes of exact models are admitted by the field equations with this geometric feature. The advantage of our approach is that the gravitational potentials have a simple form: the function $Z(x)$ can be written as a polynomial which helps to simplify the physical analysis. We consider the three polynomial functions:

(a) Case I: $Z = [(1 + dx)(1 + ex)]^2$

(b) Case II: $Z = (1 + ex + dx^2)^2$

(c) Case III: $Z = [(1 + nx)(1 + ex + dx^2)]^2$

The coefficients and degree of the polynomial in $Z(x)$ have been chosen so that integration is possible to yield elementary functions in (5.11). It is important to observe that the above choices for the function Z are physically reasonable. The forms for Z are all regular at the centre of the star and well behaved in the interior. They yield stellar models with desirable features which correspond to stellar objects as we show in §5.8. Many other forms of Z have been selected in the past as indicated in the works of Kiess (2012), Fatema and Murad (2013) and Murad (2016). Our polynomial forms for Z are new, make exact integration of the field equations possible and yield stars which are physically reasonable. The integration of the field equations is considered in the subsequent sections. It turns out that there are forms for the second gravitational potential $y(x)$ which are also regular at the centre. Regularity at the centre is a desirable feature in a stellar model. Many of the exact solutions with conformal symmetry that have been found in the past exhibit singularities at the stellar centre for the potentials.

5.4 Class I metrics

In this case, we assume that the gravitational potential has the form

$$Z = [(1+dx)(1+ex)]^2 . \tag{5.12}$$

Using the gravitational potential (5.12), the integration in (5.11) can be performed depending on the value of $d-e$. When $d \neq e$ we obtain

$$\begin{aligned} y(x) &= \frac{a\sqrt{x}}{2K}\left[K^2 x^{\frac{b}{2}}(1+dx)^{\frac{-bd}{2(d-e)}}(1+ex)^{\frac{eb}{2(d-e)}}\right. \\ &\left. +x^{-\frac{b}{2}}(1+ex)^{\frac{-be}{2(d-e)}}(1+dx)^{\frac{bd}{2(d-e)}}\right], \end{aligned} \tag{5.13}$$

where K is new constant. When $d=e$, the potential Z is

$$Z = (1+ex)^4 , \tag{5.14}$$

and (5.11) yields

$$y(x) = \frac{a\sqrt{x}}{2K}\left[K^2\left(-\frac{bex}{1+ex}\right)^{\frac{b}{2}}\exp\left(\frac{b}{2(1+ex)}\right)\right.$$

$$+\left(-\frac{1+ex}{bex}\right)^{\frac{b}{2}}\exp\left(-\frac{b}{2(1+ex)}\right)\Bigg]. \tag{5.15}$$

We observe from (5.13) and (5.15) that when $b=-1$ the potential y is regular at the centre $x=0$. We present the metric potentials in Table 5.1 for $d-e=\frac{1}{2}, d-e\gtrless\frac{1}{2}$ and $d=e$ in terms of both variables x and r.

5.5 Class II solutions

In this case, we consider the gravitational potential in the form

$$Z = \left(1+ex+dx^2\right)^2. \tag{5.16}$$

The integration in (5.11) is possible depending on the value of e^2-4d. It is convenient to introduce the new parameters

$$\alpha = \frac{e-\sqrt{e^2-4d}}{2d}, \tag{5.17a}$$

$$\beta = \frac{e+\sqrt{e^2-4d}}{2d}, \tag{5.17b}$$

in terms of e and d. When $e^2-4d<0$ then complex quantities arise which we neglect. We take $e^2-4d>0$. With $e^2>4d$ we get

$$\begin{aligned} y(x) = \frac{a\sqrt{x}}{2K}\Big[&K^2x^{\frac{b}{2\alpha\beta}}(\alpha+x)^{\frac{b}{2\alpha(\alpha-\beta)}}(\beta+x)^{-\frac{b}{2\beta(\alpha-\beta)}} \\ &+x^{-\frac{b}{2\alpha\beta}}(\alpha+x)^{-\frac{b}{2\alpha(\alpha-\beta)}}(\beta+x)^{\frac{b}{2\beta(\alpha-\beta)}}\Big], \end{aligned} \tag{5.18}$$

where K is a new constant. We note from (5.18) that with $b=-\alpha\beta$, the sphere is regular at the centre. When $e^2-4d=0$ the potential Z becomes

$$Z = \left(1+2\sqrt{d}x+dx^2\right)^2, \tag{5.19}$$

and (5.11) gives the function

$$y(x) = \frac{a}{2K}\left[\frac{K^2x^{\frac{b+1}{2}}}{(1+\sqrt{d}x)^{\frac{b}{2}}}\exp\left(\frac{b}{2(1+\sqrt{d}x)}\right)\right.$$

$$+\frac{(1+\sqrt{d}x)^{\frac{b}{2}}}{x^{\frac{b-1}{2}}}\exp\left(-\frac{b}{2(1+\sqrt{d}x)}\right)\Bigg]. \tag{5.20}$$

In this situation (5.20) is regular at the centre when $b=-1$. We present the metric potentials in Table 5.2 for $e^2-4d=0$ and $e^2-4d>0$ for both variables x and r.

5.6 Class III solutions

For this case we take the gravitational potential in the form

$$Z = \left[(1+nx)(1+ex+dx^2)\right]^2. \tag{5.21}$$

Then the integration in (5.11) can be done depending on the value of e^2-4d. We take

$$\alpha = \frac{e-\sqrt{e^2-4d}}{2d}, \tag{5.22a}$$

$$\beta = \frac{e+\sqrt{e^2-4d}}{2d}, \tag{5.22b}$$

as the new parameters expressed in terms of e and d. When $e^2-4d<0$ we obtain complex quantities, therefore this case is neglected in our study. With $e^2-4d>0$ we have

$$y(x) = \frac{a\sqrt{x}}{2K}\Bigg[\frac{K^2x^{\frac{b}{2\alpha\beta}}(\beta+x)^{\frac{b}{2\beta(\alpha-\beta)(n\beta-1)}}}{(1+nx)^{\frac{n^2b}{2(n\alpha-1)(n\beta-1)}}(\alpha+x)^{\frac{b}{2\alpha(n\alpha-1)(\alpha-\beta)}}} +\frac{(1+nx)^{\frac{n^2b}{2(n\alpha-1)(n\beta-1)}}(\alpha+x)^{\frac{b}{2\alpha(n\alpha-1)(\alpha-\beta)}}}{x^{\frac{b}{2\alpha\beta}}(\beta+x)^{-\frac{b}{2\beta(\alpha-\beta)(n\beta-1)}}}\Bigg], \tag{5.23}$$

where K is a new constant. It is convenient to know from (5.23) that with $b=-\alpha\beta$ the potential is regular at the centre. For $e^2-4d=0$, the potential Z takes the form

$$Z = \left[(1+nx)(1+2\sqrt{d}x+dx^2)\right]^2, \tag{5.24}$$

and (5.11) becomes

$$y(x) = \frac{a}{2K}\Bigg[\frac{K^2x^{\frac{b+1}{2}}(1+\sqrt{d}x)^{\frac{b(2n\sqrt{d}-d)}{2(\sqrt{d}-n)^2}}}{(1+nx)^{\frac{bn^2}{2(\sqrt{d}-n)^2}}}\exp(E)$$

$$+\frac{(1+nx)^{\frac{bn^2}{2(\sqrt{d}-n)^2}}}{x^{\frac{b-1}{2}}(1+\sqrt{d}x)^{\frac{b(2n\sqrt{d}-d)}{2(\sqrt{d}-n)^2}}}\exp\left(E\right)\Bigg], \tag{5.25}$$

where $E=\frac{b\sqrt{d}}{2(\sqrt{d}-n)(1+\sqrt{d}x)}$. So then, (5.25) is regular at the centre when we set $b=-1$. We present the metric potentials in Table 5.3 for $e^2-4d=0$ and $e^2-4d>0$ for both variables x and r.

Table 5.1 – Potentials for Class I models.

Case	Condition	Potentials in terms of x	Potentials in terms of r
Ia	$d-e=\frac{1}{2}$	$y = \frac{a}{2K}\left[\frac{K^2\left(1+(e+\frac{1}{2})x\right)^{(e+\frac{1}{2})}}{(1+ex)^e} + \frac{x(1+ex)^e}{\left(1+(e+\frac{1}{2})x\right)^{(e+\frac{1}{2})}}\right]$ $Z = \left[(1+(e+\frac{1}{2})x)\,(1+ex)\right]^2$	$e^{2\nu} = \frac{a^2A^2}{4K^2} \times\left[\frac{K^2\left(1+C(e+\frac{1}{2})r^2\right)^{(e+\frac{1}{2})}}{(1+eCr^2)^e} + \frac{Cr^2\left(1+eCr^2\right)^e}{\left(1+C(e+\frac{1}{2})r^2\right)^{(e+\frac{1}{2})}}\right]^2$ $e^{2\lambda} = \left[1+C(e+\frac{1}{2})r^2\right]^{-2} \times(1+eCr^2)^{-2}$
Ib	$d-e\gtrless\frac{1}{2}$	$y = \frac{a}{2K} \times\left[K^2\left(\frac{(1+dx)^d}{(1+ex)^e}\right)^{\frac{1}{2(d-e)}} +x\left(\frac{(1+ex)^e}{(1+dx)^d}\right)^{\frac{1}{2(d-e)}}\right]$ $Z = \left[(1+dx)\,(1+ex)\right]^2$	$e^{2\nu} = \frac{a^2A^2}{4K^2} \times\left[K^2\left(\frac{(1+dCr^2)^d}{(1+eCr^2)^e}\right)^{\frac{1}{2(d-e)}} +Cr^2\left(\frac{(1+eCr^2)^e}{(1+dCr^2)^d}\right)^{\frac{1}{2(d-e)}}\right]^2$ $e^{2\lambda} = \left[(1+dCr^2)\,(1+eCr^2)\right]^{-2}$
Id	$d=e$	$y = \frac{a}{2K} \times\left[K^2\left(\frac{-e}{1+ex}\right)^{-\frac{1}{2}}\exp\left(\frac{-1}{2(1+ex)}\right) +\left(\frac{-e}{1+ex}\right)^{\frac{1}{2}}x\exp\left(\frac{1}{2(1+ex)}\right)\right]$ $Z = (1+ex)^4$	$e^{2\nu} = \frac{a^2A^2Cr^2}{4K^2} \times\left[K^2\left(\frac{-beCr^2}{1+eCr^2}\right)^{\frac{b}{2}}\exp\left(\frac{b}{2(1+eCr^2)}\right) +\left(-\frac{1+eCr^2}{beCr^2}\right)^{\frac{b}{2}}\exp\left(\frac{-b}{2(1+eCr^2)}\right)\right]^2$ $e^{2\lambda} = (1+eCr^2)^{-4}$

Table 5.2 – Potentials for Class II models.

Case	Condition	Potentials in terms of x	Potentials in terms of r
IIa	$e^2-4d=0$	$y = \frac{a}{2K} \times \left[\frac{K^2}{(1+\sqrt{d}x)^{\frac{-1}{2}}}\exp\left(\frac{-1}{2(1+\sqrt{d}x)}\right) + \frac{x}{(1+\sqrt{d}x)^{\frac{1}{2}}}\exp\left(\frac{1}{2(1+\sqrt{d}x)}\right)\right]$ $Z = \left(1+2\sqrt{d}x+dx^2\right)^2$	$e^{2\nu} = \frac{a^2}{4K^2} \times \left[\frac{K^2}{(1+\sqrt{d}Cr^2)^{\frac{-1}{2}}}\exp\left(\frac{-1}{2(1+\sqrt{d}Cr^2)}\right) + \frac{x}{(1+\sqrt{d}Cr^2)^{\frac{1}{2}}}\exp\left(\frac{1}{2(1+\sqrt{d}Cr^2)}\right)\right]^2$ $e^{2\lambda} = \left(1+2\sqrt{d}Cr^2+dC^2r^4\right)^{-2}$
IIb	$e^2-4d>0$	$y = \frac{a}{2K}\left[K^2\left(\frac{(\beta+x)^\alpha}{(\alpha+x)^\beta}\right)^{\frac{1}{2(\alpha-\beta)}} + x\left(\frac{(\alpha+x)^\beta}{(\beta+x)^\alpha}\right)^{\frac{1}{2(\alpha-\beta)}}\right]$ $Z = (1+ex+dx^2)^2$	$e^{2\nu} = \frac{a^2}{4K^2}\left[K^2\left(\frac{(\beta+Cr^2)^\alpha}{(\alpha+Cr^2)^\beta}\right)^{\frac{1}{2(\alpha-\beta)}} + Cr^2\left(\frac{(\alpha+Cr^2)^\beta}{(\beta+Cr^2)^\alpha}\right)^{\frac{1}{2(\alpha-\beta)}}\right]^2$ $e^{2\lambda} = (1+eCr^2+dC^2r^4)^{-2}$

Table 5.3 – Potentials for Class III models.

Case	Condition	Potentials in terms of x	Potentials in terms of r
IIIa	$e^2-4d=0$	$y = \frac{aK(1+\sqrt{d}x)^{\frac{d-2n\sqrt{d}}{2(\sqrt{d}-n)^2}}}{2(1+nx)^{\frac{-n^2}{2(\sqrt{d}-n)^2}}} \times \exp\left(\frac{-\sqrt{d}}{2(\sqrt{d}-n)(1+\sqrt{d}x)}\right) + \frac{ax(1+nx)^{\frac{-n^2}{2(\sqrt{d}-n)^2}}}{2K(1+\sqrt{d}x)^{\frac{d-2n\sqrt{d}}{2(\sqrt{d}-n)^2}}} \times \exp\left(\frac{\sqrt{d}}{2(\sqrt{d}-n)(1+\sqrt{d}x)}\right)$ $Z = (1+nx)^2 \times \left(1+2\sqrt{d}x+dx^2\right)^2$	$e^{2\nu} = \frac{a^2(1+\sqrt{d}Cr^2)^{\frac{d-2n\sqrt{d}}{2(\sqrt{d}-n)^2}}}{4K^2\exp\left(\frac{-\sqrt{d}}{2(\sqrt{d}-n)(1+\sqrt{d}Cr^2)}\right)} \times \left[\frac{K^2\exp\left(\frac{-\sqrt{d}}{(\sqrt{d}-n)(1+\sqrt{d}Cr^2)}\right)}{(1+nCr^2)^{\frac{-n^2}{2(\sqrt{d}-n)^2}}} + \frac{Cr^2(1+nCr^2)^{\frac{-n^2}{2(\sqrt{d}-n)^2}}}{(1+\sqrt{d}Cr^2)^{\frac{d-2n\sqrt{d}}{(\sqrt{d}-n)^2}}}\right]^2$ $e^{2\lambda} = (1+nCr^2)^{-2} \times \left(1+2\sqrt{d}Cr^2+dC^2r^4\right)^{-2}$
IIIb	$e^2-4d>0$	$y = \frac{a(\alpha+x)^{\frac{\beta}{2(n\alpha-1)(\alpha-\beta)}}}{2K(\beta+x)^{\frac{\alpha}{2(\alpha-\beta)(1-n\beta)}}} \times \left[\frac{K^2(1+nx)^{\frac{\alpha\beta n^2}{2(n\alpha-1)(n\beta-1)}}}{(\beta+x)^{\frac{\alpha}{(\alpha-\beta)(n\beta-1)}}} + \frac{x(1+nx)^{\frac{-\alpha\beta n^2}{2(n\alpha-1)(n\beta-1)}}}{(\alpha+x)^{\frac{\beta}{(n\alpha-1)(\alpha-\beta)}}}\right]$ $Z = (1+nx)^2 \times (1+ex+dx^2)^2$	$e^{2\nu} = \frac{a^2\left(\alpha+Cr^2\right)^{\frac{\beta}{(n\alpha-1)(\alpha-\beta)}}}{4K^2(\beta+Cr^2)^{\frac{\alpha}{(\alpha-\beta)(1-n\beta)}}} \times \left[\frac{K^2\left(1+nCr^2\right)^{\frac{\alpha\beta n^2}{2(n\alpha-1)(n\beta-1)}}}{(\beta+Cr^2)^{\frac{\alpha}{(\alpha-\beta)(n\beta-1)}}} + \frac{Cr^2\left(1+nCr^2\right)^{\frac{-\alpha\beta n^2}{2(n\alpha-1)(n\beta-1)}}}{(\alpha+Cr^2)^{\frac{\beta}{(n\alpha-1)(\alpha-\beta)}}}\right]^2$ $e^{2\lambda} = (1+nCr^2)^{-2} \times (1+eCr^2+dC^2r^4)^{-2}$

5.7 Exact solutions

We have generated a number of metrics in terms of elementary functions in §5.4-§5.6. These metrics may be used to give the solution of the Einstein field equations for all geometrical and matter variables. We illustrate this with an example taken from §5.4. We use Case Ib from Table 5.1 with $d-e<\frac{1}{2}$. Then the potentials and matter quantities can be written in terms of the coordinate r:

$$e^{2\lambda} = \frac{1}{\left[(1+dCr^2)\,(1+eCr^2)\right]^2}, \tag{5.26a}$$

$$e^{2\nu} = \frac{a^2A^2}{4K^2} \times\left[K^2\left(\frac{(1+dCr^2)^d}{(1+eCr^2)^e}\right)^{\frac{1}{2(d-e)}}+Cr^2\left(\frac{(1+eCr^2)^e}{(1+dCr^2)^d}\right)^{\frac{1}{2(d-e)}}\right]^2, \tag{5.26b}$$

$$\frac{8\pi\rho}{C} = -d^2Cr^2(1+eCr^2)(5+9eCr^2) -2d(1+eCr^2)(3+7eCr^2)-e(6+5eCr^2), \tag{5.26c}$$

$$\frac{8\pi p_r}{C} = d^2e^2C^3r^6+2dC^2r^4\left(de+e^2\right)+Cr^2\left(d^2+4de+e^2\right) +2(d+e)+\left[\frac{2(1+dCr^2)(1+eCr^2)}{k^2(1+dCr^2)^{\frac{d}{d-e}}+Cr^2(1+eCr^2)^{\frac{e}{d-e}}}\right] \times\left[(1+eCr^2)^{\frac{e}{d-e}}(2+(d+e+deCr^2)Cr^2) +k^2(d+e+deCr^2)(1+dCr^2)^{\frac{d}{d-e}}\right], \tag{5.26d}$$

$$\frac{8\pi p_t}{C} = d^2(1+eCr^2)(5+9eCr^2)Cr^2 +2d(1+eCr^2)(4+7eCr^2)+e(8+5eCr^2) +\left[4(1+dCr^2)^{\frac{d}{e-d}}(1+eCr^2)^{\frac{e}{d-e}}-4dk^2(1+eCr^2)-4ek^2\right] \times\left[\frac{1}{Cr^2(1+dCr^2)^{\frac{d}{e-d}}(1+eCr^2)^{\frac{e}{d-e}}+k^2}\right], \tag{5.26e}$$

in terms of elementary functions.

It is now possible to generate several physical quantities associated with the exact model (5.26). We can compute the mass function explicitly from (5.7). Then

the total mass of the anisotropic star within the radius r has the form

$$\begin{aligned} M(r) &= -\frac{1}{6}Cr^3\left[6(d+e)+5\left(d^2+4de+e^2\right)Cr^2\right. \\ &\quad \left.+14de(d+e)C^2r^4+9d^2e^2C^3r^6\right]. \end{aligned} \tag{5.27}$$

The compactness factor is defined as

$$\mu = \frac{M(r)}{r}. \tag{5.28}$$

For this model it is given by

$$\begin{aligned} \mu(r) &= -\frac{1}{6}Cr^2\left[6(d+e)+5\left(d^2+4de+e^2\right)Cr^2\right. \\ &\quad \left.+14de(d+e)C^2r^4+9d^2e^2C^3r^6\right]. \end{aligned} \tag{5.29}$$

The surface redshift function corresponding to the compactness mass μ is given by

$$Z_s = (1-2\mu)^{\frac{1}{2}} - 1. \tag{5.30}$$

Using (5.29), we obtain

$$\begin{aligned} Z_s &= \sqrt{3}\left[3+\left(9d^2e^2C^3r^6+14de(d+e)C^2r^4\right)Cr^2\right. \\ &\quad \left.+\left(6(d+e)+5(d^2+4de+e^2)Cr^2\right)Cr^2\right]^{-\frac{1}{2}}-1. \end{aligned} \tag{5.31}$$

It is possible to study the stability of the gravitating sphere in different ways. Firstly we can use the conservation matter related to the Tolman-Oppenheimer-Volkoff (TOV) equation which describes the equilibrium condition for an anisotropic fluid in the form

$$\frac{dp_r}{dr} = -(\rho+p_r)\frac{d\nu}{dr}+\frac{2}{r}(p_t-p_r). \tag{5.32}$$

We introduce the terms for the gravitational force $F_g = -(\rho+p_r)\frac{d\nu}{dr}$, hydrostatic force $F_h = -\frac{dp_r}{dr}$ and anisotropic force $F_a = \frac{2}{r}(p_t-p_r)$. Then the TOV equation can be expressed as

$$F_g + F_h + F_a = 0. \tag{5.33}$$

In our model

$$F_a = \frac{C^2r}{2\pi}\left(d^2+4de+e^2+4de(d+e)Cr^2+3d^2e^2C^2r^4\right), \tag{5.34}$$

$$
\begin{aligned}
F_g &= \frac{C^2 r}{4\pi}\left[-\left(\frac{2\left(1+eCr^2\right)^{\frac{e}{d-e}}}{k^2(1+dCr^2)^{\frac{d}{d-e}}+Cr^2(1+eCr^2)^{\frac{e}{d-e}}}\right)^2\right. \\
&\quad +d^2(1+eCr^2)(1+3eCr^2)+e^2+2de(3+2eCr^2) \\
&\quad \left.-\frac{4deK^2}{Cr^2\left(1+dCr^2\right)^{\frac{d}{e-d}}\left(1+eCr^2\right)^{\frac{e}{d-e}}+K^2}\right], \qquad (5.35) \\
F_h &= \frac{C^2 r}{4\pi}\left[\left(\frac{2\left(1+eCr^2\right)^{\frac{e}{d-e}}}{K^2(1+dCr^2)^{\frac{d}{d-e}}+Cr^2(1+eCr^2)^{\frac{e}{d-e}}}\right)^2\right. \\
&\quad -3d^2\left(1+eCr^2\right)\left(1+3eCr^2\right)-3e^2-2de(7+6eCr^2) \\
&\quad \left.+\frac{4deK^2}{Cr^2\left(1+dCr^2\right)^{\frac{d}{e-d}}\left(1+eCr^2\right)^{\frac{e}{d-e}}+K^2}\right], \qquad (5.36)
\end{aligned}
$$

and the anisotropic star is in equilibrium. Secondly the stability is related to the adiabatic condition

$$\Gamma = \frac{\rho + p_r}{p_r}\frac{dp_r}{d\rho} > \frac{4}{3}. \qquad (5.37)$$

To maintain stability this condition has to be satisfied according to Herrera (1992). Thirdly the condition

$$\left|{v_r}^2 - {v_t}^2\right| < 1, \qquad (5.38)$$

has to be satisfied to prevent cracking and overturning of the object.

5.8 Physical features

In this section we show that the particular solution to the Einstein field equations generated in §5.7 satisfies the physical requirements. To account for the physical units and dimensional homogeneity in the dynamical and geometrical variables it is convenient to rescale constants. Since the constants d and e are expressed in dimension $length^{-2}$, and K in dimension $length^{-1}$, we use the transformation

$$\tilde{d} = R^2 d, \quad \tilde{e} = R^2 e, \quad \tilde{K} = RK,$$

where R is the parameter of geometry with dimension of length. The geometrical and matter variables are given in (5.26). A simpler form is obtained by considering

a Taylor expansion. For the particular choices of parameter values $C = 0.00051$, $\tilde{d} = -0.2$, $\tilde{e} = -0.1$, $A = 5.3737$, $\tilde{K} = 1.1778$, $a = 2$ we get forms for the exact solution to the Einstein system by expanding them in terms up to order r^2 such that

$$e^{2\lambda} \approx 1 + 0.01226r^2, \tag{5.39a}$$

$$e^{2\nu} \approx 1 + 0.02332r^2, \tag{5.39b}$$

$$\frac{8\pi\rho}{C} \approx 0.03677 - 0.27 \times 10^{-3}r^2, \tag{5.39c}$$

$$\frac{8\pi p_r}{C} \approx 0.03439 - 0.72 \times 10^{-3}r^2, \tag{5.39d}$$

$$\frac{8\pi p_t}{C} \approx 0.03439 - 0.61 \times 10^{-3}r^2. \tag{5.39e}$$

These quantities show clearly that the gravitational potentials and matter variables are finite and regular at the centre and in the region nearby the centre. Our model is not singular in the interior of the star. The behaviour of the model may be studied with the help of this particular choice of parameter values used above. It is important to observe that we can generate stars from the exact solution (5.26) which are physically reasonable. For particular choices of the parameters we generate the central density ρ_c, radius r, mass M and compactness factor $\frac{M}{r}$ for the stars SAX J1808.4-3658, EXO 1785, Cen X-3, 4U1820-30, PSR J1903+327, Vela X-1 and PSR J1614-2230 in Table 5.4. We find that these values fall in the observed range. To analyse the behaviour of the matter variables and their stability throughout the star, we make a choice of two stars: PSR J1614-2230 and SAX J1808.4-3658. The choice of these two stellar bodies is motivated by the order of magnitude of their masses: the two masses correspond to the highest and lowest masses in Table 5.4. We keep the same values $\tilde{d} = -0.2$ and $\tilde{e} = -0.1$ while C, R and $\tilde{K}$ are free, to generate numerical values of masses, radii and central density.

The metric potentials $e^{2\nu}$ and $e^{2\lambda}$ are plotted in Fig. 5.1 for PSR J1614-2230 and SAX J1808.4-3658 and the profiles are regular at the centre and continuous everywhere inside the star. The profiles of the energy density ρ for PSR J1614-2230 and SAX J1808.4-3658 are plotted in Fig. 5.2, and show that the density function is

regular at the centre and monotonically decreasing with the radius. In Fig. 5.3 the radial and tangential pressures p_r and p_t are shown respectively for PSR J1614-2230 and SAX J1808.4-3658. They are positive, decreasing continuously inside the star. The radial pressure vanishes at $r = 10.79$ km for PSR J1614-2230 and $r = 7.68$ km for SAX J1808.4-3658. At the centre we observe that $p_r = p_t$ which ensures stability of the star. Similar profiles for the pressure can be observed in the works of Bhar *et al* (2015) and Thirukkanesh and Ragel (2014). The variation of anisotropy Δ is presented in Fig. 5.4. The profiles indicate for both bodies that the anisotropic pressure increases from the centre to the surface where it has a finite value. In our model the maximum values of the pressure anisotropy are $0.37 \times 10^{36}\text{dyne/cm}^2$ for PSR J1614-2230 and $0.11 \times 10^{36}\text{dyne/cm}^2$ for SAX J1808.4-3658 which are lower compared to the maximum value found by Thirukkanesh and Ragel (2014) given as $2.0978 \times 10^{48}\text{dyne/cm}^2$. A lower bound on the anisotropy is a desirable feature.

In Fig. 5.5 it is shown that the radial and tangential speeds of sound are greater than 0 and less than 1 for both stars PSR J1614-2230 and SAX J1808.4-3658. It is important to denote that the speed of sound is monotonically decreasing away from the centre and causality is maintained. It is clear that the null energy condition, the weak energy condition and the strong energy condition for PSR J1614-2230 and SAX J1808.4-3658 respectively are satisfied everywhere in the star. This is illustrated in Fig. 5.6. The variation of compactness factor and surface redshift are plotted in Fig. 5.7 and Fig. 5.8 respectively. The values of the compactness factor are consistent with real stars in Fig. 5.7. The redshift function is increasing with increase of μ as shown in Fig. 5.8. The Buchdahl (1959) limit $\frac{2M(r)}{r} < \frac{8}{9}$ is satisfied and numerically, we have $\frac{2M}{r} = 0.5396$ for PSR J1614-2230 and $\frac{2M}{r} = 0.3476$ for SAX J1808.4-3658. The surface redshift turns out to be $Z_s = 0.4739$ for PSR J1614-2230 and $Z_s = 0.2381$ for SAX J1808.4-3658 respectively, which are compatible with observations.

Fig. 5.9 refers to the cracking of the star as proposed by Herrera (1992) for stability. We observe that $0 < {v_r}^2 - {v_t}^2 < 1$ and $-1 < {v_t}^2 - {v_r}^2 < 0$. We plotted the adiabatic index Γ in Fig. 5.10. As we can observe, everywhere inside these two

compact stars Γ is greater than 4/3. We also investigated the stability of the model through TOV equation which describes the equilibrium condition for an anisotropic fluid subject to the gravitational, hydrostatic and anisotropic forces given in (5.33). Then Fig. 5.11 shows that the gravitational force is balanced by the joint action of hydrostatic and anisotropic forces for PSR J1614-2230 and SAX J1808.4-3658. Hence all three stability criteria are satisfied. In Fig. 5.12 we have plotted the variation of the mass versus radius for stellar objects PSR J1614-2230 and SAX J1808.4-3658. In both cases the mass function is a increasing quantity with increasing radius. In the first figure we find that the upper bound on the mass is 1.971 $M_{\odot}$, and for the second figure the upper bound is 0.903 $M_{\odot}$. These figures are consistent with observations and with our results in Table 5.4.

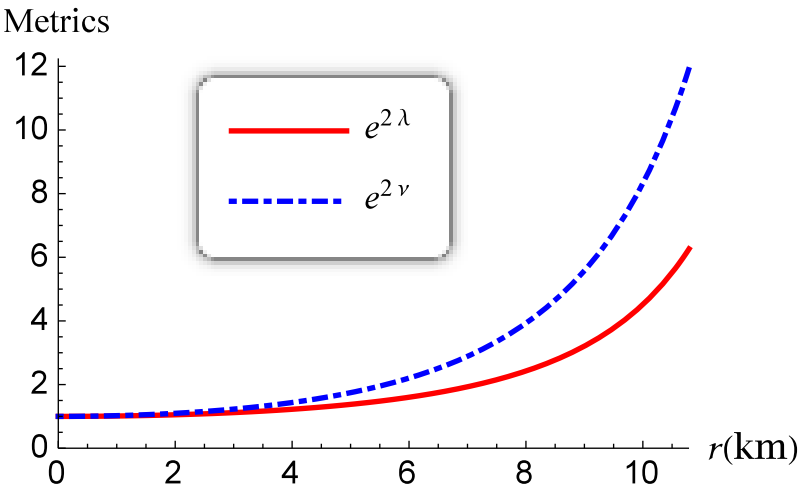

(a) PSRJ1614−2230

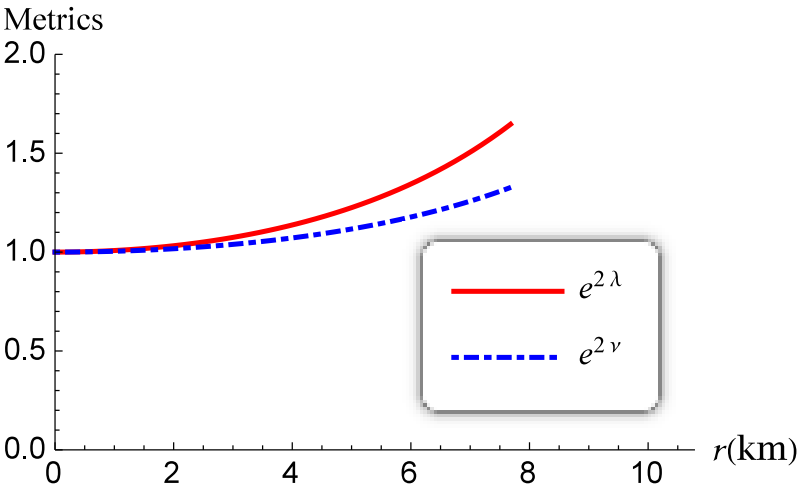

(b) SAX J1808.4−3658

Figure 5.1 – Variation of metric potentials versus the radius

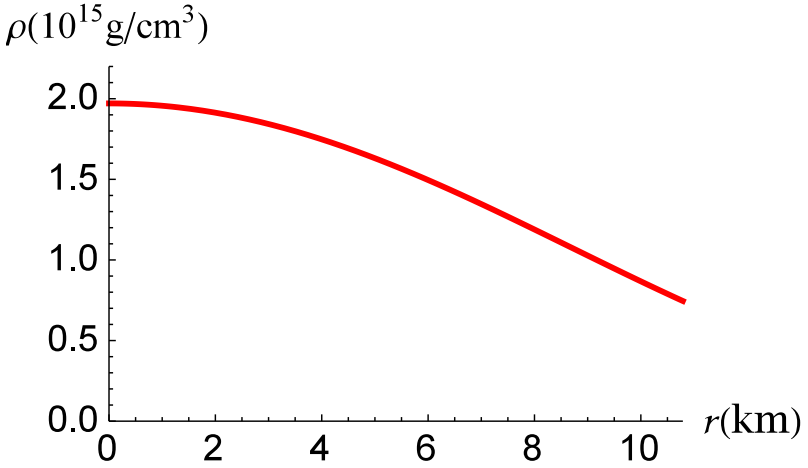

(a) PSRJ1614−2230

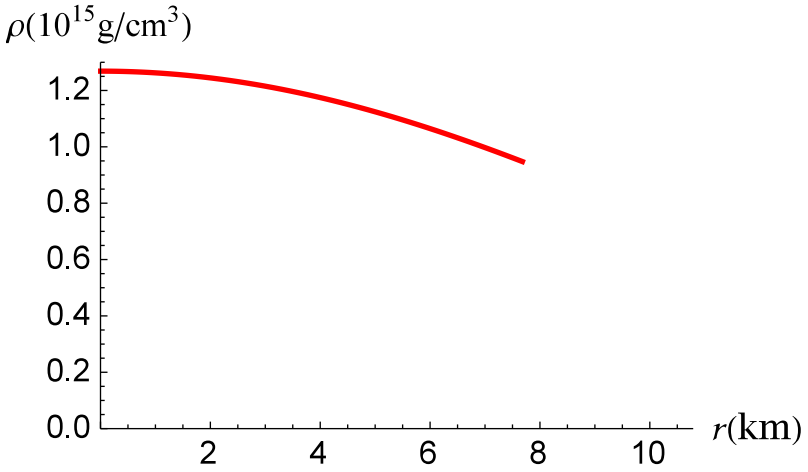

(b) SAX J1808.4−3658

Figure 5.2 – Variation of energy density versus the radius

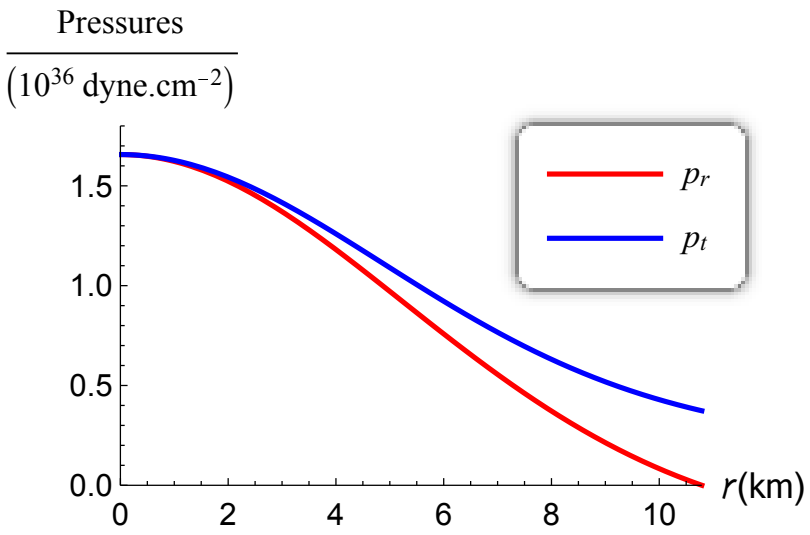

(a) PSRJ1614−2230

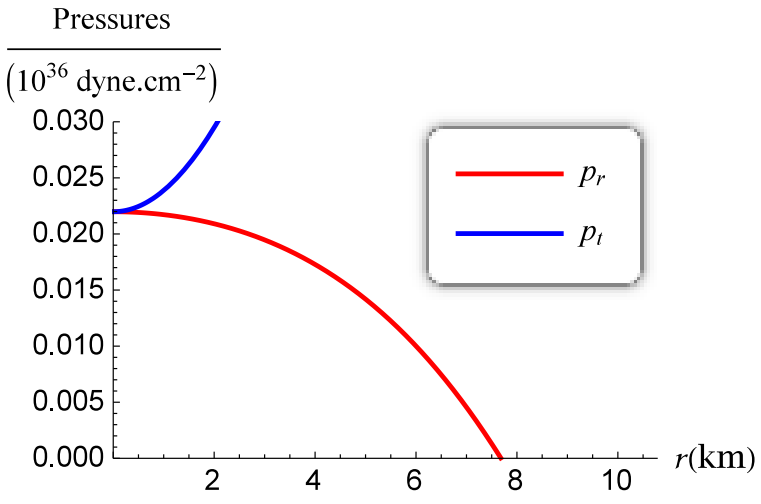

(b) SAX J1808.4−3658

Figure 5.3 – Variation of tangential and radial pressures versus the radius

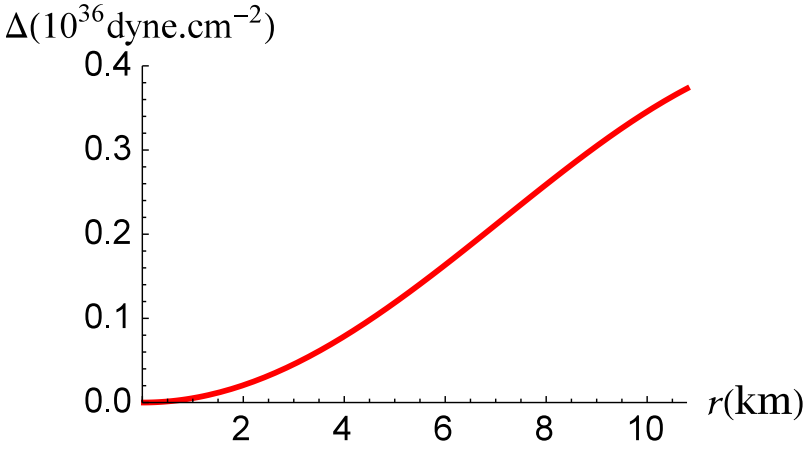

(a) PSRJ1614−2230

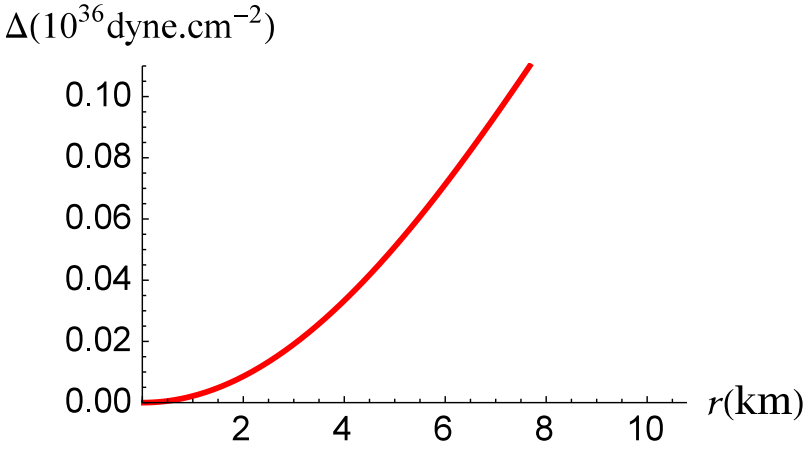

(b) SAX J1808.4−3658

Figure 5.4 – Variation of anisotropy versus the radius

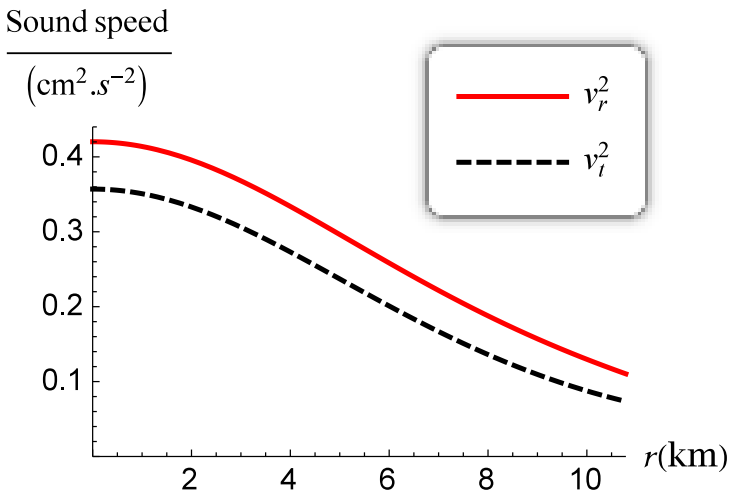

(a) PSRJ1614−2230

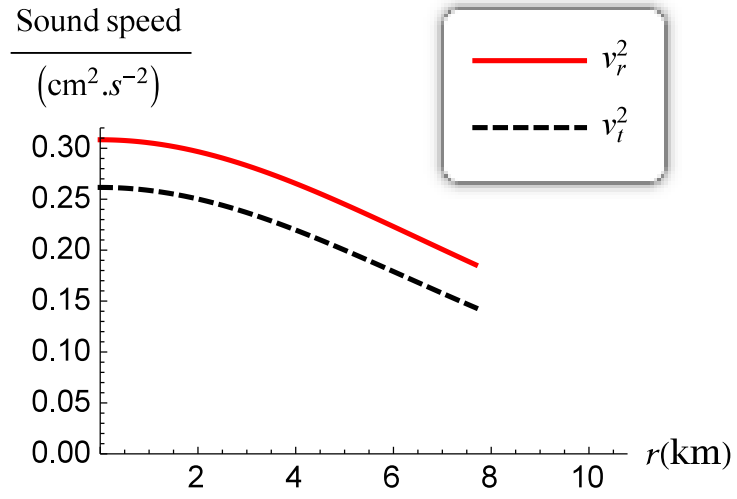

(b) SAX J1808.4−3658

Figure 5.5 – Variation of speed of sound versus the radius

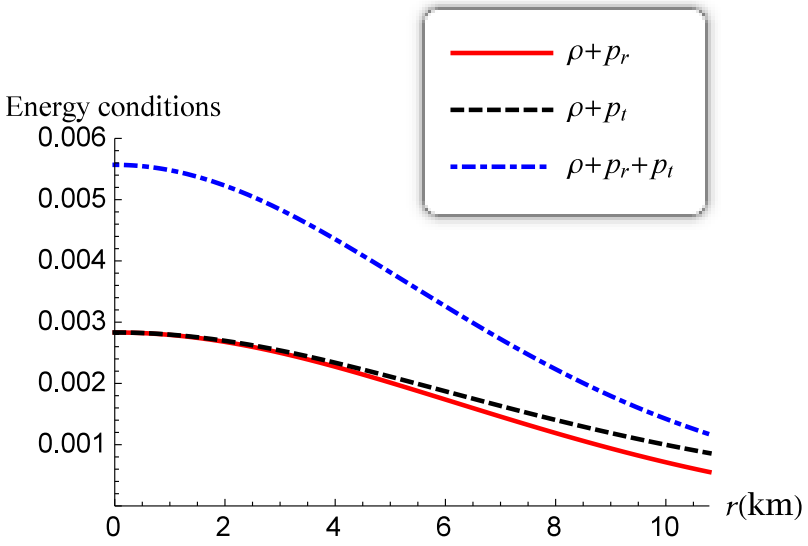

(a) PSRJ1614−2230

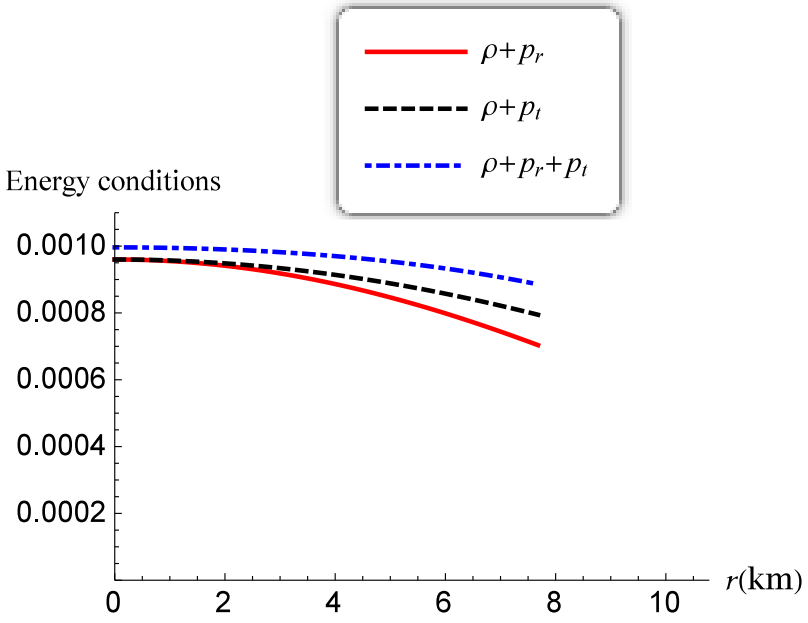

(b) SAX J1808.4−3658

Figure 5.6 – Variation of energy conditions versus the radius

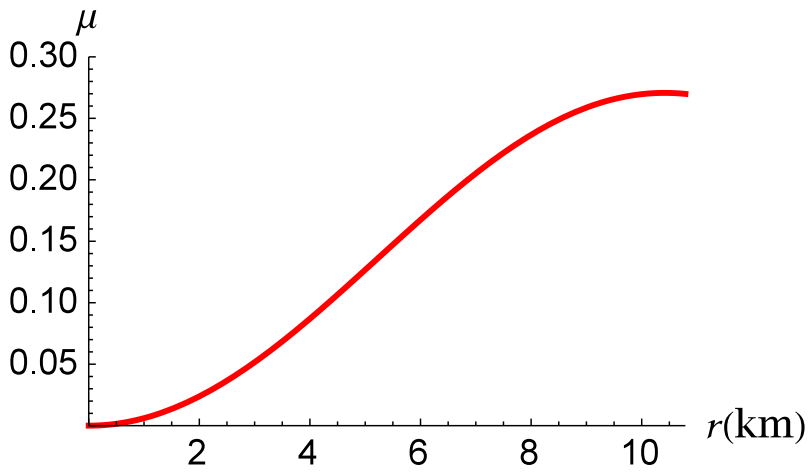

(a) PSRJ1614−2230

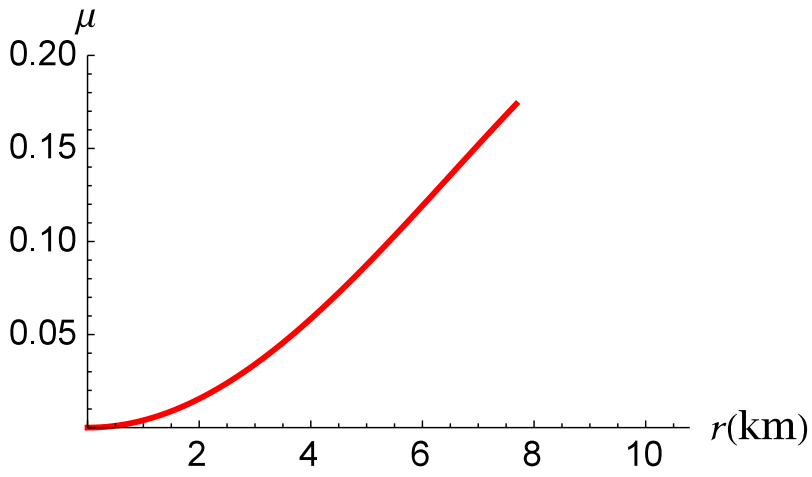

(b) SAX J1808.4−3658

Figure 5.7 – Variation of compactness factor versus the radius

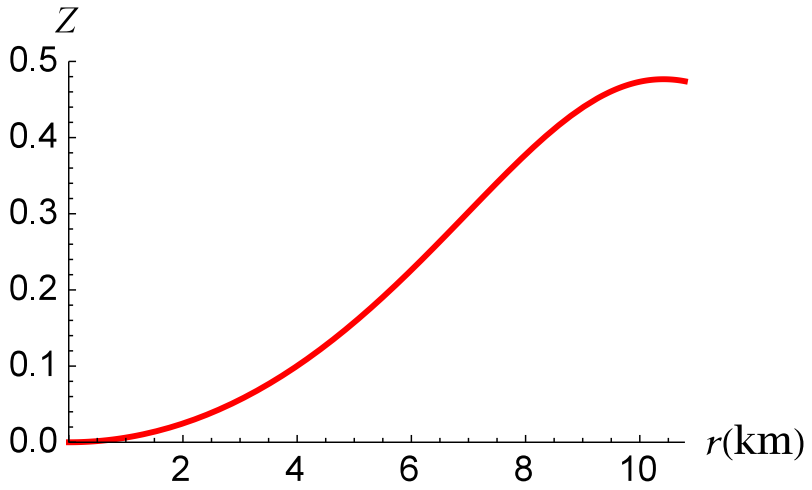

(a) PSRJ1614−2230

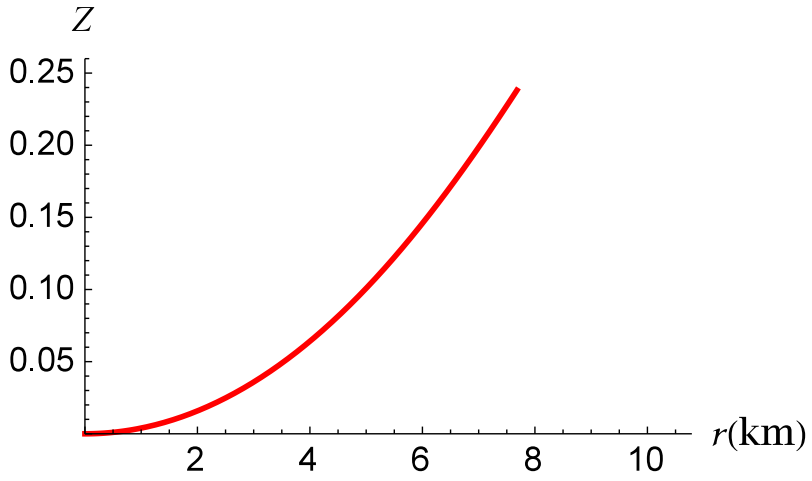

(b) SAX J1808.4−3658

Figure 5.8 – Variation of surface redshift function versus the radius

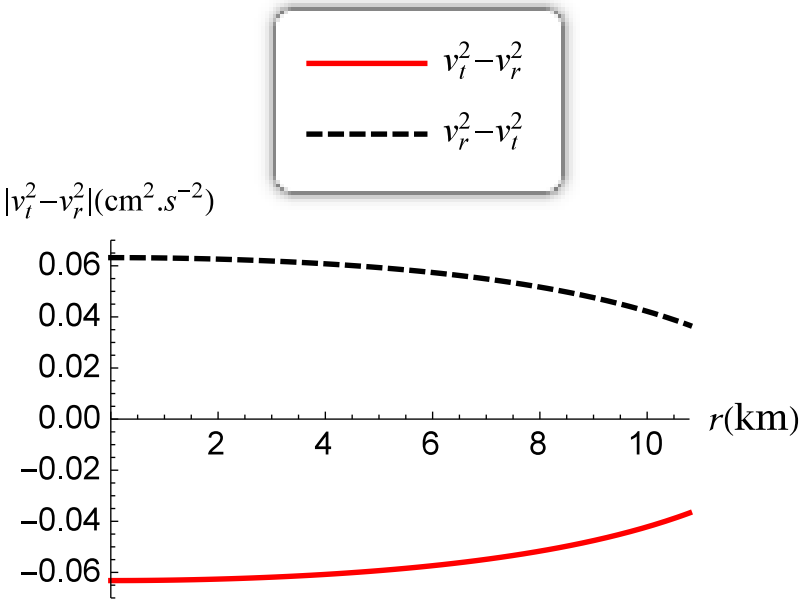

(a) PSRJ1614−2230

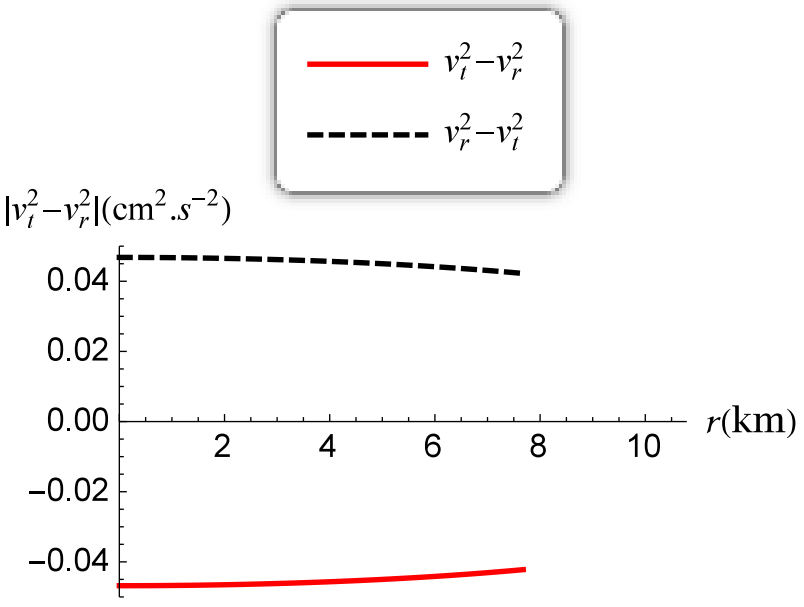

(b) SAX J1808.4−3658

Figure 5.9 – Variation of the quantity $|{v_r}^2 - {v_t}^2|$ versus the radius

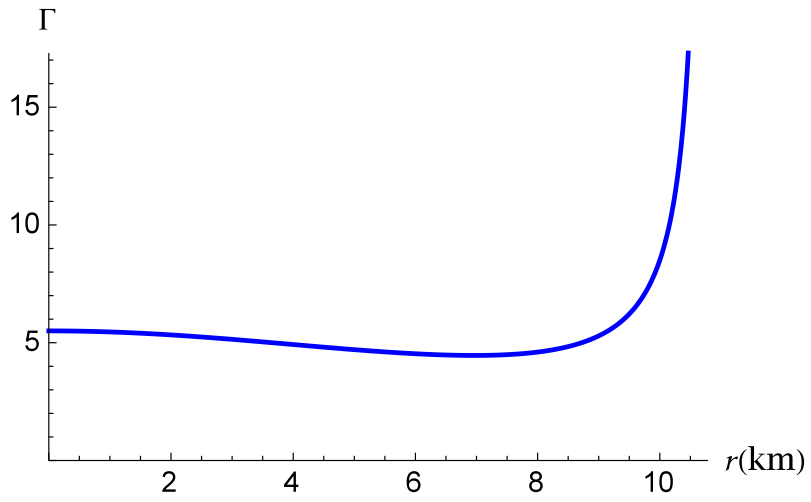

(a) PSRJ1614−2230

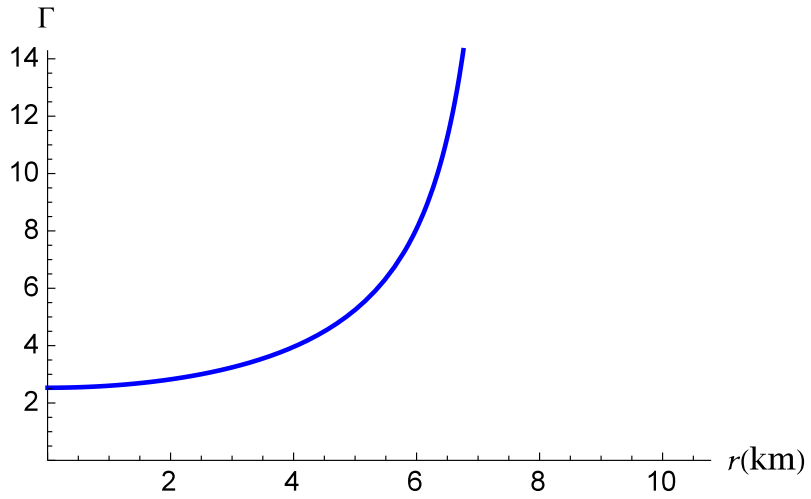

(b) SAX J1808.4−3658

Figure 5.10 – Variation of adiabatic index versus the radius

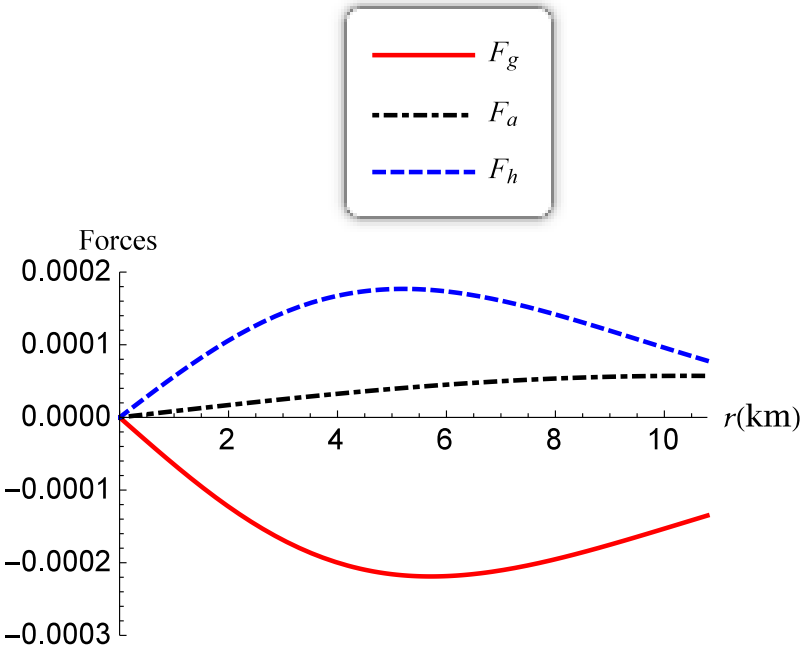

(a) PSRJ1614−2230

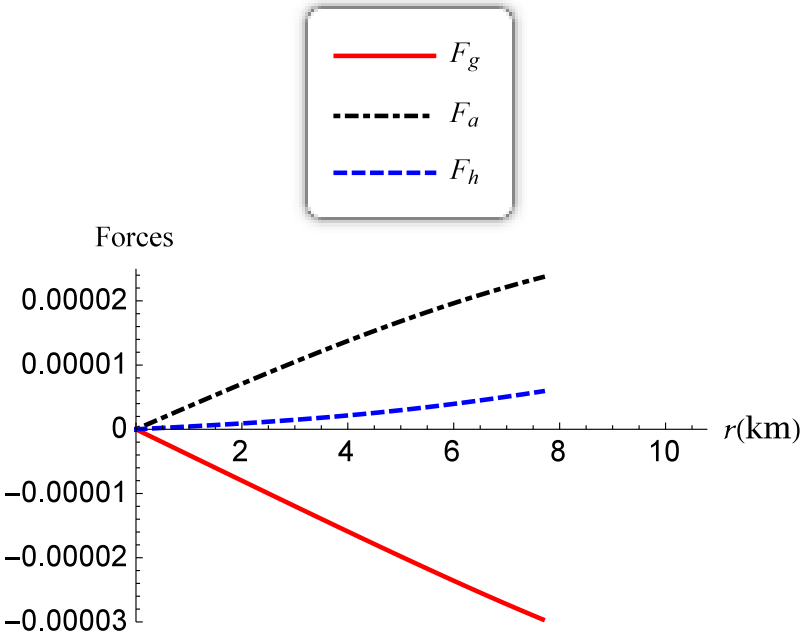

(b) SAX J1808.4−3658

Figure 5.11 – Variation of the forces versus the radius

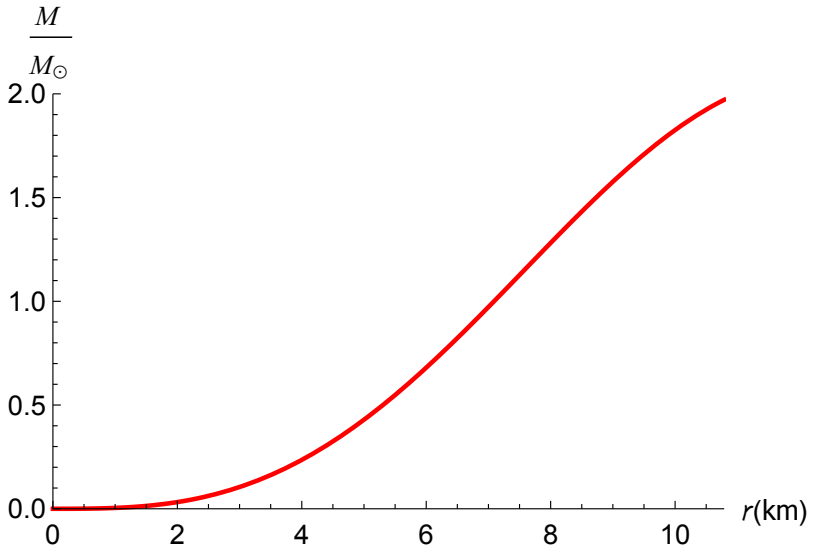

(a) PSRJ1614−2230

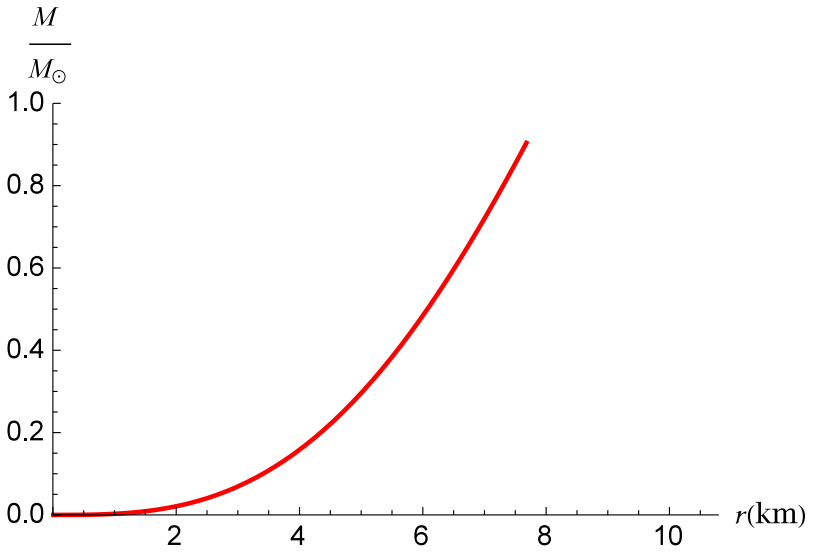

(b) SAX J1808.4−3658

Figure 5.12 – Variation of the mass versus the radius

Table 5.4 – Central density, radius, mass and compactification factor for $\tilde{d} = -0.2$ and $\tilde{e} = -0.1$.

C	$\tilde{K}$	R(km)	$\rho_c(10^{15}\mathrm{gcm}^{-3})$	r(km)	$M(M_\odot)$	$\frac{M}{r}$	Star
0.00018	1.7999	0.117	1.27	7.68	0.903	0.1738	SAX J1808.4-3658
0.00029	1.7295	0.117	2.04	8.01	1.30	0.2407	EXO 1785
0.00037	1.5914	0.118	2.56	8.31	1.493	0.2654	Cen X-3
0.00041	1.4524	0.121	2.70	8.64	1.580	0.2701	4U 1820-30
0.00045	1.3337	0.129	2.61	9.10	1.667	0.2706	PSR J1903+327
0.00049	0.9249	0.136	2.55	9.77	1.770	0.2677	Vela X-1
0.00051	1.1778	0.158	1.97	10.79	1.971	0.2698	PSR J1614-2230

Chapter 6

Charged isotropic model with conformal symmetry

6.1 Introduction

The Einstein-Maxwell system of field equations is a coupled nonlinear system of ordinary differential equations describing a localised distribution of charged gravitating matter. Solutions of this system are of importance in relativistic astrophysics and may be used to describe quark stars, gravastars, core envelope models, neutron stars and superdense compact objects. Models constructed from solutions of the Einstein-Maxwell equations are useful in describing physical features including the mass and luminosity. In recent times several models of relativistic stars have been found with anisotropic pressures. Some examples of anisotropic compact stars found recently are those of Bhar *et al* (2017), Ivanov (2017) and Maurya *et al* (2018). However it is also important to study compact stars with isotropic pressures as this is considered to be the equilibrium state of gravitating matter. Some examples of isotropic stars with an electromagnetic field are given by Thirukkanesh and Maharaj (2006), Komathiraj and Maharaj (2007b), Maharaj and Komathiraj (2007) and Thirukkanesh and Maharaj (2009). A physical analysis indicates that isotropic models may be used

to describe compact charged spheres. Other comprehensive investigations of charged isotropic spheres are contained in the works of Ivanov (2002), Kiess (2012), Murad and Fatema (2013), Fatema and Murad (2013), and Murad (2016). Of particular physical interest are exact metrics in spherical symmetry that satisfy boundary conditions and admit the limit of vanishing charge. In this way we can theoretically predict important properties of compact stars which are difficult to study otherwise.

Geometric conditions may be imposed on the spacetime manifold to produce a relativistic stellar model. An example of a geometric condition is the embedding of spacetime into a higher dimensional Euclidean space leading to an exact solution. A model of such a spherically symmetric charged compact star is given by Maurya *et al* (2017). Another geometric condition is the presence of a conformal symmetry on the manifold. Conformal symmetries generate constants of the motion and restrict the behaviour of the gravitational field. The geometrical structure of conformal symmetries have been studied in static spherical spacetimes by Maartens *et al* (1995, 1996) and Tupper *et al* (2012). Using the Weyl tensor Manjonjo *et al* (2017, 2018) showed that, in the presence of a conformal Killing vector, there is an explicit functional relationship between the metric functions. This relationship holds in general and provides an avenue to integrate the field equations. Mafa Takisa *et al* (2017) utilised this relationship to model a compact star, with anisotropic pressures, finding mass-radius limits and red shifts consistent with observational constraints. Other recent models of compact spheres which are conformally invariant are provided by Esculpi and Aloma (2010), Rahaman *et al* (2017), Shee *et al* (2016) and Deb *et al* (2017). Our objective is to extend these studies to the physically important case of isotropic pressures. This means that we have to additionally integrate the condition of pressure isotropy, a nonlinear differential equation.

In this chapter we assume the relationship between the metric functions, arising from a conformal symmetry, established by Manjonjo *et al* (2018). The matter distribution is charged with isotropic pressures. Then it is possible to integrate the Einstein-Maxwell system of equations in terms of elementary functions. In this way

we present new charged isotropic solutions for a compact star invariant under a conformal symmetry in spherical spacetimes. In §6.2 we present details of Einstein-Maxwell field equations and the relationship between the metric functions. The section §6.3 provides a differential equation, arising from the conformal symmetry, linking the gravitational potential to the electric field which is used to generate the exact solution to the Einstein-Maxwell system. Physical acceptability conditions and various physical quantities associated with the exact solution are discussed in detail in §6.4. Values for masses, radii, central densities, compactness parameters and redshifts are generated for the objects 4U 1538-52 and PSR J1614-2230. Additionally, the geometrical and matter variables are plotted for 4U 1538-52 and PSR J1614-2230 and their physical properties discussed.

6.2 The model

The gravitational field in spherically symmetric spacetimes, modelling the interior of a compact relativistic star, is given by

$$ds^2 = -e^{2\nu(r)}dt^2 + e^{2\lambda(r)}dr^2 + r^2(d\theta^2 + \sin^2\theta d\phi^2). \tag{6.1}$$

The metric quantities $e^{2\nu(r)}$ and $e^{2\lambda(r)}$ are arbitrary functions and represent gravity. The tensor $\mathbf{T}$ corresponds to energy momentum and has the general form

$$T_{ab} = \text{diag}\left(-\rho - \frac{1}{2}E^2,\ p - \frac{1}{2}E^2,\ p + \frac{1}{2}E^2,\ p + \frac{1}{2}E^2\right), \tag{6.2}$$

where the quantities ρ, p and E are the energy density, isotropic pressure and electric field intensity respectively. Then the Einstein-Maxwell system of equations can be written in the form

$$\frac{1}{r^2}\left[r(1-e^{-2\lambda})\right]' = \rho + \frac{1}{2}E^2, \tag{6.3a}$$

$$-\frac{1}{r^2}(1-e^{-2\lambda}) + \frac{2\nu'}{r}e^{-2\lambda} = p - \frac{1}{2}E^2, \tag{6.3b}$$

$$e^{-2\lambda}\left(\nu'' + \nu'^2 + \frac{\nu'}{r} - \nu'\lambda' - \frac{\lambda'}{r}\right) = p + \frac{1}{2}E^2, \tag{6.3c}$$

$$\sigma^2 = \frac{1}{r^2}(r^2E)'e^{-\lambda}, \tag{6.3d}$$

in terms of the coordinate r. Primes denote differentiation with respect to r and σ is the proper charge density. We are using units in which $4\pi G = c = 1$.

The Durgapal and Bannerji (1983) form of the field equations is obtained if we introduce the transformation

$$x = Cr^2, \quad Z(x) = e^{-2\lambda(r)}, \quad \mathcal{A}^2y^2(x) = e^{2\nu(r)}, \tag{6.4}$$

where $\mathcal{A}$ and C are constants. In terms of the new variables, the line element (6.1) has the representation

$$ds^2 = -\mathcal{A}^2y^2(x)dt^2 + \frac{1}{4CxZ(x)}dx^2 + \frac{x}{C}\left(d\theta^2 + \sin^2\theta d\phi^2\right). \tag{6.5}$$

Then the Einstein-Maxwell field equations (6.3) can be expressed as

$$\frac{1-Z}{x} - 2\dot{Z} = \frac{\rho}{C} + \frac{E^2}{2C}, \tag{6.6a}$$

$$4Z\frac{\dot{y}}{y} + \frac{Z-1}{x} = \frac{p}{C} - \frac{E^2}{2C}, \tag{6.6b}$$

$$4Zx^2\ddot{y} + 2\dot{Z}x^2\dot{y} + \left(\dot{Z}x - Z + 1 - \frac{E^2x}{C}\right)y = 0, \tag{6.6c}$$

$$\frac{\sigma^2}{C} = \frac{4Z}{x}(x\dot{E} + E)^2, \tag{6.6d}$$

which is an equivalent form. The mass function $M(x)$ contained within a radius x of the spherical star is given by the expression

$$M(x) = \frac{1}{C^{3/4}}\int_0^x \sqrt{\omega}\left(\rho(\omega) + E^2\right)d\omega, \tag{6.7}$$

which contains a contribution from the electric field. It is possible to generate a new class of exact solutions to the Einstein-Maxwell system (6.6) by choosing specific forms for the gravitational potential Z and the field electric intensity E which are physically reasonable. We assume that the line element (6.1) admits conformal symmetries. The existence of a conformal symmetry leads to a particular relationship between the gravitational potentials as established by Manjonjo et al (2018). We

have the conformal condition

$$\begin{aligned} y &= Ax^{\frac{1}{2}} \exp\left(\frac{1}{2}\sqrt{-(1+k)}\int \frac{\mathrm{d}x}{xZ^{\frac{1}{2}}}\right) \\ &\quad + Bx^{\frac{1}{2}} \exp\left(-\frac{1}{2}\sqrt{-(1+k)}\int \frac{\mathrm{d}x}{xZ^{\frac{1}{2}}}\right), \end{aligned} \tag{6.8}$$

where A, B are arbitrary constants. The parameter k is related to the Weyl tensor; $k = 0$ gives a conformally flat spacetime and $k \neq 0$ generates a non-conformally flat spacetime.

6.3 Integration

Equation (6.6c) is complicated but takes a simple form when a conformal symmetry is present. With the conformal condition (6.8), the generalized condition of pressure isotropy (6.6c) becomes

$$2x\dot{Z} - 2Z = x\frac{E^2}{C} + k. \tag{6.9}$$

It is necessary to integrate (6.9) and obtain functional forms for Z and E. There are several choices of Z and E that integrate equation (6.9). However there is a limited class of functions which generate a physically reasonable stellar model. We have isolated a family of solutions in terms of elementary functions which have the required physical characteristics. The family of solutions integrating (6.9) is given by

$$\frac{E^2}{C} = \frac{2(d-b)\left[3d-b+d(b+d)x\right]x}{(1+dx)^3}, \tag{6.10a}$$

$$Z = \frac{(1+bx)^2}{(1+dx)^2}, \tag{6.10b}$$

where b and d are constants. To avoid the singularity at the centre we must take $k = -2$. The form of E is vanishing at $x = 0$, remains bounded in the interior, and is physically reasonable for a wide range of parameter values b and d. The rational form of Z is regular at the centre and remains continuous throughout the star.

Then the exact solution to the Einstein-Maxwell system can be written as

$$e^{2\lambda} = \frac{(1+dx)^2}{(1+bx)^2}, \tag{6.11a}$$

$$e^{2\nu} = \mathcal{A}^2\left[Ax(dx+1)^{\frac{b-d}{2d}} + B(dx+1)^{-\frac{b-d}{2d}}\right]^2, \tag{6.11b}$$

$$\frac{\rho}{C} = \frac{6\left(b(d-b)x - b + d\right)}{(dx+1)^3}, \tag{6.11c}$$

$$\begin{aligned}\frac{p}{C} = {} & 2(bx+1)\left[bBd(d-b)x^2 + bB(d-b)x\right. \\ & \left.+(dx+1)^{b/d}\left(Ab(b+d)x^2 + 4Abx + 2A\right)\right] \\ & \times\left[Ax(dx+1)^{b/d} + Bdx + B\right]^{-1}(dx+1)^{-3},\end{aligned} \tag{6.11d}$$

$$\frac{E^2}{C} = \frac{2x(d-b)(dx(b+d) - b + 3d)}{(dx+1)^3}, \tag{6.11e}$$

$$\begin{aligned}\frac{\sigma^2}{C} = {} & 2C(d-b)(bx+1)^2\left[d^2(b+d)x^2 + 4d(b+d)x + 3(3d-b)\right]^2 \\ & \times\left[(dx+1)^7\left(d(b+d)x + 3d - b\right)\right]^{-1},\end{aligned} \tag{6.11f}$$

in terms of the variable x.

6.4 A stellar model

The solutions found in this chapter may be used to model a relativistic star. In this section, we investigate the applicability of the charged isotropic model and the relationship to observational data. We made choices for the parameter values A, B, b and d as given in Table 6.1. Six stars have been selected in Table 6.1 namely 4U 1538-52, LMC X-4, SMC X-1, EXO 1785-248, Vela X-1 and PSR J1614-2230. We find that our solutions produce masses and radii consistent with earlier investigations. For a more detailed physical analysis we consider the two stars PSR J1614-2230 and 4U 1538-52 which have the highest and lowest mass respectively.

The profiles of the metric potentials for PSR J1614-2230 and 4U 1538-52 in Fig. 6.1 show that they are free from singularities, regular at the centre and monotonically increasing with the radius inside the star ($e^{-2\lambda(0)} = 1, e^{2\nu(0)} = \mathcal{A}^2B^2$). The

behaviour of the metric functions are consistent with the requirements of Lake (2003) for a physically acceptable model. The variation of the energy density is plotted against the radius in Fig. 6.2. The graphs indicates that the energy densities are positive with a maximum value at the centre and decrease continuously throughout the the star ($\frac{d\rho}{dr} \leq 0$). The corresponding values of the central density are $\rho_c = 1.822 \times 10^{15}\text{gcm}^{-3}$ and $\rho_c = 10.33 \times 10^{14}\text{gcm}^{-3}$ for PSR J1614-2230 and 4U 1538-52 respectively. The variation of the isotropic pressure is presented in Fig. 6.3; We can see that the pressure is a monotonically decreasing function of r and vanishes at the boundary of the star ($p(R) = 0$). At the centre the pressure is finite ($p(0) = \frac{4AC}{B}, \frac{dp}{dr}(0) = 0$) and on the interval $0 \leq r \leq R$, the gradient of isotropic pressure $\frac{dp}{dr} < 0$. The radii of the stars are $R = 9.49$ km for PSR J1614-2230 and $R = 7.81$ km for 4U 1538-52. In Fig. 6.4, we observe that the electric field is positive and an increasing function with increasing radius. At the centre, $E(0) = 0$ and reaches a maximum value at the surface of the star. The magnitude of the surface electric field intensity is $E(R) = 8.01 \times 10^{20}\text{Vcm}^{-1}$ for PSR J1614-2230 and $E(R) = 3.94 \times 10^{20}\text{Vcm}^{-1}$ for 4U 1538-52. Fig. 6.5 shows that the proper charge density is finite at $r = 0$, regular in the interior, and evolves as a decreasing function throughout both stellar spheres PSR J1614-2230 and 4U 1538-52. The total mass of the charged isotropic model is obtained by substituting the expressions (6.11c) and (6.11e) into (6.7) and integrating. Thus we get

$$\begin{aligned} M(r) &= \frac{C^{1/4}(d-b)}{\left(Cdr^2+1\right)^2}\left[8C^{5/2}(b+d)r^5 + \frac{C^{3/2}(15b+13d)}{d}r^3\right. \\ &\left. + \frac{3C^{1/2}(3b+d)}{d^2}r - \frac{3\left(Cdr^2+1\right)^2(3b+d)}{d^{5/2}}\tan^{-1}\left(\sqrt{Cd}r\right)\right]. \quad (6.12) \end{aligned}$$

In Fig. 6.6, the mass function is plotted against the radius and the profile indicates an increasing function with increase of radius. We have calculated in Table 6.1, numerical values for six objects, and there is consistency for the stars 4U 1538-52 and PSR J1614-2230, which are consistent with the observed data. According to Buchdahl (1959), the ratio of mass to the radius for an isotropic compact star should satisfy the inequality $2M/R < 8/9$. The compactness factor $\mu(r) = M(r)/r$ can be

computed as

$$\mu = \frac{C^{1/4}(d-b)}{r(Cdr^2+1)^2}\left[8C^{5/2}(b+d)r^5+\frac{C^{3/2}(15b+13d)}{d}r^3 + \frac{3C^{1/2}(3b+d)}{d^2}r-\frac{3\left(Cdr^2+1\right)^2(3b+d)}{d^{5/2}}\tan^{-1}\left(\sqrt{Cd}r\right)\right]. \quad (6.13)$$

The compactness factor is plotted in Fig. 6.7 and the profiles reveal an increasing function of r. Table 6.2 gives the values $\mu = 0.2077(< 4/9)$ and $\mu = 0.1115(< 4/9)$ for PSR J1614-2230 and 4U 1538-52 which are consistent with the condition of Buchdahl (1959). Böhmer and Harko (2007) established the inequality for a charged compact star for the lower bound of compactness factor

$$\frac{Q^2}{R^2}\left(\frac{18R^2+Q^2}{12R^2+Q^2}\right) \leq \frac{2M}{R}. \quad (6.14)$$

Subsequently Andréasson (2009) showed that, for a charged sphere, the model must satisfy the following inequality

$$\sqrt{M} \leq \frac{\sqrt{R}}{3}+\sqrt{\frac{R}{9}+\frac{Q^2}{3R}}. \quad (6.15)$$

From (6.14) and (6.15) we obtain the range of lower and upper mass for a stellar model in the presence of charge

$$\frac{Q^2}{2R}\left(\frac{18R^2+Q^2}{12R^2+Q^2}\right) \leq M \leq \left[\frac{\sqrt{R}}{3}+\sqrt{\frac{R}{9}+\frac{Q^2}{3R}}\right]^2. \quad (6.16)$$

In this way we can obtain from (6.16) the following ranges: $0.02226 \leq M = 1.97 \leq 4.2375$ for PSR J1614-2230 and $0.72 \times 10^{-3} \leq M = 0.87 \leq 3.471$ for 4U 1538-52, which are consistent with the condition (6.16) for a stable configuration. In terms of the compactness factor, the gravitational redshift $Z = (1-2\mu)^{-1/2}-1$ can be written as

$$Z = -1+\left[1-8\frac{C^{11/4}(d^2-b^2)r^4}{\left(Cdr^2+1\right)^2}-\frac{C^{7/4}(d-b)(15b+13d)r^2}{d\left(Cdr^2+1\right)^2} - \frac{3\sqrt[4]{C}\left(3b^2-2bd-d^2\right)\arctan\left(\sqrt{dC}r\right)}{d^{5/2}r} -3\frac{C^{3/4}(d-b)(3b+d)}{d^2\left(Cdr^2+1\right)^2}\right]^{-\frac{1}{2}}. \quad (6.17)$$

The redshift function is increasing everywhere inside the star as can be seen in Fig. 6.8. For PSR J1614-2230, the surface redshift $Z_s = 0.6083$, and $Z_s = 0.2216$ for 4U 1538-52. These redshift values are consistent with the upper limit ($Z_s \leq 0.9$) proposed by Lindblom (1984) for strange stars. These values also satisfy the requirement ($Z_s \leq 2$) proposed by Buchdahl (1959). The value $Z_s = 0.6083$ for PSR J1614-2230 is in good agreement when compared to the result $Z_s = 0.596$ obtained by Kileba Matondo *et al* (2017) for the same pulsar in the case of charged isotropic stars.

For physical acceptability, the causality condition must be satisfied: the speed of sound should be smaller than the speed of light ($0 \leq {v_s}^2 = \frac{dp}{d\rho} \leq 1$) throughout the stellar configuration. For our charged isotropic model, Fig. 6.9 shows that the speed of sound remains less than the speed of light inside the star and decreases with increase of r. Bondi (1964) showed for an isotropic neutron star, the adiabatic index should satisfy the condition $\Gamma = \frac{\rho+p}{p}\frac{dp}{d\rho} > \frac{4}{3}$. The variation of Γ has been plotted against the radius for PSR J1614-2230 and 4U 1538-52, and the profiles in Fig. 6.10 show that this requirement for stability is satisfied. The Tolman-Oppenheimer-Volkoff (TOV) equation of hydrostatic equilibrium for an isotropic charged fluid is given by

$$\frac{dp}{dr} = -(\rho + p)\frac{d\nu}{dr} + \frac{E}{r^2}\frac{d}{dr}(r^2 E). \tag{6.18}$$

We introduce the terms for the gravitational force $F_g = -(\rho + p_r)\frac{d\nu}{dr}$, hydrostatic force $F_h = -\frac{dp_r}{dr}$ and electric force $F_e = \frac{E}{r^2}\frac{d}{dr}(r^2 E)$. Then the TOV equation takes the form

$$F_g + F_h + F_a = 0, \tag{6.19}$$

whose explicit expressions terms are

$$\begin{aligned} F_g \;=\; & -2C^2 r(1+bCr^2)\left(Cdr^2+1\right)^{-6}\left(ACr^2\left(Cdr^2+1\right)^{\frac{b-d}{d}}+B\right)^{-2} \\ & \times\left[B\left(b-d\right)\left(Cdr^2+1\right)-A\left(Cdr^2+1\right)^{b/d}\left(Cr^2(b+d)+2\right)\right] \\ & \times\left[B\left(b-d\right)\left(bCr^2+3\right)\left(Cdr^2+1\right)-2A\left(Cdr^2+1\right)^{\frac{b}{d}}\right. \end{aligned}$$

$$-ACr^2\left(Cdr^2+1\right)^{\frac{b}{d}}\left(bCr^2(b+d)+b+3d\right)\Big], \tag{6.20a}$$

$$\begin{aligned} F_h &= 4C^2r\left(Cdr^2+1\right)^{-4}\Bigg[\frac{A^2b^2C^4dr^8(b+d)}{(Cdr^2+1)^{-\frac{2b}{d}}} \\ &+2A^2bC^3r^6\left(-b^2+4bd+d^2\right)\left(Cdr^2+1\right)^{\frac{2b}{d}} \\ &+A^2\left(bC^2r^4(17d-5b)+8Cdr^2+2\right)\left(Cdr^2+1\right)^{\frac{2b}{d}} \\ &-b^2B^2(b-d)\left(Cdr^2+1\right)^2\left(\left(Cdr^2-2\right)Cr^2+2Cdr^2-1\right) \\ &-\frac{2ABbC^2\left(b(Cr^2(b+d)+4)+2d\right)+8AB(2bCr^4+1)}{(b-d)^{-1}\left(Cdr^2+1\right)^{-\frac{b+d}{d}}}\Bigg] \\ &\times\left(Cdr^2+1\right)^{-2}\left(ACr^2\left(Cdr^2+1\right)^{\frac{b-d}{d}}+B\right)^{-2}, \end{aligned} \tag{6.20b}$$

$$F_e = \frac{2C^2r(d-b)}{\left(Cdr^2+1\right)^4}\left[C^2d^2r^4(b+d)+4Cdr^2(b+d)-3b+9d\right]. \tag{6.20c}$$

The stability of the model has been examinated in Fig. 6.11 with the help of the TOV equation describing the equilibrium condition. The gravitational force F_g is counterbalanced by the contribution of hydrostatic force F_h and electric force F_e as we observe in Fig. 6.11. The energy condition $(\rho+p)$ is reported in Fig. 6.12, and the profile presents a decreasing function of r and remains positive inside the star for both PSR J1614-2230 and 4U 1538-52.

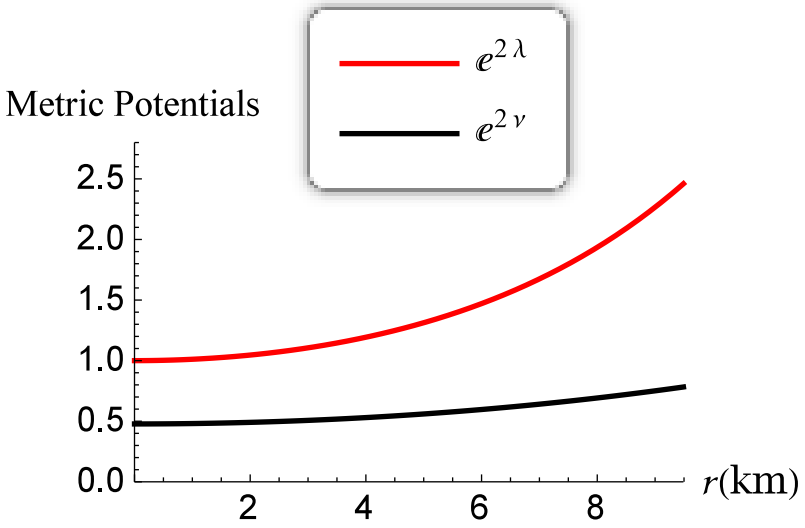

(a) PSRJ1614−2230

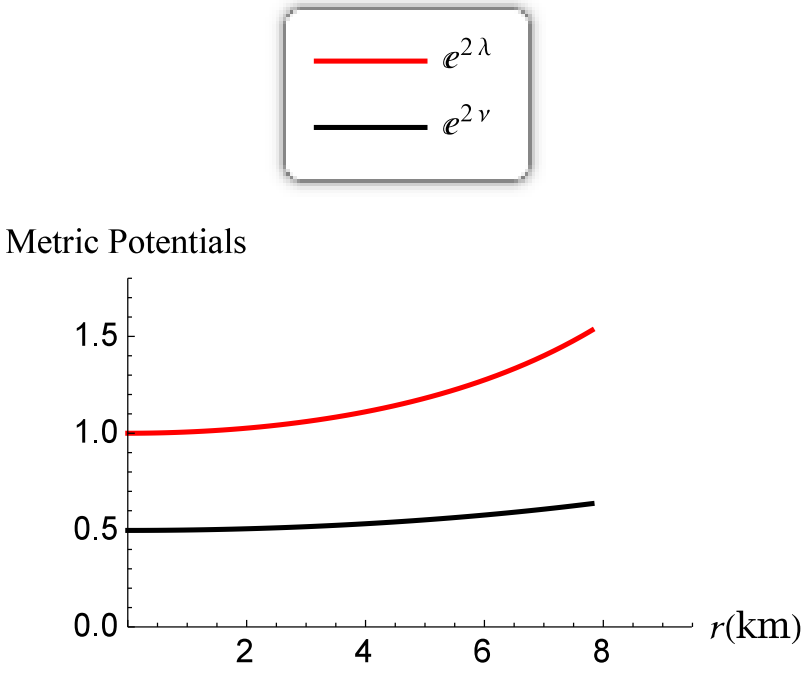

(b) 4U 1538−52

Figure 6.1 – Variation of metric potentials versus the radius

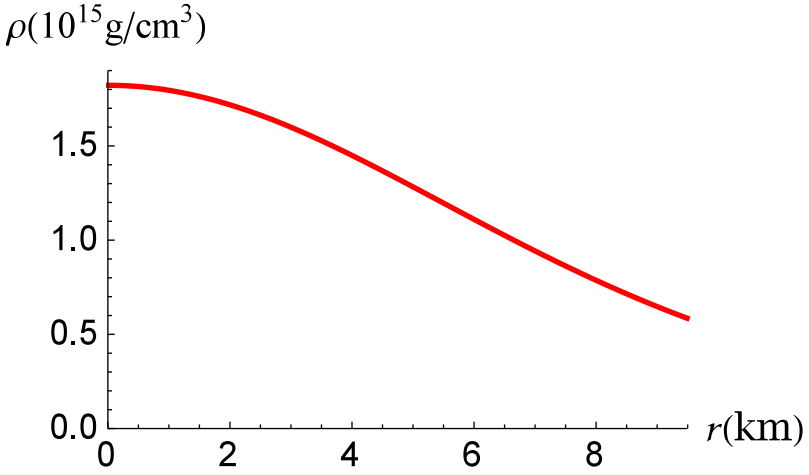

(a) PSRJ1614−2230

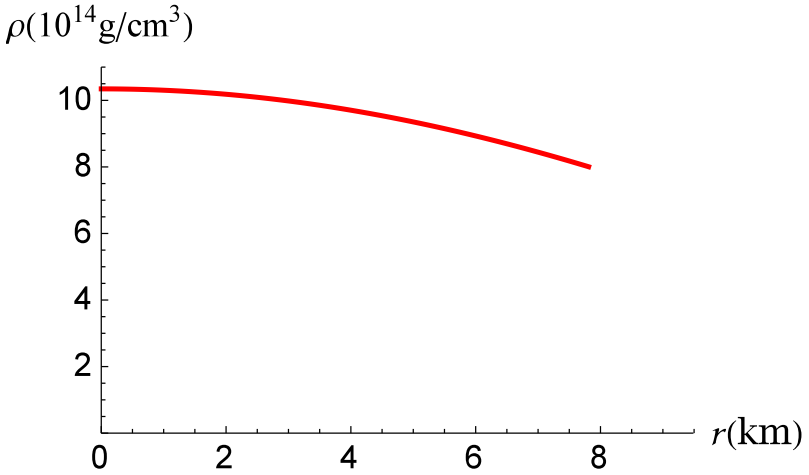

(b) 4U 1538−52

Figure 6.2 – Variation of energy density versus the radius

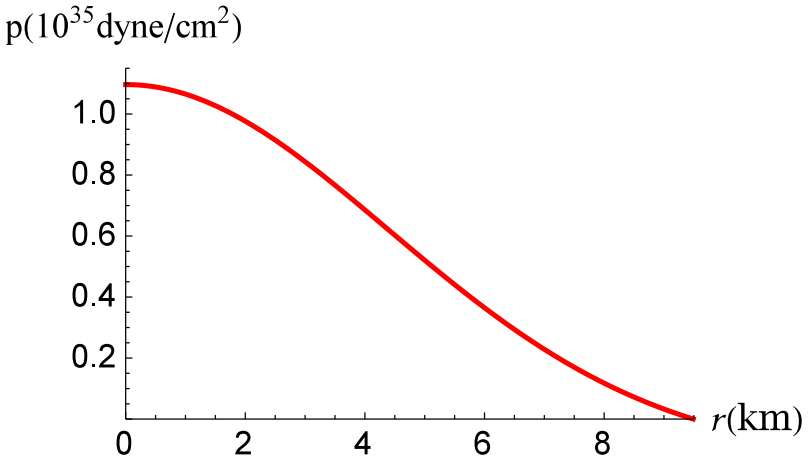

(a) PSRJ1614−2230

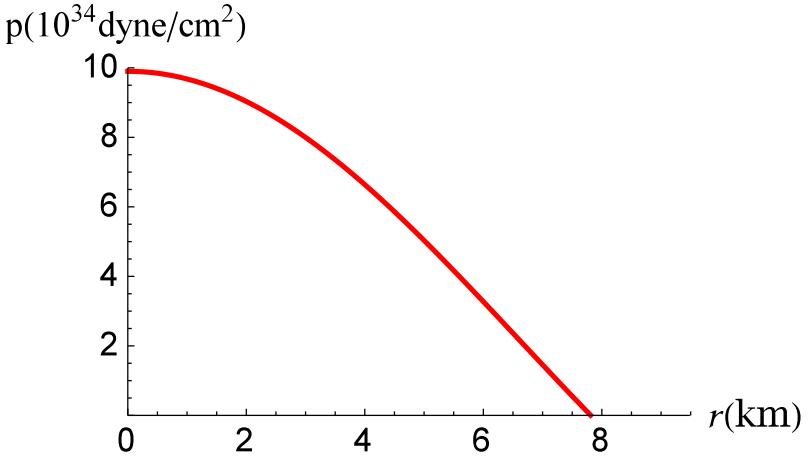

(b) 4U 1538−52

Figure 6.3 – Variation of the pressure versus the radius

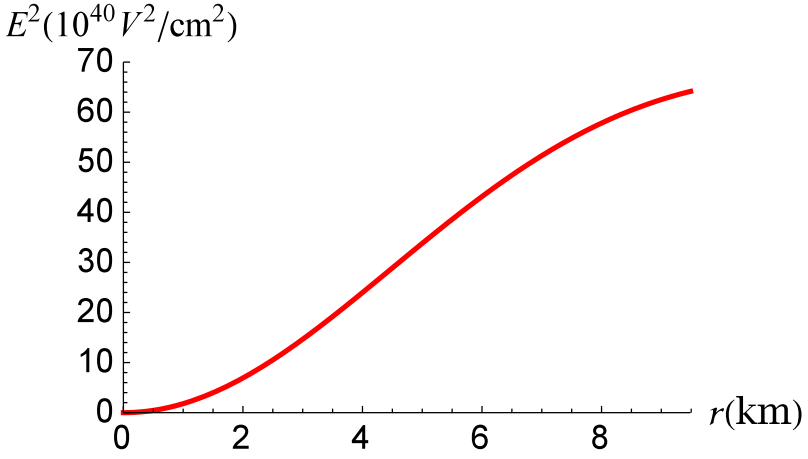

(a) PSRJ1614−2230

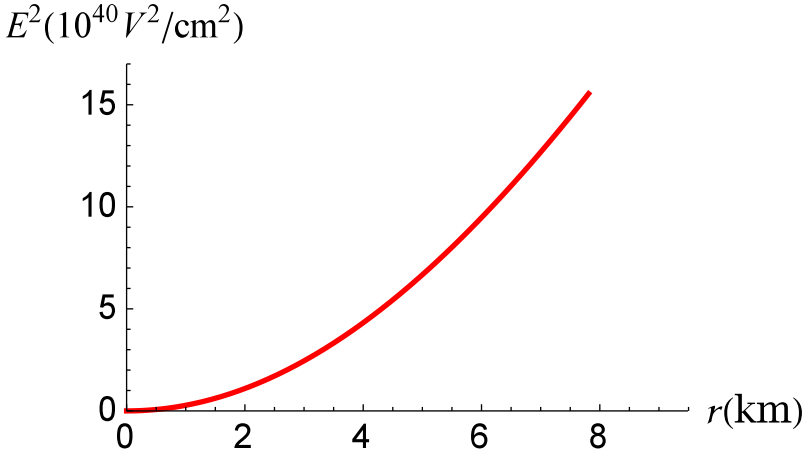

(b) 4U 1538−52

Figure 6.4 – Variation of electric field versus the radius

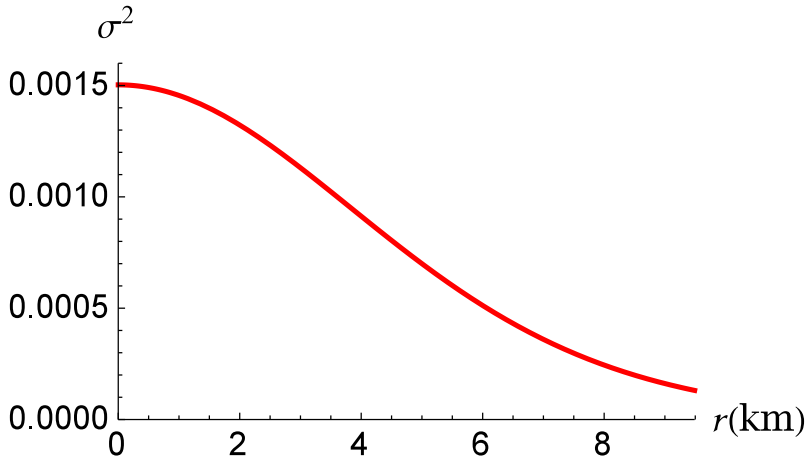

(a) PSRJ1614−2230

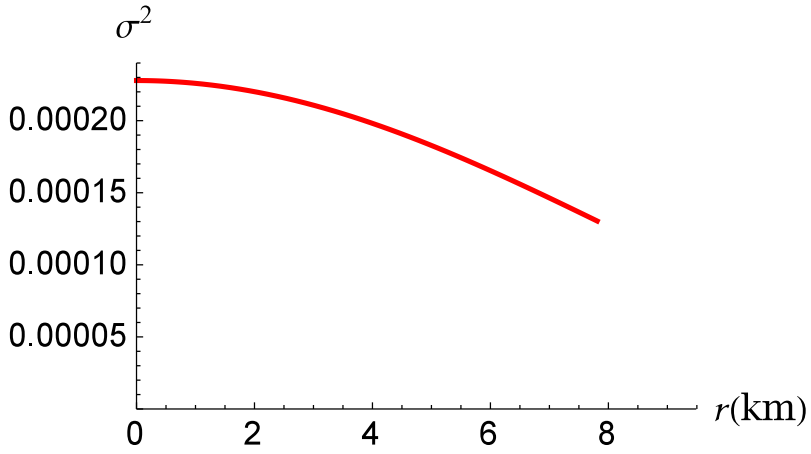

(b) 4U 1538−52

Figure 6.5 – Variation of the charge density versus the radius

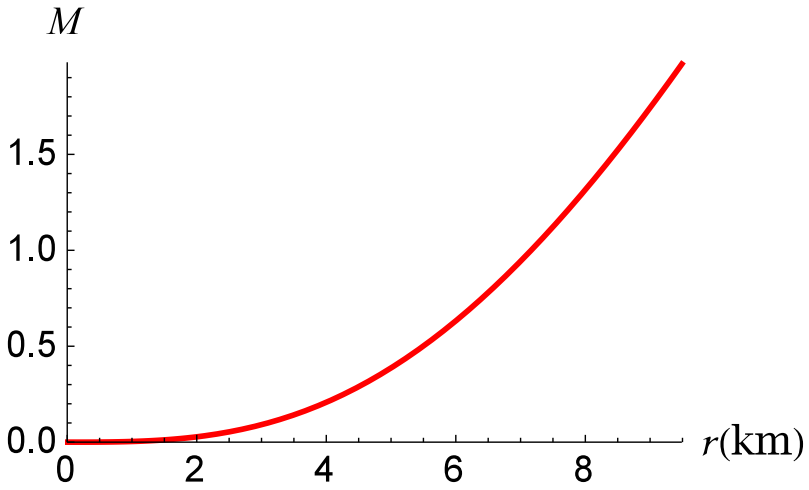

(a) PSRJ1614−2230

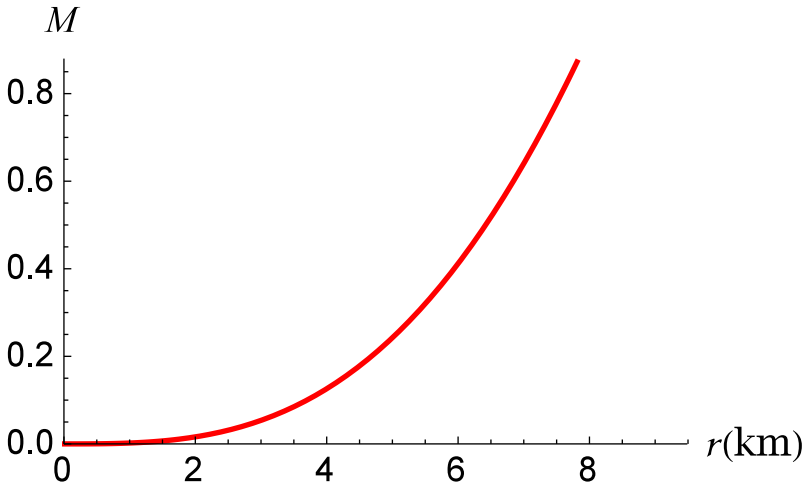

(b) 4U 1538−52

Figure 6.6 – Variation of the mass versus the radius

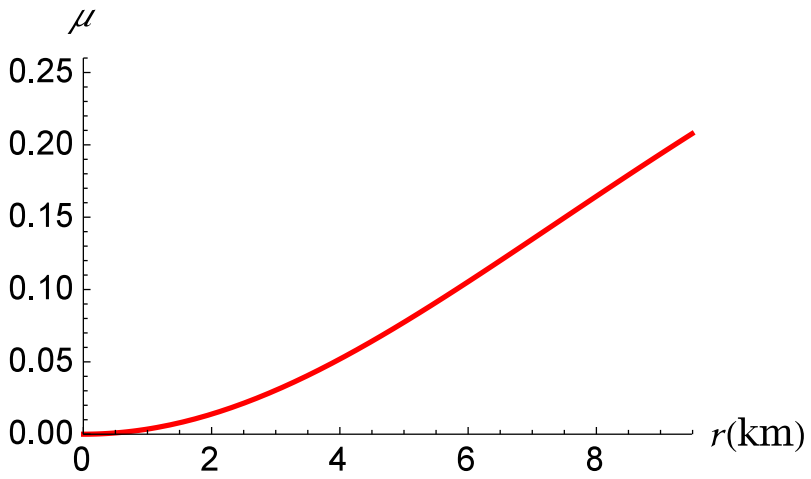

(a) PSRJ1614−2230

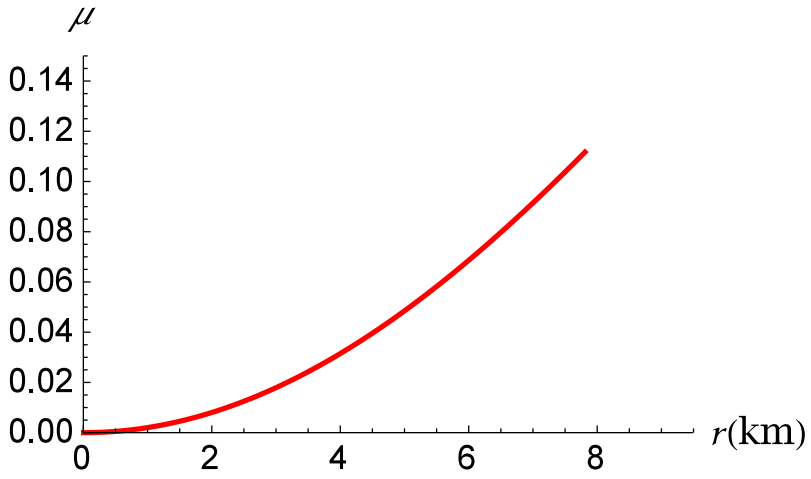

(b) 4U 1538−52

Figure 6.7 – Variation of compactness factor versus the radius

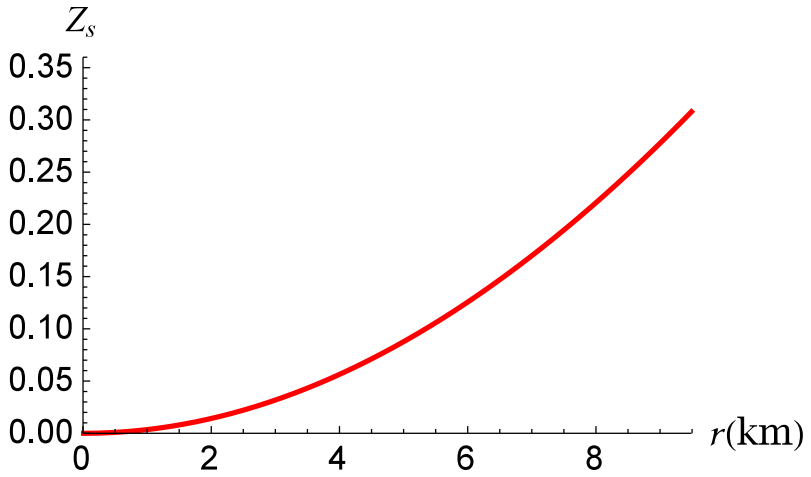

(a) PSRJ1614−2230

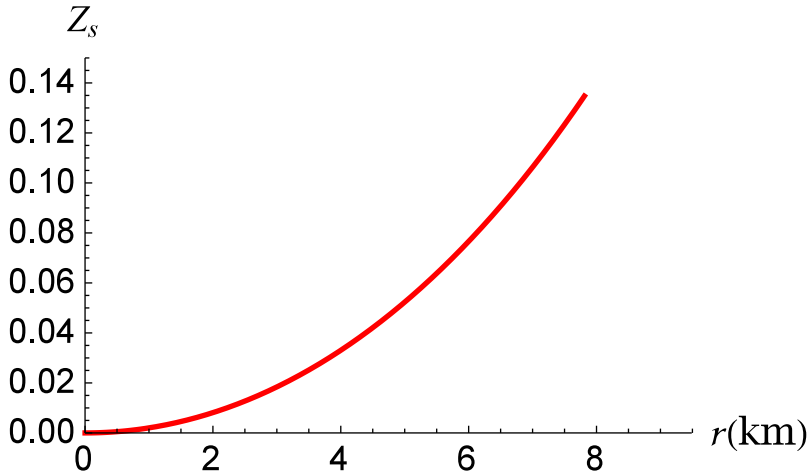

(b) 4U 1538−52

Figure 6.8 – Variation of gravitational redshift versus the radius

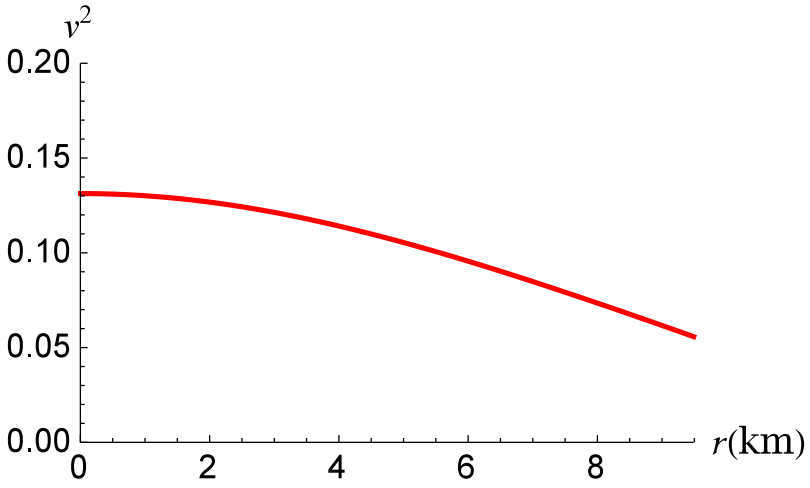

(a) PSRJ1614−2230

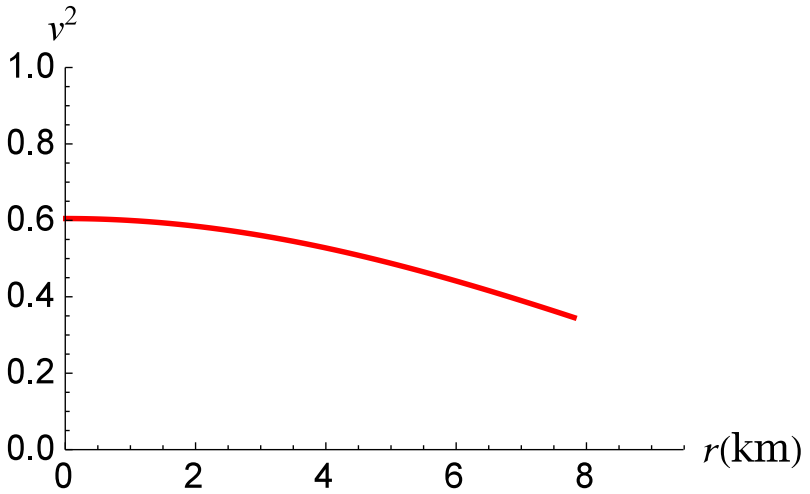

(b) 4U 1538−52

Figure 6.9 – Variation of speed of sound versus the radius

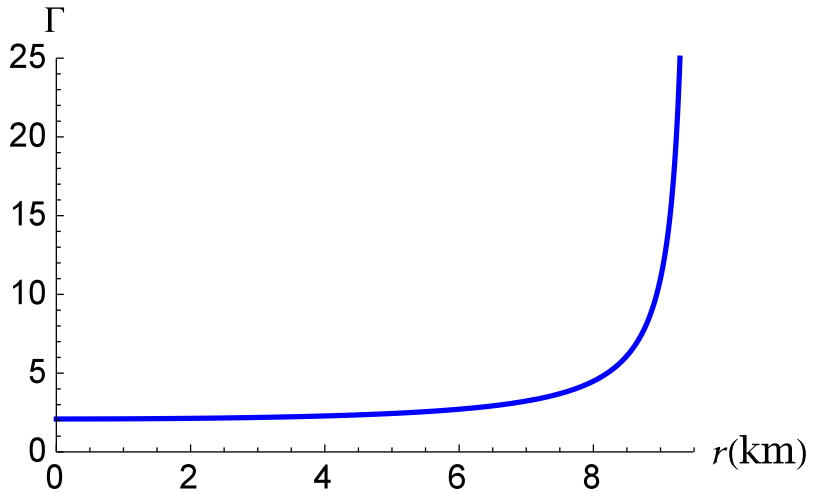

(a) PSRJ1614−2230

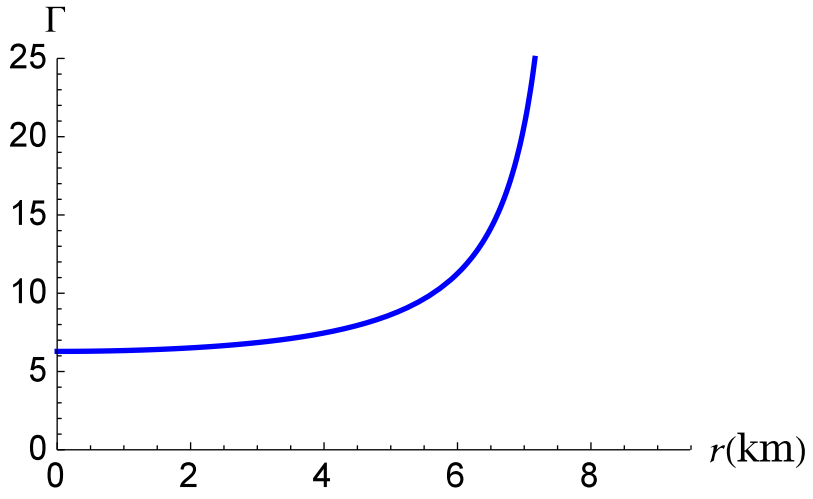

(b) 4U 1538−52

Figure 6.10 – Variation of adiabatic index versus the radius

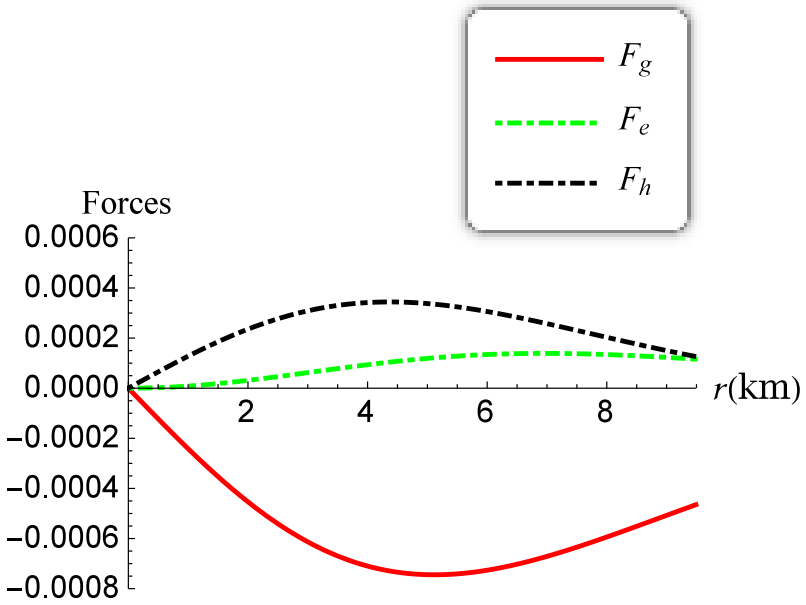

(a) PSRJ1614−2230

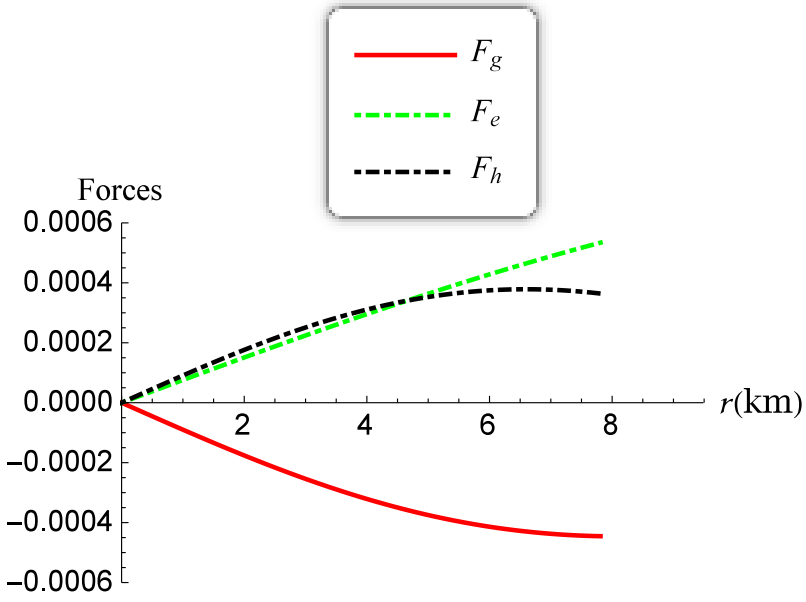

(b) 4U 1538−52

Figure 6.11 – Variation of the forces versus the radius

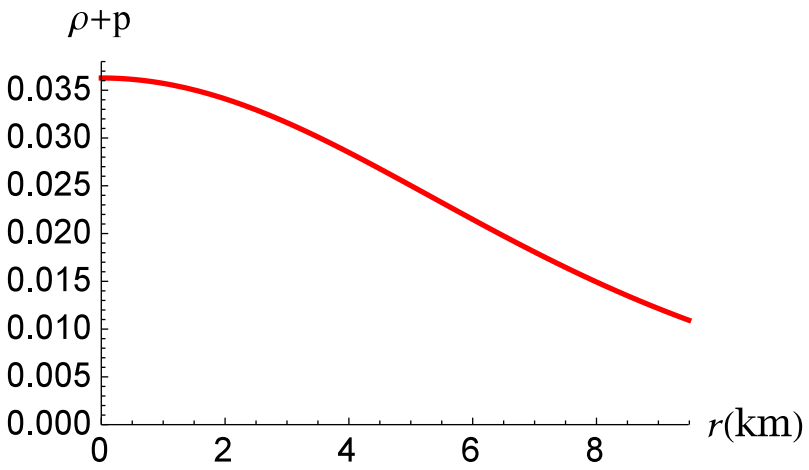

(a) PSRJ1614−2230

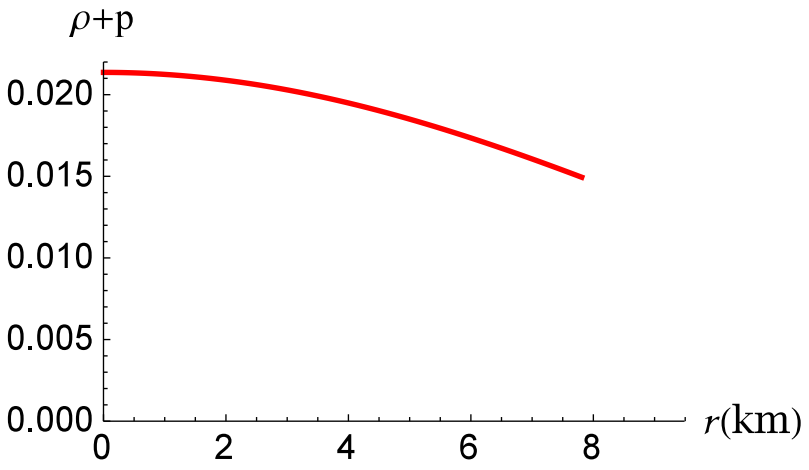

(b) 4U 1538−52

Figure 6.12 – Variation of the energy condition versus the radius

Table 6.1 – Radius and mass for six stars.

b	d	A	B	R(km)	$M(M_{\odot})$	Star
-0.0201	0.0025	0.0112	3.096	7.810	0.87	4U 1538-52
-0.0201	0.0025	0.0112	2.490	8.319	1.04	LMC X-4
-0.0201	0.0025	0.0112	1.852	8.995	1.29	SMC X-1
-0.0201	0.0025	0.0112	1.831	9.021	1.30	EXO 1785-248
-0.00797	0.0319	0.0177	5.138	9.070	1.77	Vela X-1
-0.00797	0.0319	0.0177	4.430	9.490	1.97	PSR J1614-2230

Table 6.2 – Energy density, pressure, electric field, compactness factor and redshift for 4U 1538-52 and PSR J1614-2230.

Star	ρ_c (10^{15}g/cm^3)	ρ_s (10^{15}g/cm^3)	p_c (10^{35}dyne/cm^2)	E (10^{20}V/cm)	μ	Z_s
4U 1538-52	1.033	0.7998	0.9907	3.94	0.1115	0.2216
PSR J1614-2230	1.822	0.5856	1.094	8.01	0.2077	0.6083

Chapter 7

Conclusion

The main objectives of this thesis was to generate new families of exact solutions to the Einstein and Einstein-Maxwell field equations which may be used to describe relativistic compact stars. We studied static spherically symmetric spacetimes with a linear equation of state and matter distributions with a Finch and Skea geometry including an electric field and pressure anisotropy. It was showed that new solutions are physically reasonable and earlier models are regained. We also demonstrated that the presence of a conformal symmetry leads to a new solution to the field equations. The physical analysis is detailed, matter variables are plotted, and masses and radii are generated for specific stars.

We now present an overview of the principal results obtained during the course of this research:

- In chapter 2, our purpose was to generate new class of exact solutions to the Einstein-Maxwell system. We made the following assumptions:

$$\begin{aligned} Z &= \frac{1+(a-b)\,x}{1+ax}, \\ \frac{E^2}{C} &= \frac{la^3x^3+sa^2x^2+k(3+ax)}{(1+ax)^2}. \end{aligned}$$

  The new class of solutions to the Einstein-Maxwell system of equations obtained in this chapter is physically reasonable in an astrophysical context and serves

to model relativistic stars. We have demonstrated this by graphically analysing the matter variables, and also generating various tables for the mass function for different values of the parameters in the electric field. Our general class of solutions contain the earlier models of Mafa Takisa and Maharaj (2013) and Thirukkanesh and Maharaj (2008) in the presence of charge. The models of Dey *et al* (1998, 1999) and Sharma and Maharaj (2007) are regained in the appropriate limit for vanishing charge. The stellar masses generated are consistent with earlier investigations, and we regain the stellar mass of the object SAX J1808.4-3658 as $1.434M_{\odot}$. Our new family of solutions is a further indication of the richness of the Einstein-Maxwell system of equations and their link to astrophysical applications; we studied the physical features and plotted the matter and electrical variables. A comparative table of masses for uncharged and charged matter was established which corresponds to observed astronomical objects. The parameter l does not appear to appreciably change the mass for the parameter values chosen but a different set of parameters can give a different profile for the mass.

- In chapter 3, we comprehensively studied anisotropic and charged matter with a Finch and Skea geometry. The Einstein-Maxwell system led to the differential equation

$$4(1+ax)\ddot{y} - 2a\dot{y} + (a^2-\alpha)y = 0,$$

which is the master equation governing the evolution of the model. Several families of solution are possible to the master equation in our generalized approach. Exact solutions are possible in terms of elementary functions, Bessel functions and modified Bessel functions. When a parameter becomes an integer it is possible to represent the Bessel and modified Bessel functions in terms of elementary functions. This is demonstrated for the Bessel functions $J_{\frac{1}{2}}$, $J_{-\frac{1}{2}}$, $J_{\frac{3}{2}}$, $J_{-\frac{3}{2}}$, $J_{\frac{5}{2}}$, $J_{-\frac{5}{2}}$ and the modified Bessel functions $I_{\frac{1}{2}}$, $I_{-\frac{1}{2}}$, $I_{\frac{3}{2}}$, $I_{-\frac{3}{2}}$, $I_{\frac{5}{2}}$, $I_{-\frac{5}{2}}$. In this way an infinite family of exact solutions to the master equation can be generated in terms of elementary functions. Solutions found previously are

contained in our analysis. In particular we regain the Finch and Skea (1989) solution for uncharged matter and the Hansraj and Maharaj (2006) solution in the presence of electromagnetic field. We show that the solutions found admit a barotropic equation of state so that the radial pressure can be written as a function of energy density. A graphical analysis indicates that the matter variables are well behaved and regular in the interior. In particular the speed of sound is less than the speed of light.

- In chapter 4, we have studied an exact solution in the class found by Maharaj *et al* (2016). This solution may be considered as a charged anisotropic generalisation of the Finch and Skea model. The Finch and Skea model has been widely studied and shown to satisfy all physical requirements. A detailed physical analysis of the objects PSR J1614-2230 and LMC X-4 was performed with charge and anisotropy present in this chapter. The variation of the constant parameter C allowed us to determine the upper maximum mass and the lower minimum mass of charged anisotropic fluid spheres. A numerical investigation showed that the model obtained can describe charged anisotropic fluid spheres with maximum mass 1.97 $M_{\odot}$ and radius 10.90 km which corresponds to the pulsar PSR J1614-2230 having a central energy density 4.035×10^{14} g cm^{-3}. The uncharged case leads to a maximum mass of 1.97 $M_{\odot}$ with the radius of 13.83km and a central density 1.57×10^{14} g cm^{-3}. These values are approximately similar to the results found by Andréasson (2009) with mass 1.9701 $M_{\odot}$ and radius 13.71km. It is noticed that the compactification factor $\frac{M}{R}$ of these compact stellar bodies is in the range of neutron and ultracompact stars. The uncharged stars have compactification factors lower than the charged cases, which again, contrary to the common perception, should be the other way round. We have also studied other physical aspects of the model. The surface redshift comes out to be in the range of ± 0.42 for the uncharged isotropic case, and ± 0.57 for the charged isotropic case. These redshift values are consistent with neutron and strange stars. It is observed that the Andréasson and

Buchdahl conditions related to the maximum allowable mass-radius ratio (compactification factor) limit are satisfied. All the energy conditions are shown to meet the physical requirements. The stability of the model has been checked and we have shown, via Fig. 4.3c, that $\Gamma = \dfrac{\rho + p_r}{p_r}\dfrac{dp_r}{d\rho} > \dfrac{4}{3}$ is satisfied. Moreover, the speed of sound is consistent with the causality condition and remains positive throughout the fluid sphere in the pulsars. Hence we can conclude that such a model may be utilised to construct a relevant model of a superdense star for charged anisotropic, charged isotropic and uncharged isotropic matter distributions.

- In chapter 5, we used the relationship between the potentials $e^{2\lambda(r)}$ and $e^{2\nu(r)}$ found by Manjonjo *et al* (2017) to generate three new classes of exact solutions to the Einstein field equations with an anisotropic fluid source. The relationship between the potentials arises from the conformal condition

$$\mathscr{L}_{\mathbf{X}} g_{ab} = 2\psi g_{ab},$$

where $\psi(x^a)$ is the conformal factor. The gravitational potentials are regular in the centre. A particular exact solution was selected for a detailed physical analysis. We showed that this solution produces values for the central density, radius, mass and compactification factor consistent with the stars SAX J1808.3−3658, EXO 1785, Cen X-3, 4U 1820-30, PSR J1903+327, Vela X-1 and PSR J1614−2230. The stars PSR J1614−2230 and SAX J1808.4−3658 were chosen for further study as they correspond to the highest and smallest stellar masses in Table 5.4. We find that for PSR J1614−2230 the central density is $\rho_c = 1.97 \times 10^{15}\text{gcm}^{-3}$ and for SAX J1808.4−3658 the value is $\rho_c = 1.27 \times 10^{15}\text{gcm}^{-3}$. Such high density regime pushes the matter from the nuclear density to the quark matter density. This reinforces the idea of having a quark matter core inside a neutron star, i.e., a hybrid star or a purely strange quark star. In fact, some previous attempts have been made to classify these object as strange quark stars including the work of Gangopadhyay *et al* (2013).

Our present study on gravitating bodies using conformal symmetry reinforces these claims. The stellar radius for PSR J1614−2230 is $r_s = 10.79$ km and for SAX J1808.4−3658 the radius is $r_s = 7.68$ km. Our analysis of the features show clearly that the physical criteria of a realistic star are satisfied for our model. For PSRJ1614−2230 we have $\frac{2M}{r} = 0.5396 < \frac{8}{9}$ and for SAX J1808.4−3658 we have the condition $\frac{2M}{r} = 0.3476 < \frac{8}{9}$, which satisfy the Buchdahl (1959) limit. Therefore we have showed that the conformal condition of Manjonjo *et al* (2017) can be integrated to lead to new solutions and they produce models of realistic stars.

- The objective of chapter 6 was to show that the existence of a conformal symmetry helps to find a new solution of the field equations which can then be characterised geometrically. It is desirable on physical grounds for the matter distribution to have isotropic pressures which is the assumption of this chapter. this physical constraint leads to a new mathematical equation

$$2x\dot{Z} - 2Z = x\frac{E^2}{C} + k,$$

which is the condition of pressure isotropy. We have found a new class of exact solutions to the Einstein-Maxwell system for a charged isotropic star satisfying the generalized condition of pressure isotropy with an electric field. The model is regular at the centre and well behaved in the stellar interior. We showed that for particular parameter values we can regain stellar masses and radii for six observable astronomical objects. A detailed physical analysis was carried out for the stars PSR J1614-2230 and 4U 1538-52. We showed that the matter variables have relatistic profiles and the compactness parameter satisfies the Buchdahl limit. The values for masses, radii and redshifts lie in the observable range. The model satisfies causality conditions, stability conditions and energy conditions. Therefore we have demonstrated that a stellar model, with conformal symmetry and isotropic pressures, satisfying the criteria for physical acceptability exists in general relativity.

References

[1] Andréasson H, Sharp bounds on the critical stability radius for relativistic charged spheres, *Commun. Math. Phys.* **288**, 715 (2009).

[2] Banados M, Teiltelboim C and Zanelli J, Black hole in three-dimensional spacetime, *Phys. Rev. Lett.* **69**, 1849 (1992).

[3] Banerjee A, Rahaman F, Jotania K, Sharma R and Karar I, Finch-Skea star in (2+ 1) dimensions, *Gen. Relativ. Gravit* **45**, 717 (2013).

[4] Bhar P, Strange star admitting Chaplygin equation of state in Finch-Skea spacetime, *Astrophys. Space Sci.* **359**, 41 (2015).

[5] Bhar P, Murad M H and Pant N, Relativistic anisotropic stellar models with Tolman VII spacetime, *Astrophys. Space Sci.* **359**, 13 (2015).

[6] Bhar P, Newton Singh K, Sarkar N and Rahaman F, A comparative study on generalized model of anisotropic compact star satisfying the Karmarkar condition, *Eur. Phys. J. C* **77**, 596 (2017).

[7] Bhar P, Rahaman F, Biswas R and Fatima H I, Exact solution of a (2+1) - dimensional anisotropic star in Finch and Skea spacetime, *Commun. Theor. Phys.* **62**, 221 (2014).

[8] Böhmer C G and Harko T, Minimum mass-radius ratio for charged gravitational objects, *Gen. Relativ. Gravit.* **39**, 757 (2007).

[9] Bondi H, The contraction of gravitating spheres, *Proc. R. Soc. London A* **281**, 39 (1964).

[10] Bonnor W B, The equilibrium of a charged sphere, *Mon. Not. R. Astron. Soc.* **129**, 443 (1965).

[11] Bowers R L and Liang E P T, Anisotropic spheres in general relativity, *Astrophys. J.* **188**, 657 (1974).

[12] Buchdahl H A, General relativistic fluid spheres, *Phys. Rev.* **116**, 1027 (1959).

[13] Canuto V, Equation of state at ultrahigh densities, *Ann. Rev. Astron. Astrophys.* **12**, 167 (1974).

[14] Chilambwe B and Hansraj S, n-dimensional isotropic Finch-Skea stars, *Eur. Phys. J. Plus* **130**, 19 (2015).

[15] Coley A A and Tupper B O J, Spherically symmetric spacetimes admitting inheriting conformal Killing vector fields, *Class. Quantum Grav.* **7**, 1961 (1990).

[16] Davies P, The new physics (Cambridge: Cambridge University Press) (1989).

[17] Deb D, Chowdhury S R, Ray S, Rahaman F and Guha B K, Relativistic model for anisotropic strange stars, *Ann. Phys.* **387**, 239 (2017).

[18] Delgaty M S R and Lake K, Physical acceptability of isolated, static, spherically symmetric, perfect fluid solutions of Einstein's equations, *Comput. Phys. Commun.* **115**, 395 (1998).

[19] Dev K and Gleiser M, Anisotropic stars: exact solutions, *Gen. Relativ. Gravit.* **34**, 1793 (2002).

[20] Dev K and Gleiser M, Anisotropic stars II: stability, *Gen. Relativ. Gravit.* **35**, 1435 (2003).

[21] Dey M, Bombaci I, Dey J, Ray S and Samanta B C, Strange stars with realistic quark vector interaction and phenomenogical density-dependent scalar potential, *Phys. Lett. B* **438**, 123 (1998).

[22] Dey M, Bombaci I, Dey J, Ray S and Samanta B C, Strange stars with realistic quark vector interaction and density-dependent scalar potential, *Phys. Lett. B* **467**, 303 (1999).

[23] Durgapal M C and Bannerji R, New analytical stellar model in general relativity, *Phys. Rev.* **27**, 328 (1983).

[24] Esculpi M and Aloma E, Conformal anisotropic relativistic charged fluid spheres with a linear equation of state, *Eur. Phys. J. C* **67**, 521 (2010).

[25] Fatema S and Murad M H, An exact family of Einstein-Maxwell Wyman-Adler solution in general relativity, *Int. J. Theor. Phys.* **52**, 2508 (2013).

[26] Feroze T and Siddiqui A A, Some exact solutions of the Einstein-Maxwell equations with a quadratic equation of state, *J. Korean Phys. Soc.* **65**, 944 (2014).

[27] Finch M R and Skea J E F, A relativistic stellar model based on an ansatz of Duorah and Ray, *Class. Quantum Grav.* **6**, 467 (1989).

[28] Gangopadhyay T, Ray S, Li X-D, Dey J and Dey M, Strange star equation of state fits the refined mass measurement of 12 pulsars and predicts their radii, *Mon. Not. R. Astron. Soc.* **431**, 3216 (2013).

[29] Gleiser M and Dev K, Anisotropic stars: Exact solutions and stability, *Int. J. Mod. Phys. D* **13**, 1389 (2004).

[30] Glendenning N K, Compact Stars: Nuclear physics, particle physics and general relativity (Berlin: Springer) (2000).

[31] Gupta Y K, Pratibha and Kumar J, A new class of charged analogues of Vaidya-Tikekar type super-dense star, *Astrophys. Space Sci.* **333**, 143 (2017).

[32] Hansraj S and Maharaj S D, Charged analogue of Finch-Skea stars, *Int. J. Mod. Phys. D* **15**, 1311 (2006).

[33] Hansraj S, Chilambwe B and Maharaj S D, Exact EGB models for spherical static perfect fluids, *Eur. Phys. J. C* **75**, 277 (2015).

[34] Herrera L, Cracking of self-gravitating compact objects, *Phys. Lett. A* **165**, 206 (1992).

[35] Herrera L, Jimenez J, Leal L, Ponce de Leon J, Esculpi M, and Galino V, Anisotropic fluids and conformal motions in general relativity, *J. Math. Phys.* **25**, 3274 (1984).

[36] Herrera L and Ponce de Leon J, Perfect fluid spheres admitting a one-parameter group of conformal motions, *J. Math. Phys.* **26**, 778 (1985a).

[37] Herrera L and Ponce de Leon J, Anisotropic spheres admitting a one-parameter group of conformal motions, *J. Math. Phys.* **26**, 2018 (1985b).

[38] Herrera L and Ponce de Leon J, Isotropic and anisotropic charged spheres admitting a one-parameter group of conformal motions, *J. Math. Phys.* **26**, 2302 (1985c).

[39] Herrera L and Santos N O, Local anisotropy in self-gravitating systems, *Phys. Rep.* **53**, 286 (1997).

[40] Ivanov B V, Static charged perfect fluid spheres in general relativity, *Phys. Rev. D* **65**, 104001 (2002).

[41] Ivanov B V, Analytical study of anisotropic compact star models, *Eur. Phys. J. C* **77**, 738 (2017).

[42] Kalam M, Rahaman F, Molla S and Hossein S M, Anisotropic quintessence stars, *Astrophys. Space Sci.* **349**, 865 (2014).

[43] Kerr R P, Gravitational field of a spinning mass as an example of algebraically special metrics, *Phys. Rev. Lett.* **11**, 237 (1963).

[44] Kiess T E, Exact physical Maxwell-Einstein Tolman-VII solution and its use in stellar models, *Astrophys. Space Sci.* **339**, 329 (2012).

[45] Kileba Matondo D, Mafa Takisa P, Maharaj S D and Ray S, Prediction of stellar masses with Finch and Skea geometry, *Astrophys. Space Sci.* **362**, 186 (2017).

[46] Kileba Matondo D and Maharaj S D, New charged anisotropic compact model, *Astrophys. Space Sci.* **361**, 221 (2016).

[47] Kippenhahn R and Weigert A, Stellar Structure and Evolution (Berlin: Springer-Verlag) (1990).

[48] Komathiraj K and Maharaj S D, Classes of exact Einstein-Maxwell solutions, *Gen. Relativ. Gravit.* **39**, 2079 (2007a).

[49] Komathiraj K and Maharaj S D, Tikekar superdense stars in electric fields, *J. Math. Phys.* **48**, 042501 (2007b).

[50] Lake K, All static spherically symmetric perfect-fluid solutions of Einstein's equations, *Phys. Rev. D* **67**, 104015 (2003).

[51] Lindblom L, Limits on the gravitational redshift form neutron stars, *Astrophys. J.* **278**, 364 (1984).

[52] Maartens R and Maharaj S D, Conformally symmetric static fluid spheres, *J. Math. Phys.* **31**, 151 (1990).

[53] Maartens R, Maharaj S D and Tupper B O J, General solution and classification of conformal motions in static spherical spacetimes, *Class. Quantum Grav.* **12**, 2577 (1995).

[54] Maartens R, Maharaj S D and Tupper B O J, Conformal motions in static spherical spacetimes, *Class. Quantum Grav.* **13**, 317 (1996).

[55] Maartens R, Mason D P and Tsampolis M, Kinematic and dynamic properties of conformal Killing vectors in anisotropic fluids, *J. Math. Phys.* **27**, 2987 (1986).

[56] Mafa Takisa P and Maharaj S D, Compact models with regular charge distributions, *Astrophys. Space Sci.* **343**, 569 (2013a).

[57] Mafa Takisa P and Maharaj S D, Some charged polytropic models, *Gen. Relativ. Gravit.* **45**, 1951 (2013b).

[58] Mafa Takisa P, Maharaj S D, Manjonjo A M and Moopanar S, Spherical conformal models for compact stars, *Eur. Phys. J. C* **77**, 713 (2017).

[59] Mafa Takisa P, Maharaj S D and Ray S, Stellar objects in the quadratic regime, *Astrophys. Space Sci.* **354**, 463 (2014a).

[60] Mafa Takisa P, Ray S and Maharaj S D, Charged compact objects in the linear regime, *Astrophys. Space Sci.* **350**, 733 (2014b).

[61] Maharaj S D, Kileba Matondo D and Mafa Takisa P, A family of Finch and Skea relativistic stars, *Int. J. Mod. Phys. D* **26**, 1750014 (2016).

[62] Maharaj S D and Komathiraj K, Generalized compact spheres in electric fields, *Class. Quantum Grav.* **24**, 4513 (2007).

[63] Maharaj S D and Mafa Takisa P, Regular model with quadratic equation of state, *Gen. Relativ. Gravit.* **44**, 1419 (2012).

[64] Mak M K and Harko T, Quark stars admitting a one-parameter group of conformal motion, *Int. J. Mod. Phys. D* **13**, 149 (2004).

[65] Malaver M, Models for quark stars with charged anisotropic matter, *Research Journal of Modeling and Simulation* **1**, 65 (2014).

[66] Manjonjo A M, Maharaj S D and Moopanar S, Conformal vectors and stellar models, *Eur. Phys. J. Plus* **132**, 62 (2017).

[67] Manjonjo A M, Maharaj S D and Moopanar S, Static models with conformal symmetry, *Class. Quantum Grav.* **25**, 045015 (2018).

[68] Maurya S K, Banerjee A and Hansraj S, Role of pressure anisotropy on relativistic compact stars, *Phys. Rev. D* **97**, 044022 (2018).

[69] Maurya S K and Gupta Y K, A new class of relativistic charged anisotropic super dense star models, *Astrophys. Space Sci.* **353**, 657 (2014).

[70] Maurya S K, Gupta Y K, Ray S and Dayanandan B, Anisotropic models for compact stars, *Eur. Phys. J. C* **75**, 225 (2015).

[71] Maurya S K, Gupta Y K, Ray S and Deb D, A new model for spherically symmetric charged compact stars of embedding class 1, *Eur. Phys. J. C* **11**, 45 (2017).

[72] Murad M H, Some analytical models of anisotropic strange stars, *Astrophys. Space Sci.* **361**, 20 (2016).

[73] Murad M H and Fatema S, Some exact relativistic models of electrically charged self-bound stars, *Int. J. Theor. Phys.* **52**, 4342 (2013).

[74] Newman E T and Janis A I, Note on the Kerr spinning particle metric, *J. Math. Phys.* **6**, 915 (1965).

[75] Nördstrom G, On the energy of the gravitational field in Einstein's theory, *Proc. Kon. Ned. Akad. Wet.* **20**, 1238 (1918).

[76] Pandya D M, Thomas V O and Sharma R, Modified Finch and Skea stellar model compatible with observational data, *Astrophys. Space Sci.* **356**, 285 (2015).

[77] Patel L K, Mehta N P and Maharaj S D, Higher-dimensional relativistic-fluid spheres, *Il Nuovo Cimento B* **112**, 1037 (1997).

[78] Paul B C, Chattopadhyay P K, Karmakar S and Tikekar R, Relativistic strange stars with anisotropy, *Mod. Phys. Lett. A* **26**, 575 (2011).

[79] Picanço R and Malheiro M, Charged relativistic stars and the anisotropic formalism, *Int. J. Mod. Phys. D* **16**, 303 (2007).

[80] Picanço R, Malheiro M and Ray S, Charged polytropic stars and a generalisation of Lane-Emden equation, *Int. J. Mod. Phys. D* **13**, 1441 (2004).

[81] Rahaman F, Maharaj S D, Sardar I H and Chakraborty K, Conformally symmetric relativistic star, *Mod. Phys. Lett. A* **32**, 1750053 (2017).

[82] Rahaman F, Sharma R, Ray S, Maulick R and Karar I, Strange stars in Krori-Barua spacetime, *Eur. Phys. J. C* **72**, 2071 (2012).

[83] Rahaman F, Paul N, De S S, Ray S and Kayum Jafry Md A, The Finslerian compact star model, *Eur. Phys. J. C* **75**, 564 (2015).

[84] Ray S, Espindola A L, Malheiro M, Lemos J P S, Zanchin V T, Electrically charged compact stars and formation of charged black holes, *Phys. Rev. D* **68**, 084004 (2003).

[85] Reissner H, Uber die Eigengravitation des elektrischen Feldes nach der Einstein-schen Theorie, *Ann. Phys.* **59**, 106 (1916).

[86] Ruderman R, Pulsars: Structure and dynamics, *Ann. Rev. Astron. Astrophys.* **10**, 427 (1972).

[87] Sawyer R F, Condensed π^- Phase in neutron star matter, *Phys. Rev. Lett.* **29**, 823 (1972).

[88] Sawyer R F and Scalapino D J, Pion condensation in superdense nuclear matter, *Phys. Rev. D* **7**, 953 (1973).

[89] Schwarzschild K, Uber das gravitationsfeld eines massenpunktes nach der Einsteinschen theorie, *Sitz. Deut.Akad. Wiss. Berlin, Kl. Math. Phys.* 189 (1916a).

[90] Schwarzschild K, Uber das gravitationsfeld eines kugel aus inkompressibler flussigkeit nach der Einsteinschen theorie, *Sitz. Deut. Akad. Wiss. Berlin, Kl. Math. Phys.* 424 (1916b).

[91] Sharma R and Maharaj S D, A class of relativistic stars with a linear equation of state, *Mon. Not. R. Astron. Soc.* **375**, 1265 (2007).

[92] Sharma R and Ratanpal B S, Relativistic stellar model admitting a quadratic equation of state, *Int. J. Mod. Phys. D* **22**, 1350074 (2013).

[93] Sharma R, Mukherjee S and Maharaj S D, General solution for a class of static charged spheres, *Gen. Relativ. Gravit.* **33**, 999 (2001).

[94] Shee D, Rahaman F, Guha B K and Ray S, Anisotropic stars with non-static conformal symmetry, *Astrophys. Space Sci.* **361**, 167 (2016).

[95] Singh K N, Pant N and Govender M, Some analytic models of relativistic compact stars, *Indian J. Phys.* **90**, 1215 (2016).

[96] Sokolov A I, Phase transitions in a superfluid neutron liquid, *J.E.T.P.* **79**, 1137 (1980).

[97] Sunzu J M, Maharaj S D and Ray S, Charged anisotropy models for quark stars, *Astrophys. Space Sci.* **352**, 719 (2014a).

[98] Sunzu J M, Maharaj S D and Ray S, Quark star model with charged anisotropic matter, *Astrophys. Space Sci.* **354**, 517 (2014b).

[99] Thirukkanesh S and Maharaj S D, Exact models for isotropic matter, *Class. Quantum Grav.* **23**, 2697 (2006).

[100] Thirukkanesh S and Maharaj S D, Charged anisotropic matter with a linear equation of state, *Class. Quantum Grav.* **25**, 235001 (2008).

[101] Thirukkanesh S and Maharaj S D, Charged relativistic spheres with generalized potentials, *Math. Meth. Appl. Sci.* **32**, 684 (2009).

[102] Thirukkanesh S and Ragel F C, Anisotropic compact sphere with Van der Waals equation of state, *Astrophys. Space Sci.* **354**, 415 (2014).

[103] Tikekar R, Exact model for a relativistic star, *J. Math. Phys.* **31**, 2454 (1990).

[104] Tikekar R and Jotania K, On relativistic models of strange stars, *Pramana - J. Phys.* **68**, 397 (2007).

[105] Tupper B O J, Keane A J and Carot J, A classification of spherically symmetric spacetimes, *Class. Quantum Grav.* **29**, 145016 (2012).

[106] Usov V V, Electric fields at the quark surface of strange stars in the color-flavor locked phase, *Phys. Rev. D* **70**, 067301 (2004).

[107] Varela V, Rahaman F, Ray S, Chakraborty K and Kalam M, Charged anisotropic matter with linear or nonlinear equation of state, *Phys. Rev. D* **82**, 044052 (2010).

[108] Watson G N, A treatise on the theory of Bessel functions (Cambridge: Cambridge University Press) (1996).

[109] Weber F, Strange quark matter and compact stars, *Prog. Part. Nucl. Phys.* **54**, 193 (2005).

[110] Wolfram S, Mathematica (Cambridge: Cambridge University Press) (2010).